FCT Fundação para a Ciência e a Tecnologia

MINISTÉRIO DA CIÊNCIA, TECNOLOGIA E ENSINO SUPERIOR

FREEZE - Submarine FREsh water dischargEs: characteriZation and Evaluation (PTDC/MAR/102030/2008)

2010 – 2013: Activity Report

ipma instituto português do mar e da atmosfera

Div. de Geologia Marinha e Georecursos

LNEG

Unidade das Águas Subterrâneas

CENTRO DE OCEANOGRAFIA

Centro de Oceanografia, CO-FCUL

UAlg UNIVERSIDADE DO ALGARVE

Universidade do Algarve

INSTITUTO SUPERIOR TÉCNICO Universidade Técnica de Lisboa

Instituto Superior Técnico, Lisboa

1. INTRODUCTION: FREEZE PROJECT

The flow of terrestrial groundwater towards the sea is an important natural component of the hydrological cycle (Church, 1996). Hydrological studies have shown that land derived fresh groundwater may discharge through the sea floor through a process known as submarine groundwater discharge (SGD, Taniguchi et al., 2002). Many studies have highlighted the ubiquitous occurrence on the near-shore environment (Bratton, 2004) and for carbonate acquiferous (limestones or dolomite) with dissolution flow conduits discharge in the form of submarine freshwater springs is a well-known phenomenon (Moore, 2008; Taniguchi et al., 2002).

In Portugal, groundwater supplies about 70% of the fresh water needs and most of the aquifers are hosted in sandstones and limestones along the Portuguese coastline where more than 60% of the whole population dwells. It is assumed in various cases that the aquifers discharge to the sea based on the hydraulic heads, geology and geometry of the aquifers, and on the results of numerical models. The identification and quantification of groundwater submarine discharge is crucial for water and ecosystem management. At present, the over-exploitation observed in the main deep aquifers located in the Beira-Litoral, SetúbalPeninsula and Algarve regions (north, centre and south of Portuguese littoral) led to the prohibition of drilling new boreholes, which limits local investment and economic development.

The project FREEZE - Submarine FREsh water dischargEs: characteriZation and Evaluation study on their impact on the Algarve coastal ecosystem (PTDC/MAR/102030/2008) is a Portuguese national research project funded by FCT.

The project started officially in January 2010 and was devoted to the study of the freshwater submarine groundwater discharges (SGD's) at sea off Olhos de Água area (Algarve, South Portugal). The project focused part of its activity on mapping an area in the continental shelf where SGDs are known to occur in the intertidal zone and their monitoring; a remote sensing methodology for detection of SGDs in the offshore have been tested leading to shallow water physical oceanographic parameters acquisition. Estimation of freshwater SGD respect to the local groundwater reserves was another key project aim in the scope to evaluate a possible exploitation or to increase attention to the monitoring of present boreholes exploitation in the studied area. In addition particular attention was dedicated to the analysis and monitoring of the submarine ecosystems and biological communities associated to the discovered SGDs. To achieve all these goals a multidisciplinary team of geologists, geophysicists,

oceanographers, hydro-geologists, geochemists and biologists has been gathered in the scope to collaborate approaching the same topic by different point of view. Most of the time, the various investigations/activities have been strictly connected one to each other assuring an immediate feedback and helping in this way to the planning of further initiatives.

1.1Study area

The study area is located in the Algarve region, the southernmost province of Portugal, characterized by a warm Mediterranean, semi-arid climate. The Algarve mean annual temperature and precipitation are around 17º C and 600 mm, respectively. The precipitation regime is irregular, having intermittent periods with heavy rains in the winter and a long dry period in the summer.

The southern coast of Portugal is characterized by an important development of the tourism sector, particularly demanding in water supply directly but also indirectly for the irrigation of the numerous hotels, resorts and golf courses flanking the coast of the area. Furthermore the water abstraction for agricultural purpose, such as the irrigated market gardening, represents a significant need of water. The vegetation is mainly composed by citrus tree used for cultivation and other commercially attractive trees such as olive, almond and cork oak trees.

The geomorphology of the Algarve littoral is characterized on the East by a shore line of sandy deposit and the West by a platform forming a cliff well observed between Albufeira and Olhos de Água. Inland, the area can be described as coastal plain with low relief, bordered on the north by Jurassic limestone with a more pronounced relief. Several characteristic karstic features can also be observed such as doline and dry valleys.

1.2 Geological setting

The onshore Meso-Cenozoic Algarve basin is located on southwestern border of the Iberian Peninsula and is known as Orla Meridional or Orla Sedimentar Algarvia. It is an E-W trending sedimentary basin extending from the São Vicente cape to the Spanish border (represented by the Guadiana river) with in some areas a sedimentary infill more than 4000 m thick. These Meso-Cenozoic sedimentary units lie on a Hercinian basement made by Carboniferous schists and greywackes.

During Middle to Upper Triassic begun an extensional tectonic regime related to the Pangaea fragmentation (Terrinha, 1998), promoting the deposition of a transgressive mega-sequence since the Upper Triassic to the Sinemurian (Azerêdo et al., 2003).

The pre-rift phase sedimentation begins with a positive sequence of sandstones and conglomerates, the "Arenitos de Silves", discordantly above the Paleozoic basement (Palain, 1976, 1979; Rocha, 1976; Manuppella et al., 1988; Ramalho, 1988; Manuppella et al., 1992). Toward the top these arenites evolve progressively to a transitional facies composed by sequences of fine sandstones, siltstones, claystones and clayey dolostones (Azerêdo et al., 2003), that form an evaporitic carbonate pelitic complex known in literature as "Complexo Pelítico Carbonatado-Evaporítico" (Manuppella et al., 1992).

This sedimentary cycle ends with a volcanic-sedimentary complex related to the first rifting phase, represented by tholeitic basalts, volcanic breccias, tuffs and dolostones (Manuppella et al., 1992) that with the carboniferous schists and greywackes constitutes an impermeable substratum.

The Algarve Basin starts its structuration since Lower Lias forming in the E-W direction some sub-basins with distinct tectono-sedimentary domains. In the eastern sub-basin, located between Lagoa and Tavira, Lias is represented by limestones and dolomites (600 m of thickness) deposited in a confined and subsiding internal shelf.

The transition to the Dogger is marked by an erosional phase and general aerial exposure, registered by sedimentary disconformities promoting a hiatus between the middle Toarcian and the Aalenian (Azerêdo et al., 2003). In the Dogger occurs a change in the sedimentary environments which is characterized by alternations between inner platform and hemipelagic environments, where oolitic limestones and marls are formed (350 to 500m of thickness), conditioned by sea level variations (Manuppella et al., 1992).

Lias and Dogger formations present good hydraulic properties, great thickness and outcrop extensively supporting some of the most important aquifers of the region. These formations have been affected by an intense secondary dolomitization process that produced their great porosity and permeability.

The period between the upper Callovian and lower Oxfordian is marked by a compressive episode of tectonic inversion (Terrinha, 1998).

During Malm, mainly in the Upper Oxfordian and Middle Kimmeridgian, the variation between sedimentary environments increases due to a second phase of rifting. Since Upper Kimmeridgian an inner platform environment develops promoting the deposition of a thick regressive carbonate sequence that reaches its maximum in Tithonian-Cretaceous.

These formations, like the Lias-Dogger ones, present good hydrogeological properties and support important aquifers systems although with minor areal extension.

The transition to Cretaceous is marked by another compressive tectonic episode (Terrinha, 1998). During Hauterivian and Barremian the sedimentation has marine and fluvial characteristics, while in the lower Aptian the subsidence increases and begins a transgressive episode due to the North Atlantic expansion (Rey, 1983).

The lower Cretaceous sediments composed by marls, limestones, dolostones and a few sandy and conglomeratic levels, doesn't show the same flow rates of the Jurassic formations, even if the flow rate starts to be important when they became thicker and areally extended.

The absence of Upper Cretaceous sediments in the Algarve Basin is probably associated with an important event of tectonic inversion occurred between Aptian and Middle Miocene (Terrinha, 1998) although there's a much more complete geological record, from Paleogene to Quaternary, on the immerse region to the south in the offshore of Algarve.

The Lagos-Portimão Formation corresponds to deposits of "temperate carbonate platform" sedimentological type, developed during a long time span (Lower Burdigalian to Upper Serravallian). Boreholes indicate an 80m maximum thickness. Strongly affected by karst phenomena, this formation overlies the Carboniferous, Jurassic, Cretaceous and possible Paleogene units with angular unconformity, stratigraphical hiatuses or paraconformaties (Pais et al., 2000).

From hydrogeological point of view this formation is very interesting being an important source for fresh water supply and irrigation.

A major change in sedimentation conditions (carbonate to siliciclastic environments occurred in the Lower Tortonian with the deposition of yellowish sands (Pais et al., 2000).

A detailed palaeoichnological study of the Oura hardground permitted to confirm the existence of an important intra-Miocene stratigraphic gap (ca. 3 Ma hiatus), represented by a razor-sharp erosional contact that separates the lower carbonate sequence of Lagos–Portimão Formation from the upper siliciclastic sequence of Cacela Formation (Upper

Tortonian) (Cachão et al. 2009). The bioeroded hardground of Oura can be correlated with a single transgressive event that took place during that period of time. At the same time, it is possible to state the relationship between this stratigraphic gap and the tectonic phase that took place in the Betic Chain and Alboran Sea domain (Cachão et al. 2009).

Continental sedimentation keeps on Quaternary with the deposition of Faro-Quarteira Sands reaching a maximum thickness of 50m. It is made by siliciclastic deposits with reddish colors, due to its high content in iron oxides, with human lithic artifacts of quartz, quartzite and greywacke pebbles, Muestirien type (relative to the Riss-Würm interglacial or early Würm glaciation).

It is one of the most extended formations of the Algarve Basin, outcropping in all Algarve region, covering older formations and overlaying in some places Paleozoic rocks.

This formation was intensely investigated and drilled for irrigation purposes. Nowadays, large wells and the traditionally “noras” are still active.

1.2.1 Tectonics

The Algarve Basin, located in South Portugal, can be sub-divided into two distinct superposed sedimentary basins, the Mesozoic and the Cenozoic basins. The Mesozoic basin formed by lithospheric thinning caused by the southeastwards drifting of Africa with respect to Iberia from Triassic to Late Cretaceous times. Rifting was followed by tectonic inversion caused by N-S compression associated with the northwards movement of Africa with respect to Eurasia which started in the Late Cretaceous. Whilst the Algarve was subjected to uplift, compression and alkaline magmatism in the Late Cretaceous, the westernmost Mediterranean was undergoing subduction of the Tethyan oceanic sea floor.

Onshore Algarve only Neogene and Quaternary sediments are recorded. Offshore, the Paleogene was drilled by exploration oil industry wells. The stratigraphic relationships and tectonic regimes between the Mesozoic, Paleogene and Neogene show that the inversion tectonics regime occurred in various phases. A first phase occurred during the Late Cretaceous during which the Monchique laccolith was emplaced, the rifting extensional faults were inverted and the proximal continental margin was extensively uplifted. Uplift and compression continued during the Paleogene as recorded by well dated deposits offshore Terrinha (1998); Terrinha et al. (2003); Lopes et al. (2006); Roque (2007); Terrinha et al. (2013).

The formation of the Neogene Algarve basin postdates the tectonic inversion of the Mesozoic and Paleogene deposits. It has been shown that the Neogene proximal deposits thicken from less than 200m onshore to more than 1.5 km in the depocentre of the offshore basin and that this thickening is not associated to faulting. The Neogene basin is a sag basin, formed by lithospheric flexural processes associated with the late stages of the evolution of the southwest Iberia margin, such as the formation of the Gibraltar arc after subduction of the Tethyan oceanic lithosphere in the West Mediterranean and slab roll-back into the Atlantic. The Neogene basin is limited to the south by the Guadalquivir-Portimão banks which form the limit of the well-recognized continental crust. To the south of these structural highs, extends oceanic crust as reported by Sellares et al. (2013) and Martínez-Loriente et al. (2013) based on seismic refraction profiles. The Guadalquivir-Portimão banks were the southern limit of the Algarve rift basin during the Mesozoic and are at Present undergoing uplift and deformation as attested by instrumental seismicity.

The stratigraphy of the Neogene of the Algarve basin has been matter of discussion. Recent synthesis were produced by Pais, Cunha et al. (2012); Cachão, Silva et al. (2009); Matias, Kress et al. (2011); Roque, Duarte et al. (2012); Terrinha, Rocha et al. (2013). These works taken together encompass the stratigraphy from the onshore across the deep offshore. Onshore, the sedimentary record of the Miocene is unconformably overlying the folded and thrust Mesozoic deposits. The Miocene consists of shallow water high energy limestones.

The earliest deposits were dated of Burdigalian times Pais et al. (2012). A main unconformity between the Tortonian and Serravalian times, i.e. between the Lagos-Portimão Formation and the Cacela Formation was described in the area of Oura as corresponding to a hiatus of 3 Ma (Cachão et al., 2009).

The seismic reflection record shows the continuity of these deposits offshore until the shelf break, to the south of which the stratigraphic record thickens and has a different origin as described by Matias, Kress et al. (2011) and Roque, Duarte et al. (2012). The Lower and Mid Miocene record is made up of deep water turbidites and the Upper Miocene through Quaternary shows a very important record of contournite sedimentation associated with the onset of the Mediterranean Outflow Water, which formed after the reopening of the Mediterranean-Atlantic circulation gateway, the Gibraltar Straits.

1.3 Hydrogeological setting

The ARQ aquifer system (M6 in Fig. 1.1) was characterized by Almeida and Lourenço da Silva (1990) and Almeida et al. (2000). These last authors defined the limit of the ARQ, as shown in Fig. 1.1, with the aim to define inventory and management units.

The water-bearing formations are composed by detritic-carbonate rocks dating from Miocene and upper Jurassic (Table 1.1 and Fig.1.1). Both formations, called from here Jurassic and Miocene aquifer respectively, are supposely separated by the Cretaceous aquitard, identified in Fig.1.2 (upper). Structural conditions allow, in some sectors, the contact between the two water-bearing formations, making possible hydraulic connection. Between Albufeira and the Quarteira stream, the subtabular Miocene is tilting slightly towards S-SE (Fig.1.2 bottom). Miocene formations are sedimented with strong angular unconformity over the Cretaceous and Jurassic formations (Fig.1.2 bottom). They all are partly recovered by the Plio-Quaternary formations that act as an aquitard, confining unit.

The diapir west of Albufeira (Figs. 1.1 and 1.2 upper) was responsible for the strong angular unconformity (near 90°) be-tween the Miocene and Cretaceous. Another not outcropping diapir, but whose presence is denounced by hydrochemical characteristics of the groundwater, is located E of Escarpão, extending southwards to the vicinity of Patã de Baixo, i.e. on the west border of the ARQ, along the Quarteira stream.

The aquifer system boundaries are defined by three tectonic major accidents (Fig.1.1):

- East: the NW-SE Quarteira fault, which conditioned the Miocene sedimentation since the eastern compartment (M7 aquifer) is thicker (180 m) than the western compartment (80 m, ARQ-M6 aquifer);

- North: W-E Sagres-Algoz-Vila Real de Santo António flexure zone (see also Fig. 1.2 upper);

- West: N-S Albufeira fault and Albufeira diapir (see also Fig.1.2 upper).

The south boundary is formed by the seacoast. Inter and sub-tidal springs of fresh to brackish water along the coast line, in particular at Olhos de Água (Fig. 1.1), indicate that ARQ discharges into the sea. Another discharge area is the Quarteira stream (Almeida et al. 2000; Reis, 2007).

Recharge occurs in the northern side, through direct infiltration in the Escarpão plateau. Its plain topography and abundant epikarstic forms (sinkholes, sinks and dry valleys) is

favourable to an important recharge and, in a minor scale, in the Cretaceous and Miocene formations. Due to their considerable clay fraction, the Miocene coverage formations make direct recharge more difficult. It was proved through tracers that part of the recharge that takes place in the Escarpão plateau flows east and northeastwards and feeds the exsurgences in the Quarteira streambed (Almeida and Crispim, 1987).However, southwards of this plateau, groundwater probably flows southwards. The Quarteira stream is effluent in its last section, located southwards of Ponte do Barão and influent in a section located upwards.

Recharge was originally estimated for the ARQ as 8.7×106 m^3.year-1 (Almeida et al., 2000), based on an average rainfall of 550 mm and considering recharge rates of 50% for the Jurassic and 15% to the Miocenelithologies. Monteiro et al. (2007) presented a value of 5.4×106 m^3.year-1 based on an average precipitation of 593 mm/yr and corresponding to the infiltration of 23% of the rainfall on the areas of occurrence of formations with an intergranular porosity, and between 63% and 69% on the areas of occurrence of karst formations.

Transmissivity was estimated in 30 boreholes exploiting the Miocene formation. It ranges between 84 e 3080 m^2.day-1, with average of 540 m^2.day-1 and median of 235 m^2.day-1 (Almeida and Lourenço da Silva, 1990).

Groundwater abstraction for public supply extracted 3.3×106 m^3/year in 1993 (Almeida et al., 2000) and 8.43×106 m^3/year (~30% of the estimated average annual recharge) in 1999 (Hugman et al., 2013). After 1999, public water supply was mainly ensured by surface water. Almeida et al. (2000) estimated as 3.5×106 m^3.year-1 (~12% of the estimated average annual recharge) the water extractions for irrigation in 1979.

Recently numerical flow models were applied to quantify the SGD and the impact of changes in groundwater use (Monteiro et al., 2007). These authors used the ARQ boundaries defined by Almeida et al. (2000) and shown in Fig 1.1.

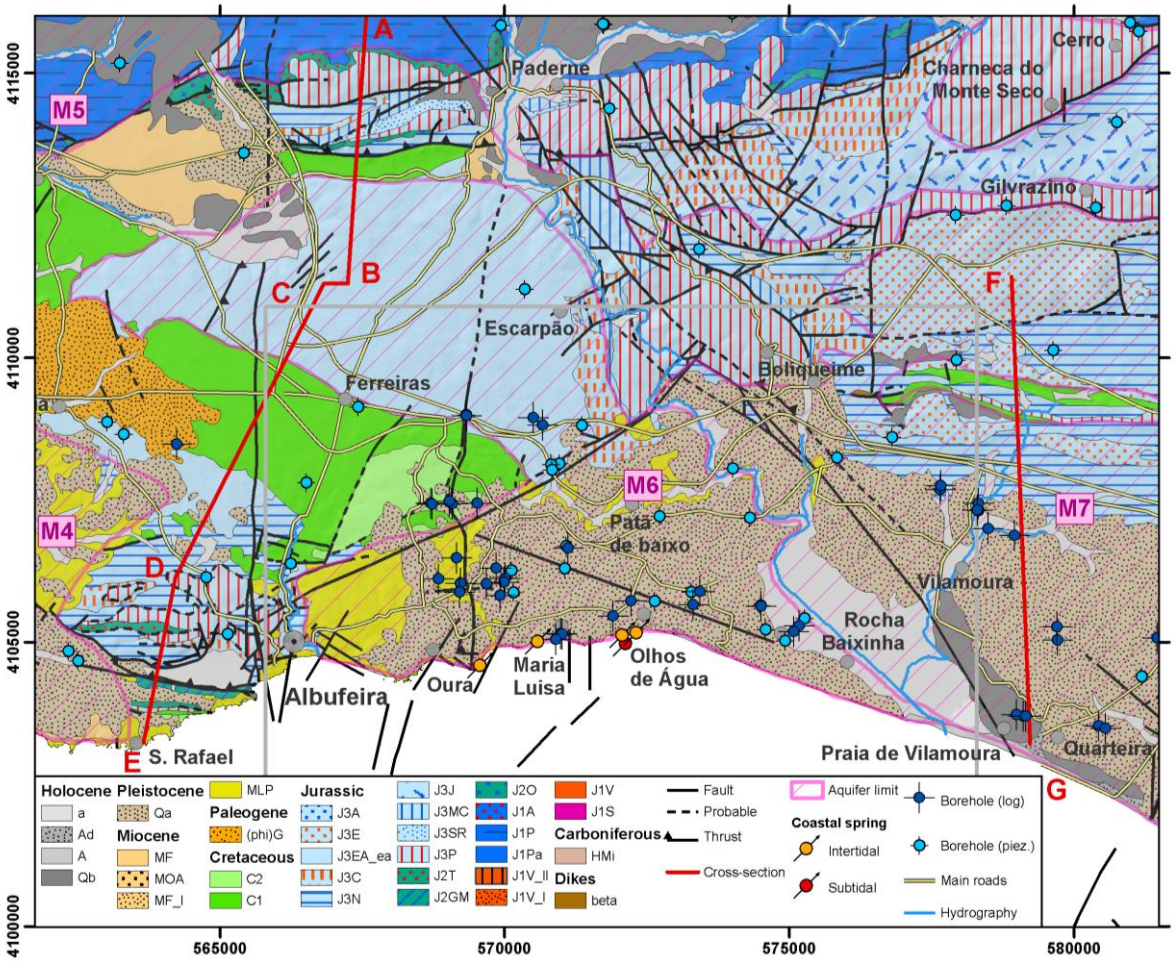

Fig 1.1 - Geological map of the study area (adapted from Manuppella, 1992). Grey rectangle indicates the position of Fig.2.16 on Task1. Coordinates system: UTM N29, WGS 84. Aquifer systems abbreviations (Almeida et al., 2000): M4 Ferragudo - Albufeira; M5 Querença - Silves; M6 Albufeira - Ribeira de Quarteira; M7 Quarteira.

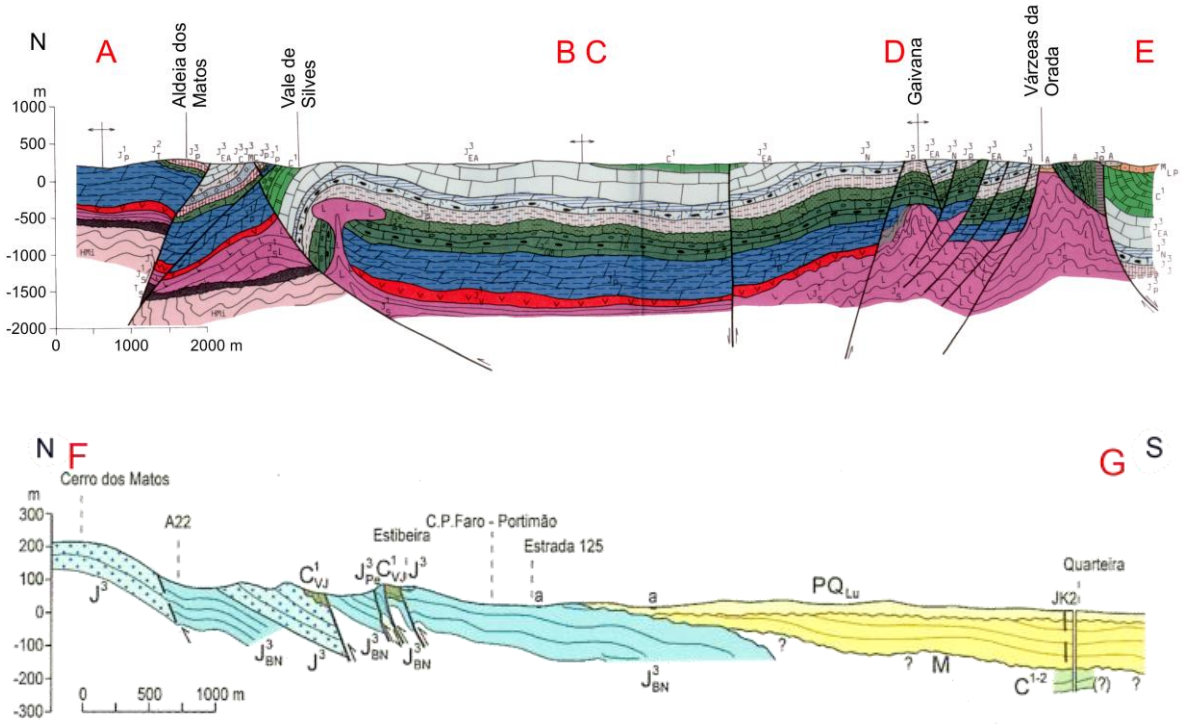

Fig. 1.2 – Geological cross-sections (Top: Manuppella (1992); bottom: Manuppella et al. (2007)), location in Fig. 1.1.

Epoch	Age	Symb.	Formation	Lithology	Thickness	Main lithology	Hydrostratigraphy
Pleistocene?	?	Qa	Faro-Quarteira sands	Reddish and yellowish clayey sandstones with pebbles intercalations	10-30m	Detritic	Aquitard
Pliocene	Piazencian	MOA	Olhos de Água sands	White and yellow feldspathic sands, pebbles			
Miocene	Burdigalian-Serravian	MLP	Lagos-Portimão Formation	Biocalcarenites, yellow or pink, sandy limestones and sandstones, abundant fossils	30-85 m	Limestone	Aquifer
Lower Cretaceous	Aptian	C2	Porto de Mós marls and limestones Luz marls Limestones and marls with *Palorbitolina lenticularis*	Marls and limestones Green and purple marls Massive limestones and marls, brownish	100 m	Marl and limestone	Aquitard

Epoch	Age	Symb.	Formation		Lithology	Thickness	Main lithology	Hydrostratigraphy
	Barremian	C2	Marls with *Choffatella decipiens*		Marls, sandstones, marly limestones and dolomites	50 m		
	Berriasian	C1	Limestones with *Choffatella pyrenaica* Sobral sandstones Limestones with *Trocholina* Purbeck facies marls and limestones		Limestones and marls, yellow to purple Sandstones with quartz gravels, pebbles and pelites, redish to purple Oolithic limestones Limestones, conglomerates, marls and dolomites	100 m	Detritic	
Upper Jurassic	Titonian	J3A	Limestones with *A. Lusitanica*		Massive limestones whitish with calciclastic intercalations	650 m	Limestone and dolomite	Aquifer
	Kimmeridgian	J3_EA	Escarpão limestones	Transition limestones	Massive limestones whitish with clayey intercalations			
		J3E		Limestones with *V. striata* and *C. jurassica*	Massive limestones, whitish to grey			
		J3_EA		Limestones with *A. jaccardi*	Massive limestones, whitish, with Nerineas and oncolithes			
		J3N	Sta Bárbara de Nexe dolomitic limestones and dolomites		Dolomitic limestones and dolomites, pinkish or yellowish			
		J3C	Cerro da Cabeça biolimestones		Massive limestones with recif fossiles			
	Oxfordian-Lower Kimmeridgian	J3P	Peral marls and limestones		Alternance of sandy and or marly limestones, massive, yellow and grey, with blue/grey marls	80-100 m	Marl and marly limestone	Aquiclude

Table 1.1 – Lithostratigraphy and hydrostratigraphy of the study area (adapted from Almeida and Lourenço da Silva, 1990; Almeida et al., 2000; Manuppella, 1992; Pais et al., 2000; Rey, 2006).

1.4 Oceanographic setting

The area off the Algarve coast has been surveyed for decades, during many oceanographic campaigns where the main objective was the physical characterization of the Mediterranean Outflow Water in the Gulf of Cadiz (Ambar and Howe, 1979; Baringer and Price, 1997; Mauritzen*et al.*, 2001; Ambar *et al.*, 2002; Potter and Lozier, 2004).

The surface circulation in the Gulf of Cadiz has not been investigated so extensively and most of the studies were based on satellite-derived sea surface temperature (SST) or climatological data (Fiúza *et al.*, 1982; Fiúza, 1983; Folkard *et al.*, 1997; Vargas *et al.*, 2003; Sánchez and Relvas, 2003).

To characterize the surface circulation in the Gulf of Cadiz, Garcia-Lafuente *et al.* (2006) used current-meter, meteorological and remote sensing data along with *in situ* observations gathered during the GOLFO-2001 survey carried out in May-June 2001. The analysis of the whole data sets allowed the aforementioned authors to summarize the surface circulation in the Gulf of Cadiz as presented in Fig. 1.3, valid for depths greater than 200 m.

For the western part of the Gulf of Cadiz, the area under study in the FREEZE project, Garcia-Lafuente *et al.* (2006) suggested that the continental shelf circulation is constituted by core N2 around the cyclonic eddy off Cape S. Vicente (SVE in Fig. 1.3). Core N2 is a branch of the larger-scale Portuguese-Canary eastern boundary current that veers eastward into the Gulf of Cadiz and the SVE is a quasi-permanent feature of the circulation in the Gulf associated with the local wind field.

The area surveyed under the FREEZE project has not been included in the tens of oceanographic campaigns conducted in the Gulf of Cadiz, because is located on the continental shelf off the Olhos de Água region (Albufeira), very near from the coast and with depths much lower than the shelf break (≈ 200 m).

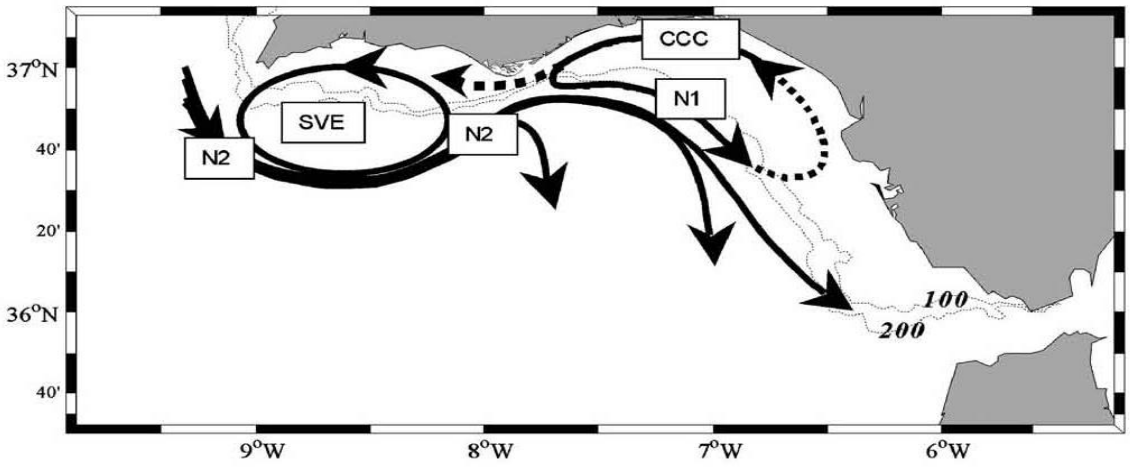

Fig.1.3 – Sketch of the surface circulation in the Gulf of Cadiz proposed by Garcia-Lafuente et al. (2006). In the western part of the Gulf, Core N2 is a branch of the larger-scale Portuguese-Canary eastern boundary current that veers eastward into the Gulf of Cadiz and the cyclonic eddy off Cape S. Vicente (SVE) is a quasi-permanent feature of the circulation in the Gulf associated with the local wind field.

1.5 Biologic state of the art in the study area

Submarine Groundwater Discharge (SGD) can be, volumetrically and chemically, significant for coastal waters worldwide, influencing productivity, species biomass, composition and zonation (Johannes, 1980). Estimates of 2-4 x 1013 m^3 yr-1 have been made for the Atlantic Ocean, which is around the same amount of freshwater that enters this ocean from rivers (Moore et al., 2008). This flow of fluids through shelf sediments transport nutrients like silica, nitrogen and phosphorous (Waska and Kim, 2011) to the coastal zone, which in turn have the ability to affect the biological zonation. For these conceptual similarities, SGD have been termed 'submarine estuaries' (Moore, 1999).

Literature dealing with SGD is scarce and mainly focused on coastal bays, lagoons or estuaries (Miller and Ullman, 2004; Dale and Miller, 2008). In Portugal, only two studies reported the effect of SGD both in Algarve, South Portugal: i) in Arade Estuary (Silva et al. 2012) and ii) Guadiana estuary (Carvalho Dill, 2014). However, the existence of SGD in Olhos de Água beach is known for a long time and was already described in 1841 by João Baptista Lopes on a document concerning the Algarve "kingdom" (Lopes, 1841).The volume of water discharged fluctuates according to the aquifer water table. However, freshwater discharges are observed throughout the year, with several discharge points in intertidal and

subtidal areas (Almeida et al., 2000). Despite the difficulties associated with measuring the volumes of discharged groundwater to Olhos de Água beach, estimations of 100 litres per second have been proposed(Almeida and Silva, 1990).

As in “conventional” estuaries, where the freshwater inflow is a major structuring factor of biological communities (Montagna and Kalke, 1992), changes in salinity due to freshwater flow from SGD also has the ability to influence the distribution of organisms (Miller and Ullman, 2004). For its life history characteristics, namely ubiquitous distribution, rapid generation times, direct benthic development and sessile life-style (Kennedy and Jacoby, 1999), meiofauna and macrofauna holds a high potential for environmental monitoring program. Environmental indicators have taken on such importance because they provide ‘‘a sign or signal that relays a complex message, potentially from numerous sources, in a simplified and useful manner’’ (Jackson et al., 2000).

2. TASK 1– Onshore characterization of Albufeira-Quarteira costal aquifer system

2.1 Objectives

This task deals with the necessity of characterizing the Albufeira-Quarteira aquifer system by the combination of (1) geological and (2) hydrogeological studies, (3) geophysical and (4) geochemical methods and evaluates the hydrodynamic conditions for offshore groundwater discharge.

The task was very complex and articulated and included the following actions:

1. Structural interpretation of the geology of the study area started with analysis and interpretation of already available aerial photos at the approximate scale of 1/32.000, followed by field mapping. A detailed structural map was produced with the typical geometrical, kinematic and chronological information of structural features. The map was inserted in a GIS project and thus easily merged with the offshore data acquired in the frame of task 2.

2. The hydrogeological investigation included recompilation of the available hydrogeological data and a detailed inventory of the existing wells and springs. Groundwater levels and spring discharge were measured in the aquifer and a detailed piezometric contour map was prepared to show main flow paths and recharge/discharge areas.A water balance approach was used to estimate the fresh groundwater component of SGD as the total volume of groundwater discharging to the sea. Finally, to evaluate the distribution and the nature of SGD over the discharge area, numerical models neglecting or considering density effects were used. These models include both the near shore part of the aquifer as well as the part lying below the sea bottom, where density effects are relevant, and provide both the fresh groundwater discharge as well as the discharge of the seawater re-circulated in the aquifer.

3. The geophysical methods included the use of radio frequency electromagnetic (RF-EM), 1D time domain electromagnetics (TDEM), quasi-2D frequency domain electromagnetics (FDEM) and 2D continuous vertical electrical soundings (CVES) on land and on intertidal zone (5m below s.l.) to: (i) detect the freshwater–saltwater interface (FSWI) position and geometry along the coastline; (ii) identify the water-bearing layers and aquitards and relate them with the geological formations and SGD localization. The hydrogeophysics results

contributed to review and upgrade the aquifer geometry, boundary and structure, including hydraulic relationships between the hydrogeological formations.

4. The geochemical methods included the sampling and analysis of groundwater and spring water samples on land and on intertidal and subtidal zones for major, minor and trace elements, and also for some specific tracers such as a suite of naturally occurring isotopic tracers in the U/Th decay chain – 222Rn and 223,224,226,228Ra. Radon-222, an inert gas produced by the decay of 226Ra in sediments, is typically present in groundwater at much greater activities than in surface waters. Its short half-life of 3.8 days and its conservative geochemical nature make this isotope ideal to study exchange processes across the sediment/water interface over daily to weekly timescales. Other isotopic tracers to be analyzed include O-18 and H-2. The geochemical study was complemented with a detailed multiparameters monitoring of the known intertidal springs existing at “Olhos de Água” beach.

The results of Task 1 were the following: (1) production of a detailed structural map of the study area; (2) development of the conceptual and the numerical groundwater models of the aquifer system; (3) calculation of the water balance; (4) flow paths and location of SGD areas; (5) estimates of SGD; and, (6) approximate location of the fresh/sea water interface.

2.2 Geology, Structure and Karstification

With the goal of characterizing the geometry and 3D structure (compartments and boundaries), hydraulic connections and preferential flow paths of the Albufeira-Ribeira de Quarteira aquifer system, the existing wide bibliography was compiled, boreholes logs were interpreted and geological, hydrogeological and geophysical surveys comprising several field work campaigns were conducted.

Structural interpretation of the geology of the study area started with the analysis and interpretation of existing aerial photos at the approximate scale of 1/32.000, followed by field mapping. A detailed structural map was produced with the typical geometrical, kinematic and chronological information of structural features. The map was inserted in a GIS project and thus easily merged with the offshore data acquired within the frame of task 2, Fig. 3.19.

Some onshore structures were detected with the geophysical surveys, such as the Olhos de Água fault, the Mosqueira fault and the Oura fault.

The Oura fault is an accident trending N-S towards NNE-SSW. Its probable trace extends about 10km from Balaia beach until the S. Marcos-Quarteira fault, near Paderne. It is a Mesozoic accident, parallel to Albufeira fault that just like this one may has functioned as an extensional structure during the extensive Mesozoic phase. This accident was later reactivated as a dextral strike-slip fault, probably during the post-Cretaceous and pre-Miocene inversion. In the geophysical profile A2 (see Fig. 2.20), there is a gap in the fault zone, affecting Miocene and Plio-Quaternary formations, that indicates a vertical movement component.

The Mosqueira fault is a structure trending ENE-WSW that extends from the Albufeira fault, located W, until the S. Marcos-Quarteira fault, located E, with an extension of 9 km. It is cut by the Oura fault, separating it into two segments, respectively with 4 km and 5 km of extension. This structure has neotectonic activity, as a reverse fault (Dias, 2001). It is intersected in profiles B2 and B3, see Fig. 2.22.

The Olhos de Água fault is a structure trending WNW-ESE with reverse dip-slip movement. It is intersected in profiles B3, B5 and B6, see Fig. 2.22.

The lithological information of 45 borehole logs (Fig. 2.1) obtained from drilling companies reports were collected in the archives of several institutions (Laboratório Nacional de Energia e Geologia – LNEG, Administração de Região Hidrográfica do Algarve - ARHAlgarve). The boreholes logs were interpreted so that an association of the described lithologies with the geological and hydrogeological formations referred in Table 1**Erro! A origem da referência não foi encontrada.**.1 could be made (Fig. 2.2). This information was used to support the interpretation of the hydrogeophysics results.

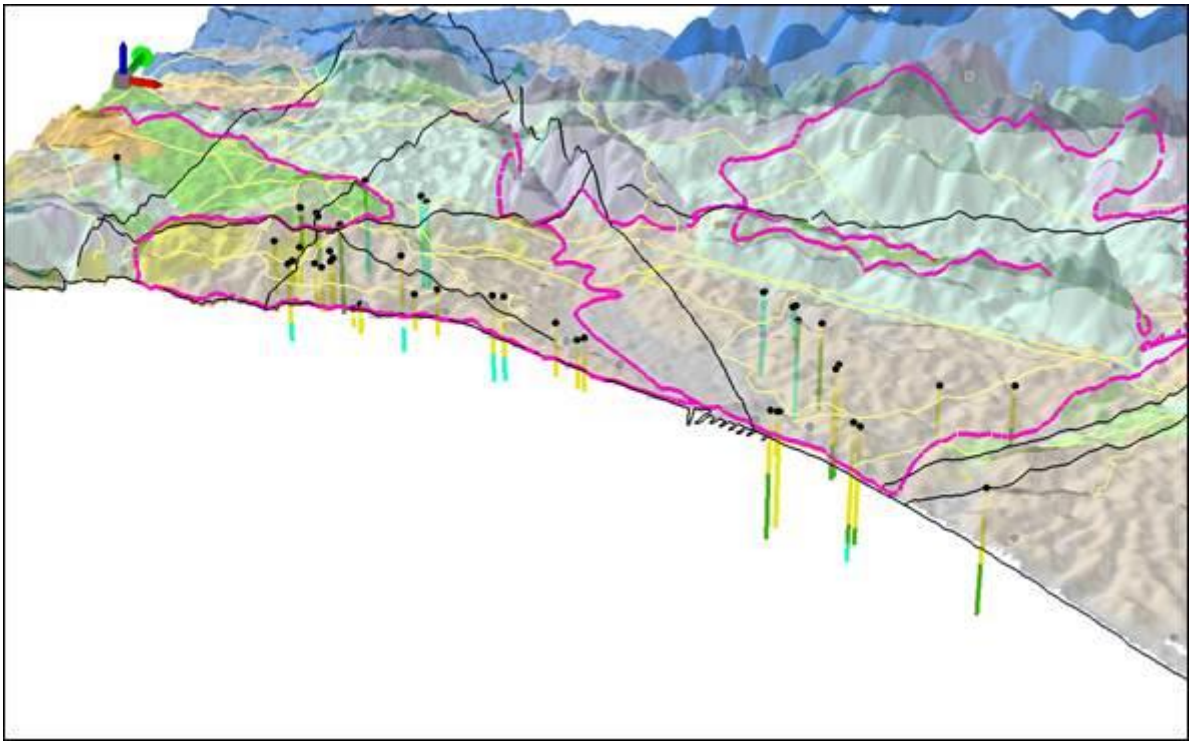

Fig. 2.1 – 3D view of the study area geology with boreholes logs (vertical exaggeration x10).

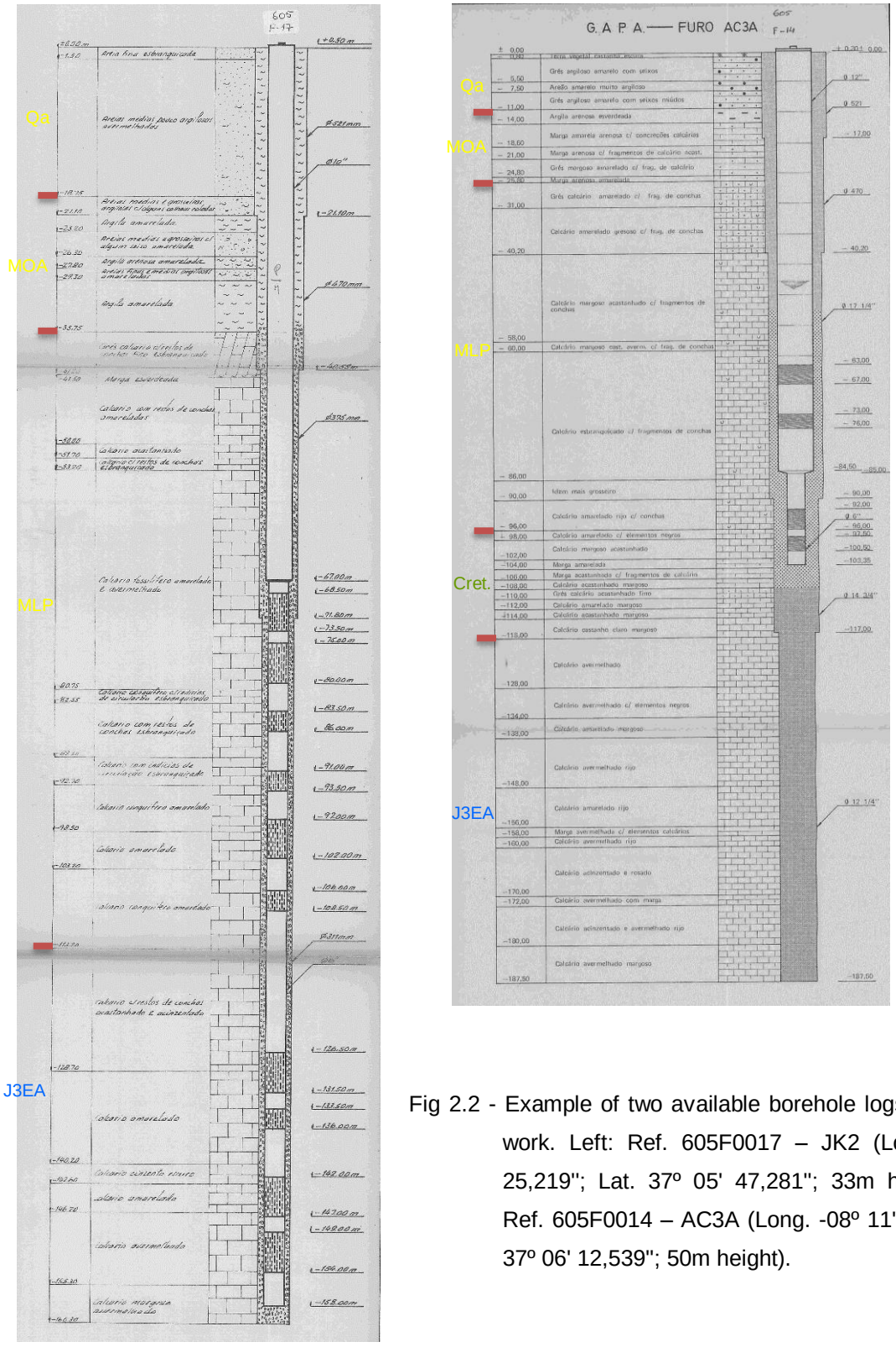

Fig 2.2 - Example of two available borehole logs used in this work. Left: Ref. 605F0017 – JK2 (Long. -08º 10' 25,219"; Lat. 37º 05' 47,281"; 33m height). Right: Ref. 605F0014 – AC3A (Long. -08º 11' 58,785"; Lat. 37º 06' 12,539"; 50m height).

In the aquifer system, the karstification processes seem to be very active. Dias & Cabral (1998) identified a large number of structures affecting the Plio-Quaternary coverage detrital

deposits, probably related with a plastic or fragile behavior of this sedimentary coverage. This occurs as a response to the progressive subsidence or sudden collapse in the karstified bedrock of subjacent dolines (see Fig. 2.3). These structures include i) stratification with accentuated dipping, sometimes near the vertical, ii) mesoscopic scale foldings and iii) fractures either in normal faults and more rarely in reverse faults or fractures without outcrop observable shear (joints, *sensu lato*).

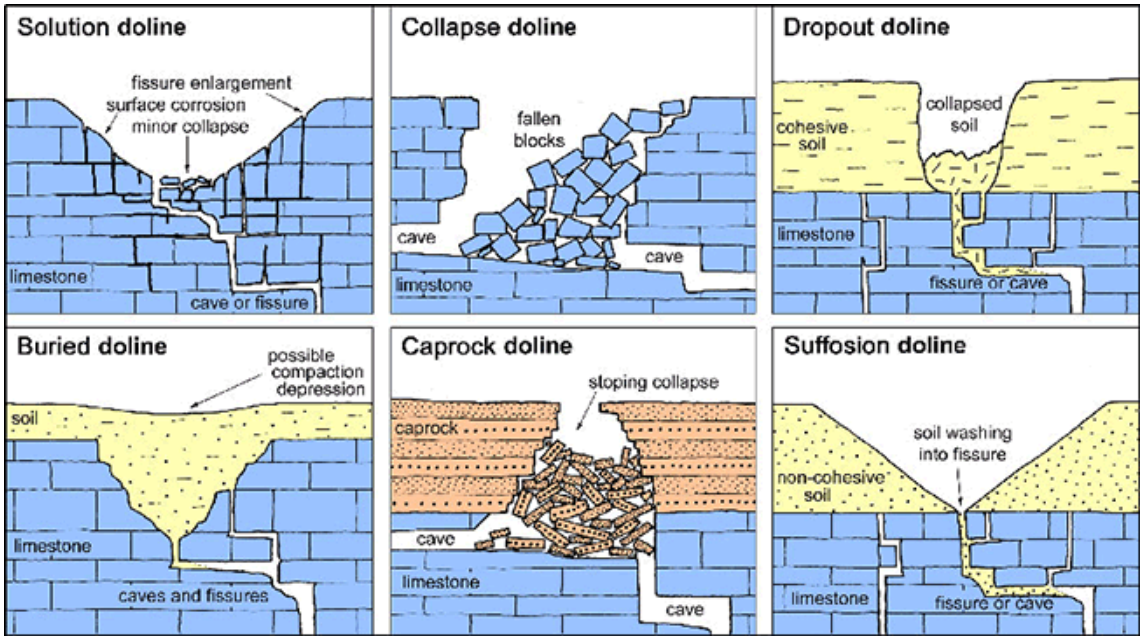

Fig. 2.3 - Sinkholes (or dolines) and subsidence: karst and cavernous rocks in engineering and construction (Modified from the BGS Engineering Geology (Superficial) map of the UK, 2011; adapted from Waltham, A C, Bell, F G and Culshaw, M G. 2005).

During field surveys it was possible to observe the enlargement of dissolution conducts in the carbonate Miocene (Fig. 2.4 a)) and groundwater circulation in the bedding planes and joints (Fig. 2.4 b)). In a rock landslide along a joint, it was possible to see thinner material deposits that have circulated between strata.

a) b)

Fig. 2.4 – a) Top: reddish Plio-Quaternary formations; Middle: yellow detrital fine carbonate sandstone from Miocene; Bottom: yellow carbonate Miocene with intersected pipelines. b) Dissolution on bedding planes and joints of the Miocene.

Along the beaches, in the discharge front of the aquifer system towards the sea, there are several grottos and subsidence dolines infilled by Plio-Quaternary deposits (see Fig. 2.5).

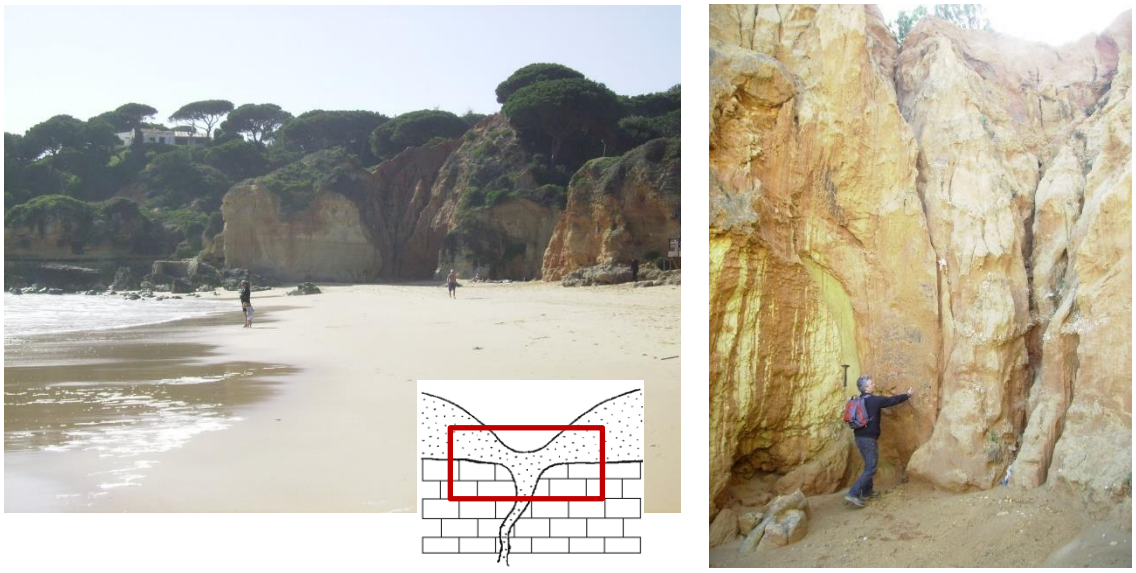

a) b)

Fig. 2.5 – Karst developed in the Lagos Portimão Formation (Miocene), infilled by Faro-Quarteira Sands (Quaternary deposits) (a) affected by faults either with normal geometry or reverse, probably with karstic origin (b) in Olhos de Água beach.

The subsidence dolines are formed when the karst is covered by a surface deposit, collapsing suddenly or progressively towards a cavity in the carbonate rocks (Fig. 2.6). A progressive subsidence with plastic behavior of the sediments may settle them in the interior of a cavity. On the other hand, with fragile behavior, it may result in high deformation velocities associated to an underground sudden collapse.

A particular case of progressive subsidence is related with the down-washing of non-cohesive soil into fissures in bedrock (Fig.2.6 bottom).

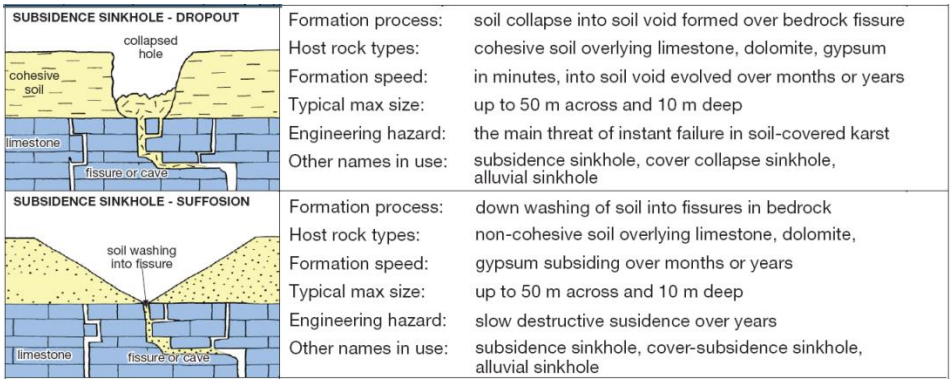

Fig. 2.6 – Top: subsidence sinkhole/doline - dropout; Bottom: subsidence sinkhole/doline – Suffosion (extract from the BGS Engineering Geology (Superficial) map of the UK, 2011).

The surface expression of the subsidence processes, with numerous and small depressions, was identified in several areas, as seen in Fig. 2.7 (left). A satellite image approach to the observed pattern can be seen in Fig. 2.7 (right). Fig. 2.8 shows a field photo of one of the depressions showed in Fig 2.7 (right).

Fig. 2.7 - Overview of the identified subsidence dolines areas (green contour) in the aquifer system (pink contour) (left). Satellite image detail of the depression areas (right). Main faults – red lines. ©Google 2014.

Fig 2.8 – Two close-up views of the same depression.

2.2.1 Onshore geophysical survey using RF-EM method

Onshore geophysical surveys were conducted to detect geological structures and their orientation and preferential groundwater flow paths.

This method has been successfully applied in wetlands, onshore and in shallow coastal waters. Previous works carried out on the Tróia peninsula (south of Setúbal) (Carvalho Dill et al., 2009), Ria Formosa (Stigter et al., 2013) and at the Guadiana estuary (Carvalho Dill &

Stigter, 2008; Carvalho Dill et al., 2012) had already shown that, despite of the attenuation effect of the salt water, very valuable information could be obtained with the use of electromagnetic methods. Structures like fractures and faults are revealed by the presence of freshwater, which circulates along them, creating significant measurable contrasts with the salt water, so that anomalies detected on land are also detectable in shallow salt waters. This fact not only validates the use of this method in coastal environments, in order to detect geological structures and their orientation, but can also be a helpful tool to understand the genesis of some coastal features, including SGD.

The Radio-frequency Electro-magnetics (RF-EM) method uses radio frequencies ranging from 12 up to 300 kHz. The device has been designed for fast and extensive mapping of geological contacts by combining a Data logger, which registers every second and a Global Positioning System. The gathered field data are georreferenced, transformed into 2D data profiles and coupled with all the available information, by means of GIS software. The direction of the profiles should be as much as possible perpendicular to the structure strikes, so that its 2D effect induces a vertical component of the magnetic field. Fig. 2.9 shows the measuring device coupled on a vehicle.

Fig. 2.9 - RF-EM equipment coupled on a vehicle: the receiver antenna is self-orientated and captures the horizontal primary field and the vertical components of the secondary magnetic fields, which are in-phase or out-of-phase with the primary field.

The relationship between the secondary (Hs) and primary (Hp) magnetic fields is studied as a percentage-expressed Hs/Hp ratio (Fig. 2.10). The investigation depth is a function of the resistivity (Rho) of the strata and the radio frequency (F, in Hertz) used:

$$P = 503\sqrt{\frac{Rho_{ap}}{F}}$$

This method cannot be used near electric power lines (EPLs), since the anomalies they cause may mask the geological ones, as shown in Fig. 2.10, where we can see natural anomalies caused by caverns and karst channels and the ones caused by EPLs.

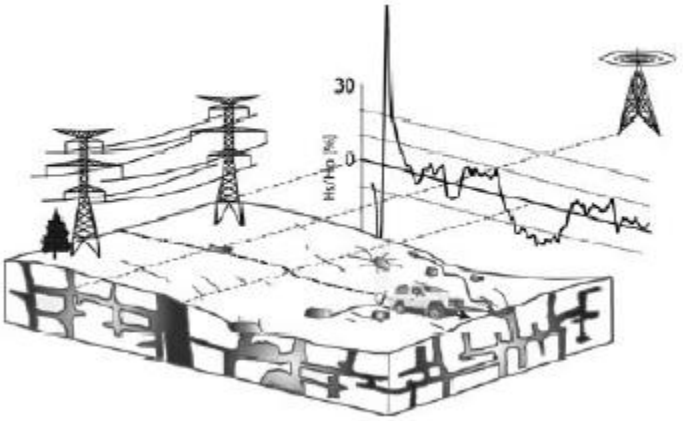

Fig. 2.10 – RF-EM results expressed a ratio [in %] between primary field (Hp) and secondary field (Hs), caused by natural (karst system) and artificial anomalies – after Carvalho Dill et al, 2009.

About 41 kilometers of profiles were conducted with the self-oriented antenna mounted on a jeep in March 2012. The profiles direction (Fig. 2.11) was conditioned by the existent roads. Unfortunately, due to EPLs and electric cables, natural anomalies didn't come out very often.

Fig. 2.11 – RF-EM Profiles (~41 km) conducted at Olhos de Água region, Aldeia das Açoteias and surroundings. ©Google 2014.

In profiles 3 (Fig. 2.12) and 7 (Fig. 2.13) important anomalies were detected. Both profiles are located in two of the areas identified as dolines subsidence areas (Fig. 2.7 (left) and Fig. 2.14).

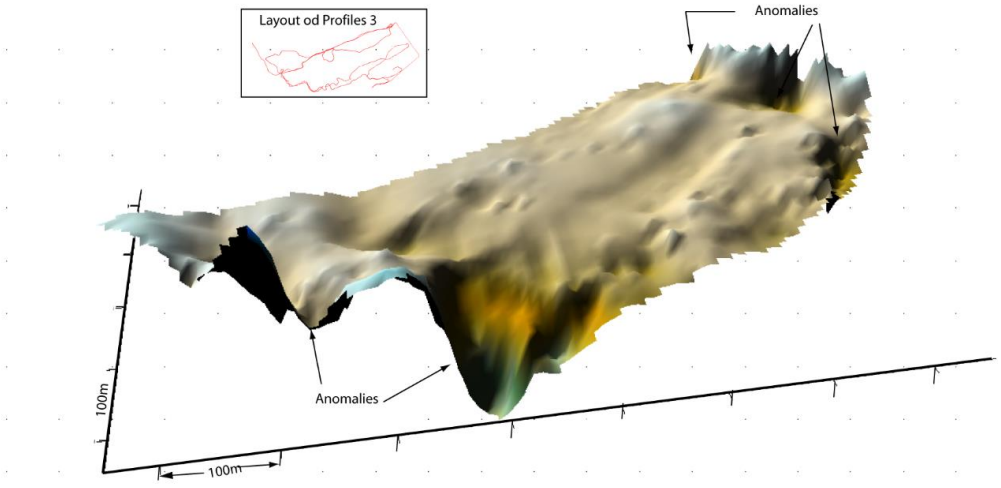

Fig. 2.12- Outphase 3-D anomalies due to fracturing (Profiles 3), which in turn is causing cliffs erosion and retreating and are also related to the interception of the Olhos de Água fault in an area where subsidence dolines ocours – see also Profiles 3 location at Fig. 2.11.

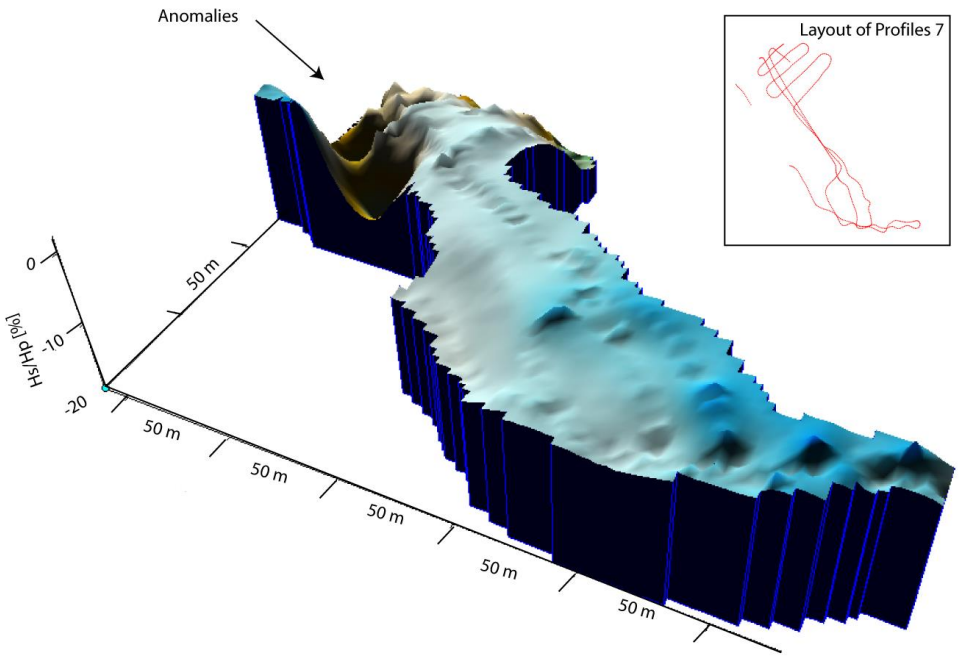

Fig. 2.13 - Anomalies related with the existence of subsidence dolines in Profiles 7. The 3D surface was obtained by the Outphase interpolation obtained in parallel and transversal profiles. [see profiles locations at Fig. 2.11.]

NE-SW and NW-SE regional joints directions that control, for instance, the setting of a river bed (V lines, yellow in Fig. 2.14) and the final set of the Quarteira Stream are possible to observe in Fig. 2.14. NW-SE direction is the same as S. Marcos-Quarteira Fault. Joints directions are also visible in offshore linements.

Another linement can be defined, with the same NW-SE joint direction, between anomalies detected in profiles 3 and 7 and respective direction and several areas identified with subsidence dolines that may indicate one of the preferential groundwater flowpaths towards Quarteira Stream (Fig. 2.14). This linement is located over an area where underground karstification and/or evaporite dissolution are very active, being part in one of the areas that are nowadays in subsidence, that are mapped and described in the next section.

In addition, the Olhos de Água fault is intersected in profiles 3 (Fig. 2.12 and 2.14), in the ending section mapped eastwards. In profiles 7 (Fig. 2.13 and 2.14) there is not any mapped accident, although its existence is not impossible.

Fig. 2.14 - Overview of the joints direction (yellow), subsidence dolines areas (green contour) and present subsidence area (orange line) in the aquifer system (pink contour). Profiles 3 and 7 – light blue lines. Main faults – black lines. ©Google 2014.

2.2.2 Pangeo data

The spatial distribution of the subsidence areas was crossed with Pangeo Project data (http://www.pangeoproject.eu/).

PanGeo (Enabling Access to Geological Information in Support of GMES) is an EC Project of the Seventh Framework Program. It is a 3-year Collaborative project, started on 1 February 2011, that has the objective of enabling free and open access to geohazard information in support of the program Copernicus (former GMES - Global Monitoring for Environment and Security), based on the collection of environmental data via satellites (space component, in charge of the European Space Agency ESA) and *in situ* (in charge of the European Environment Agency EEA) (http://copernicus.eu/). The goal of PanGeo will be achieved by providing an INSPIRE-compliant, free, online geohazard information service for 52 of the most populated towns in Europe, covering approximately 13% of the EC citizens.

The geohazard information has been made accessible in a standard format by the 27 EU national Geological Surveys by means of a modified version of the “shared access” infrastructure devised for One-Geology Europe, as well as via Google Earth™. The information to be served (a new ground stability data-layer and accompanying interpretation) has been made by each Geological Survey, and compiled from the integration of Satellite Persistent Scatterer InSAR processing (providing measurements of terrain-motion), geological and geohazard information, already held by national Geological Surveys (together with their expertise), the exposure data contained within the GMES Land Theme’s Urban Atlas (1:10,000, 20-class, landcover data).

Permanenent Scatterer Interferometry (PSI) is a radar-based remote-sensing technique to measure and monitor land deformation from space borne synthetic aperture radar (SAR) imagery.

In particular, the technique denominated SAR interferometry (InSAR), computes the interference pattern caused by the phase difference between two SAR images acquired at different times with slightly different look angles, giving a measurement of the ground deformation projected along the satellite line of sight (LOS) with millimeter accuracy and high spatial resolution.(Gabriel et al, 1989; Burgmann et al., 2000; Massonnet & Feigl, 1998).

Its intrinsic limits due to temporal and geometric decorrelations can be partly overcome by the joint exploitation of large groups of SAR images, allowing the detection of sub-millimetric movements of the ground at locations characterized by stability of the radar backscattering. This procedure, first developed by Ferretti et al. (2000, 2001), is referred to as Permanent Scatterers Interferometry (PSInSAR).

This is an operational tool for precise ground deformation mapping on a sparse grid of phase stable radar targets (the so-called Permanent Scatterers, PS), acting as a “natural” geodetic network. The application of PSInSAR to detect and monitor surface deformations has advanced rapidly during the last decade, and it is now routinely applied to a wide range of natural hazards: landslides, natural subsidence and subsidence induced by urbanization, land surface deformation due to ground water abstraction or seasonal groundwater fluctuation, tectonic or salt motions, etc.

This technique has been applied through the Pangeo Project over the Albufeira to Olhão area of the Algarve region.

PSI data were obtained either from ERS or ENVISAT satellites. From ERS, 44 images were used spanning the timeline from 13-06-1995 to 28-11-2000, approximately 5.5 years. From

ENVISAT, 21 images were processed covering the timeline from 11-05-2003 to 20-12-2009, approximately 6.5 years.

The density of the PS is of 57 PS/km^2 in ERS data and 38 PS/km^2 in ENVISAT data, which results in a sparse coverage outside the main localities, especially in vegetated or agricultural areas. This fact is more evident in the case of the ENVISAT data.

The ground deformation measurements are given in mm/year. These velocities are projected in a color scale, where the red to orange points correspond to subsidence, the green to stable areas and the blue to uplift zones, in the periods of time considered for each satelite.

Crossing data results led to the following remarks (see Fig. 2.15):

- In the already collapsed areas (green light polygons), there is no visible register of movement, except for the area among Roja Pé, Aldeia das Açoteias and Várzea de Quarteira (A), that although with depressions, is still in subsidence with a -1 to -1,99 mm/year rate.
- Extention following a linement towards NW-SE (B) of a mapped fault in the coastal cliff by Terrinha (1998).
- The subsidence areas probably related with salt/gypsum/limestone dissolution and/or salt movement are:
    - Patã de Baixo (C), with -1 to -1,99 mm/year rate);
    - E of Pedreira do Escarpão (D), with -1 to -2,99 mm/year rate;
    - Torre da Mosqueira-Fontainhas (E) , with -1 to -2,99 mm/year rate;
    - Ferreiras-Caliços (F), with -1 to -1,99 mm/year rate);
- The uplift areas with a frequent 1-2 mm/year rate are registered. They are probably related with diapirism, namely:
    - E of Patã de Cima (G), with 1-2 mm/year rate;
    - between Patã de Cima and Pinhal (H), with 1-3 mm/year rate;
    - southern of Vale de Serves (I), with 1-3 mm/year rate;
    - between Brejos and Mosqueira (J), with 1-2 mm/year rate;
    - between Vale de Navio and Val da Azinheira (L), with 1-2 mm/year rate;
    - among Branqueira, Torre da Medronheira and Olhos de Água (M), with 1-2 mm/year rate.

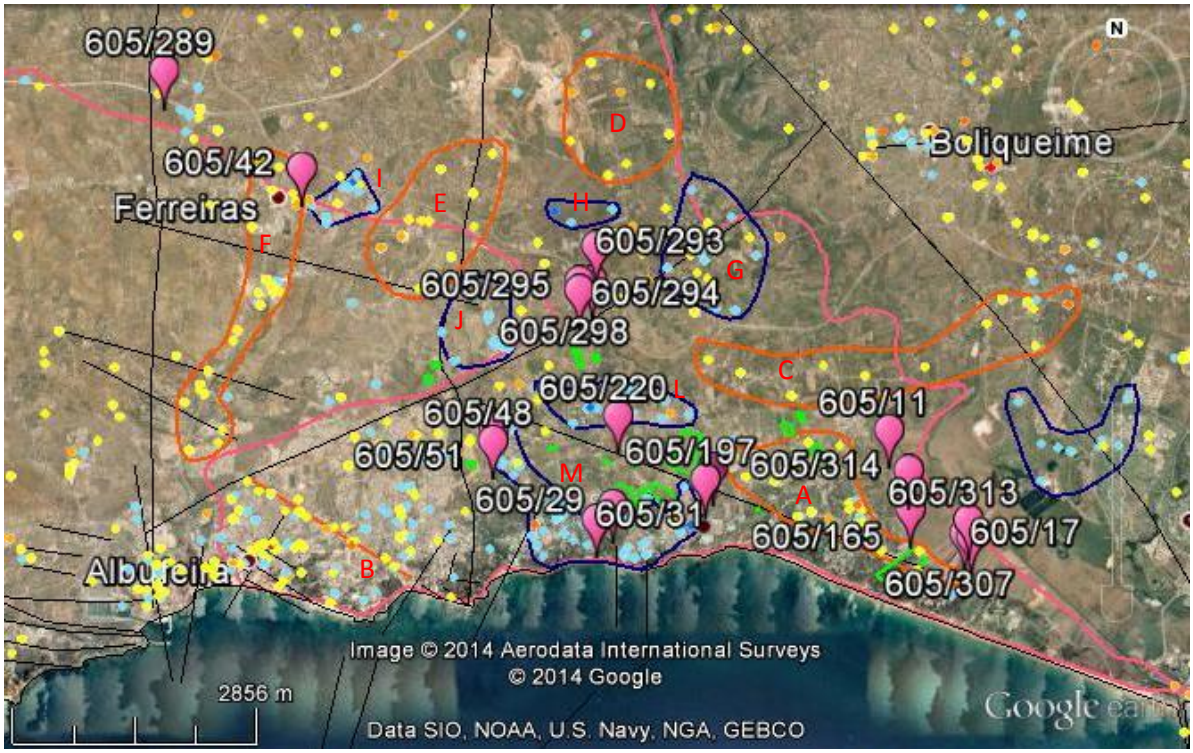

Fig. 2.15 – Uplift (blue) and subsidence (orange) mapped areas. Pangeo data: Yellow and orange points related to subsidence; light and dark blue related to uplift. Pink drops: groundwater with high concentrations of SO_4, Ca, Mg, Na, Cl. Black lines: main faults. Light green polygons: collapsed mapped areas. Pink contour: Aquifer system. ©Google 2014.

There are evidences of high concentrations of sulfates, calcium, magnesium, sodium and chlorides in groundwater chemical analysis (pink drops Fig. 2.15) pointing out to the existence of evaporites in depth, without surface cartographic expression (Almeida at al., 2000). Most of these waters were sampled in boreholes located nearby faults.

In the Vale de Navio geoelectrical profile (B5 in Fig. 2.22), that crosses the Olhos de Água fault, there is a deep very low electrical resistive formation, compatible with the existence of salt and/or salt water. A similar situation occurs in profiles A1 and A2, (Fig. 2.20). It is still important to highlight that in the profile A2, intersecting the Oura fault, the uplift that is observed E of the fault is in line with Pangeo data. Moreover, in Montechoro area, while drilling a borehole, salt was extracted (Almeida, oral information).

Indeed, the pelite evaporite Silves Complex of Hetangian age is the origin of salt/gypsum that is injected in many faults of the Algarve region. While moving, the salt behaves as a viscous fluid, creating uplifts in the areas where its displacement takes place. It also creates

subsidence due to the void space created when it moves and due its ability to dissolve in groundwater.

Pinhal boreholes (ref. 605/293, 605/294, 605/295, 605/298, see Fig. 2.15) are located next to the Mosqueira reverse fault and also in the center of 4 uplift areas. These groundwaters indicate evaporite dissolution. Similar situation occurs in the Balaia (ref, 605/48, 605/51), Torre da Medronheira (ref. 605/29) and Olhos de Água (ref. 605/197, 605/199) boreholes, located in one of the uplift areas (M, see Fig. 2.15).

The pattern defined by these 5 areas resembling a salt dome surrounded by subsidence areas. Although the subsidence caused by the endokarst evolution is important in the aquifer system, the subsidence due to the salt movement and dissolution should be more important.

Salt movement is conditioned by tectonics. The recognized neotectonic activity is marked by a regional uplift and by mesoscopic faults with an inverse movement component and variable orientations, indicating the action of a compressive stress field, generating a constritive regional finite deformation in the last 2 to 3 My. This evolution can be explained within the interaction context of the involved lithospheric plates, namely the convergence in NW-SE direction, between Iberia and Africa, a rate of about 4 mm/y in the Gorringe-Gibraltar sector, and the convergence Atlantic-Iberia induced at W by means of this interaction (Ribeiro, 2002), overlayed by the propagation towards W of the accrecionary prism of the Gibraltar Arch (Gutscher et al, 2002; Gutscher, 2004). Relatively low deformation (0.02-0.04 mm/year) inferred in the emerse territory suggest that interplated deformation is distributed through numerous structures, most of them located offshore (Terrinha et al., 2013).

Weinberger et al. (2006) shows that the uplift rate of Mount Sedom salt diapir (Dead Sea Rift, Israel) varies from 5.5 mm/yr to 8.3 mm/yr and the current strain rate is about 9×10^{-13} s^{-1}. Typical pre-emergent diapirs in the US Gulf Coast and Germany show uplift rates of 0.2 mm/yr and 0.1–0.5 mm/yr, respectively (Jackson and Talbot, 1986; Jartiz, 1987, in Weinberger et al. (2006)). Bruthans et al. (2010) show for Namakdan diapir (Persian Gulf, Iran) an uplift rate of ~4 mm/yr, constant for the last 50 Kyr, and for host rocks an uplift rate of 0.4-0.6 mm/yr, which is 2-3 times greater than regional uplift rate. In Algarve, the Loulé diapir has an uplift rate of 0.08 mm/yr, not detected by InSAR and appears as a stable zone in Pangeo data.

Regarding the geodynamic context of the eventual Pinhal-Olhos de Água saline dome compared with other world diapir uplift contexts, an 1-2 mm/yr uplift rate seems plausible,

although 2-3 times greater than onshore deformation. More research in this domain is still needed.

2.3 Hydrodynamics and freshwater–saltwater interface

Hydraulic heads and regional static piezometric surface

The objective of the piezometric analysis was not to obtain a regional piezometric surface *per se*, but to highlight high and low hydraulic gradient areas to detect hydraulic barriers, preferential flow zones and other relevant hydrogeological features. The retrieval of a reliable static piezometric surface requires the availability of a good spatial distribution of boreholes and measurements made during a short period with same hydrological conditions. Although a high boreholes density was available in the ARQ CA, most of them are under exploration and equipped with pumps, which does not allow us to use a dipper (high risk of blocking the dipper's tape with the pump's cables). Hydraulic heads measurements were only possible in 22 boreholes equipped with dip tube and belonging to the Albufeira municipality (CMA). Hydraulic heads were also available from 69 boreholes belonging to the monitoring program of the Portuguese Water Institute (INAG, snirh.pt). We thus compiled the historical data from INAG and CMA archives to obtain the final hydraulic heads dataset composed by records from March 1978 to December 2013 of 91 boreholes. Note that the piezometric measurements in the CMA boreholes were made after being deactivated, i.e. from 2001. They thus correspond to the static piezometric level.

The maximum number of concomitant hydraulic heads was only 29 (8 of them inside the ARQ area). We thus elaborated the static piezometric surface using the lowest hydraulic head at each of the 91 boreholes to retrieve the regional piezometric surface. We assumed that the lowest hydraulic head is the most reliable value in absence of pumping because the recession part of the well hydrograph follows an exponential decay that is asymptotic towards the local base level (Dingman, 2002). After selecting the lowest hydraulic heads, we interpolated it using simple kriging.

Analytical models of the freshwater–saltwater interface

The Dupuit-Ghijben-Herzberg model (Dingman, 2002; Fetter, 2001) allow to compute the position of the freshwater–saltwater interface (FSWI) under the assumptions of sharp interface and 1D flow in a homogeneous unconfined coastal aquifer, as following:

$$z = \sqrt{2xq_tG/K} \quad (1)$$

Where*z* is the depth of the interface below sea level, *x* is the distance inland from the coast, q_t is the groundwater discharge at the coastline per unit width, *G* is equal to $\rho_w/(\rho_s - \rho_w) \simeq 40$, with ρ_w and ρ_s density of fresh and salt water respectively, and *K* is hydraulic conductivity.

However in this model the FSWI intercepts the water table at the coastline, which doesn't correspond to the real situation. The Glover model (Dingman, 2002; Fetter, 2001) considers an outflow face of freshwater discharge into the sea as following:

$$Z = \sqrt{2xq_tG/K + {q_t}^2G^2/K^2} \quad (2)$$

$$x_0 = -q_tG/2K \quad (3)$$

$$h = \sqrt{2xq_t/GK} \quad (4)$$

where x_0 is the width of the outflow face and *h* is the height of the water table above sea level.

2.3.1 Results

2.3.1.1 Regional static piezometric surface

The regional static piezometric surface obtained by interpolation of the lowest hydraulic heads of 91 boreholes is shown in Fig. 2.16. The depth of most of these boreholes is unknown. However, from the analysis of the borehole with logs (Figs. 2.1 and 2.2), we observed that boreholes screen the shallowest aquifer and are connected with only one aquifer.

The regional static piezometric surface (Fig. 2.16) highlighted the limits of the ARQ aquifer and its compartments. It confirms the north limit that is marked by a clear contrast between high hydraulic heads in ARQ and low hydraulic heads in Querença-Silves aquifer (respectively M5 and M6 aquifers in Fig.1.1). The east boundary is also confirmed since the computed equipotential lines are parallel to the Quarteira streamwhen boreholes are available at the both side of the river. The west boundary is also strongly marked by a strong contrast of hydraulic heads between ARQ and Ferragudo – Albufeira aquifer (M4). A clear distinction can also be made between the hydraulic heads in the Jurassic and the Miocene

formations inside the ARQ, showing clearly that these two aquifers are not fully hydraulically connected. The general flow direction is towards South in the Miocene aquifer while it is south and SE in the Jurassic aquifer. Note that the increase of hydraulic heads between Oura and Albufeira, i.e. in an area of Miocene outcrops, seems to be an artifact because no boreholes are available in this area. At north of this sector, the hydraulic heads in the Cretaceous outcrops are in continuity with the one of the Jurassic formations. This fact is supported by the hydraulic heads of 3 boreholes located in the Cretaceous outcrops. Although the depth of these boreholes is unknown, it is very probable that they are implemented in the Jurassic aquifer, which means that the Jurassic aquifer extends towards the sea below the Cretaceous and the Miocene formations.

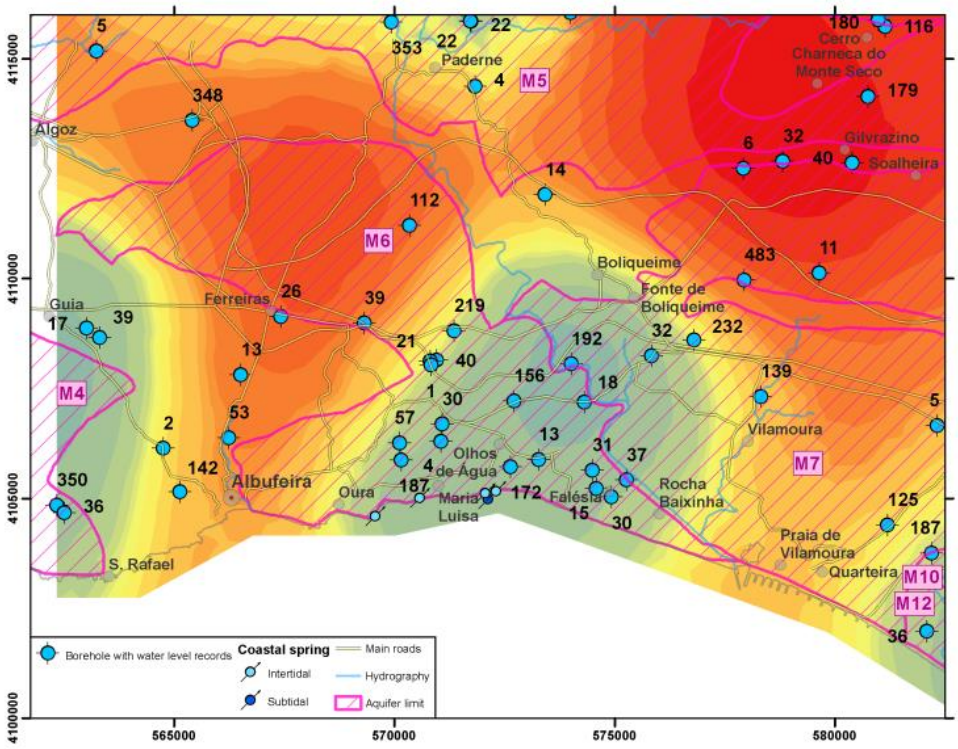

Fig. 2.16 – Regional static piezometric surface retrieved using the lowest hydraulic head of each borehole (black label next to the borehole symbol indicates the number of values). Red colors indicate high hydraulic heads, blue colors indicate low hydraulic heads.

2.3.1.2 Analytical models

The analytical models were applied using the collected information of the aquifer system, i.e. hydraulic conductivity of 1 and 5 $m.d^{-1}$ (minimum and intermediate values) and recharge of 23800 $m^3.d^{-1}$. We tested the impact of low and high recharge by applying a multiplier factor *n* with value of 0.5, 1.0 and 2.0.

The application of the analytical models (Fig. 2.17) shows that:

- the width of the outflow interface (x_0) varies from 119 m to 6 m, while the depth of the FSWI at coast line varies between 238.0 and 11.9 m. Subtidal springs were indeed observed during diving at ~120m from the coast (Fig.1.1).
- high recharge and low K, as they increase the hydraulic gradient, provokes wider outflow face as well as deeper and steeper FSWI.
- the interface inclination is smooth for the intermediate case (i.e. K = 5, n = 1). At 200 m from the coast line towards inland, the FSWI is only 100 m deep. With the lowest recharge (n = 0.2), the depth is 100 m at 400 m of the coast and 150 m at 1 km. Note that with the maximum K (100 $m.day^{-1}$), the Glover model indicate much shallower FSWI (plot not shown here).

Although these facts indicate a high risk of upconing since boreholes in the ARQ area reach the depth of the modelled FSWI, the real hydrogeological settings (high heterogeneities with spatially variable *K*, karstification and confining units) are much more complex that the one assumed in the model. Nevertheless, the Glover model gives a valuable information about the FSWI position and its dynamic.

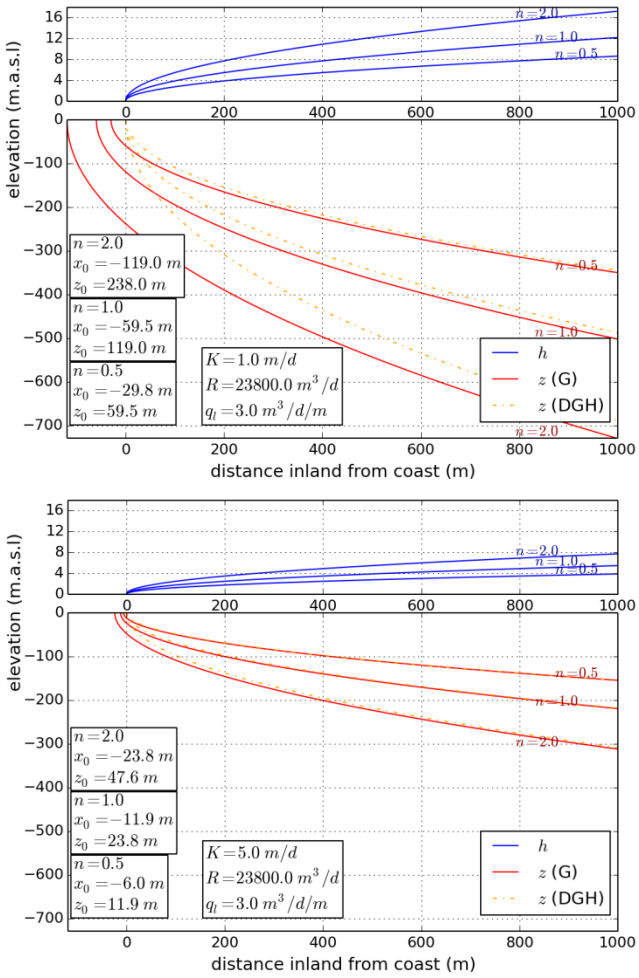

Fig.2.17 – Analytical model of the freshwater-saltwater interface (note the difference of vertical scale above and below sea water level). G: Glover model; GDH: Dupuit-Ghyben-Herzberg model; z0: depth of the interface at the coast line; n: recharge multiplier. See text for other abbreviations.

2.3.1.3 Aquifer tests based on tidal effect

The effect of tidal sinusoidal movement on the piezometric level in this costal aquifer was studied by Razack et al (1980) and now in a borehole near Quarteira stream (Long. - 8° 9' 10.62"; Lat. 37° 5' 31.34").

By comparing both sinusoidal curves (see Fig. 2.18) and knowing the distance to shoreline it is possible to calculate hydraulic diffusivity of the aquifer based on:

a) Delay time (φ) between experimental curve and theoretical tide curve;

b) Relation between tide amplitude and piezometric amplitude.

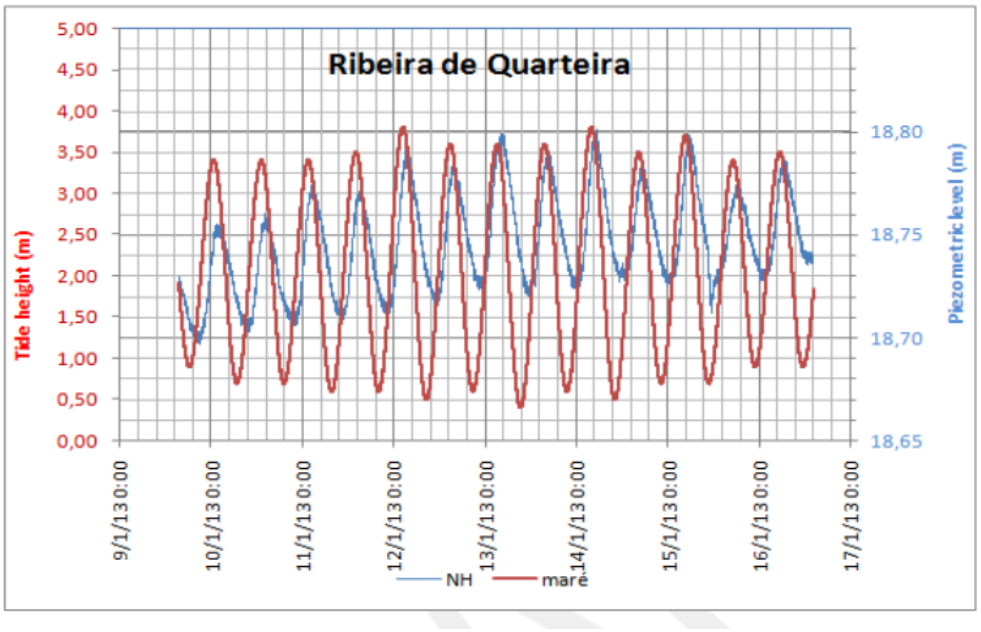

Fig. 2.18 – Theoretical tide curve and piezometric curve observed in Ribeira de Quarteira borehole.

The lag time calculated by linear regression, as proposed by Costa (2013), was 1,5 hour. Other parameters calculated are presented on column 1 of table X, where the other four columns shows results obtained by Razack et al. (1980) in other boreholes of this aquifer.

The interpretation of this test leads to the following conclusions:

- The aquifer is semi-infinite, meaning that it discharges to the sea in the area;
- The aquifer is semi-confined, with significant leakage, since ρ=2,2 (so very different from 1);
- The hydraulic diffusivity is 13,6 x 106 m/dia.

These conclusions seem to agree, in general, with Razack et al. (1980) concerning the conceptual model of this aquifer and its high heterogeneity. Nevertheless, the highest value of hydraulic diffusivity was now obtained in the east sector of this aquifer, where lower values also exists. This confirms that this aquifer is very heterogeneous concerning transmissivity and leakage.

Piezometer	Ribeira de Quarteira	Penta	Monte Choro	JK2	Poço Velho
ρ	2,21	1,40	1,1261	1,2784	2,8029
x0 (m)	1100,0	252,3	848	392,8	625,1
B (m)	712,2	209,6	1.224,40	388,6	224,8
B/x0	0,65	0,83	1,444	0,989	0,359
D (m^2/hr.)	564894	15650	176500	37800	95800
h (cm)	5,2	13	7,5	16,5	12,5
φ (hr.)	1,5	1,5	3,2	1,5	0,5

Table 2.1 – Aquifer tests based on tidal effect: comparison between calculated parameters for Ribeira de Quarteira borehole (column 1) and results obtained by Razack et al. (1980) in other boreholes of this aquifer (columns 2 to 5).

Another similar test was made in a borehole called Sesmarias, north of Albufeira (Long. -8° 17' 48.44"; Lat. 37° 5' 10.67"). The hydraulic diffusivity was higher, but this borehole is related with Jurassic limestone and not with the Miocene Albufeira aquifer.

2.4 Hydrogeophysics

As there are still uncertainties in the ARQ conceptual model, we applied hydrogeophysic methods to contribute to review and hypothetically upgrade the ARQ geometry, boundary and structure, including hydraulic relationships between the hydrogeological formations. The geophysical methods we used consisted on: (i) 1D time domain electromagnetics (TDEM); (ii) quasi-2D frequency domain electromagnetics (FDEM); (iii) 2D continuous vertical electrical soundings (CVES).

2.4.1 Field surveys

Time domain electromagnetics

We used a TEM-FAST 48 from Applied Electromagnetic Research (AEMR) company with square loop of 25 or 50 m side (1 turn) in coincident loop configuration with an input current

of 24 V and 4 A. A minimum of 3 curves at each site was acquired to confirm the repeatability of the measurement and the absence of EM noise induced by galvanic and/or capacitive coupling (Danielsen et al., 2003). The data were inverted using the software TEM-RES v7 from AEMR. When necessary, noisy data were firstly removed. Afterwards, using automatic inversion and trial and error method, a theoretical curve was fitted on observed data. The criterion of selection of the final solution was based on the minimum number of layers for the same quality of fitting, as well as hydrogeological knowledge of the area completed by local observation or borehole logs and coherency with the other geophysical methods.

Frequency domain electromagnetics

We used an EM-34 from Geonics instrument. The Geonics EM-34 device allows conducting a fast mapping of the lateral geolectrical variability of the subsurface, being particularly suitable to map saline intrusions (McNeill, 1980). It is composed by a transmitter coil Tx and a receiver coil Rx located at a predefined distance from Tx. This method is extremely easy and fast to use in the field and requires a minimum of 2 operators, one at each coil. During the data acquisition operations, special care must be taken regarding possible electrical interferences (industrial noise, transport lines of 50/60 Hz or even atmospheric noise).

At each measurement point, we obtained a vertical sounding with the 6 possible configurations, i.e. horizontal and vertical dipoles with cable spacings of 10, 20 and 40 m, allowing to reach investigation depths between 7.5 and 60.0 m. With several soundings along a line and applying a proper inversion algorithm, it is possible to obtain a subsurface 2D profile of the electrical resistivity variation. In this study, geoelectrical 2D modeling was conducted using the algorithm EM34-2D, which applies a 1D laterally constrained method (Santos, 2004). The obtained profiles allow to visualize a model of the vertical distribution of electrical conductivities. The inverse problem is solved using a smooth inversion, where each 1D conductivity model, obtained beneath each measurement site, is constrained by its neighbors.

Geoelectrical

CVES were acquired in the field using an IRIS Syscal pro and an ABEM Terrameter SAS-4000. The former was configured with 4 cables 90 m long and a total of 72 electrodes, the latter with 4 cables 100m long and a total of 64 electrodes. We used several arrays such as schlumberger, wenner and dipole-dipole. We also used a Scintrex TSQ-3 device with 18 electrodes in dipole-dipole array with 1350 m length to detect large geological structures. Inversions were performed using RES2DINV v3.53, generally using model refinement and

robust inversion. Bad datum points and points with RMSE > 60 or 80 % were removed from the inversion.

2.4.2 Results

Based on the previous analysis, we detected the following questions in relation to the current ARQ limits and structure:

- Is the Cretaceous present between the Miocene and Jurassic aquifers?
- Is the Cretaceous stripe outcropping between the Jurassic and the Miocene in the central west part of the aquifer, i.e. between Ferreiras and Albufeira, a hydraulic barrier or just aquitard semi-confining the Jurassic aquifer?
- What is the shape and position of the FWSI, and its spatial variation along the coast?
- How can we explain the concentration of the SGD, namely at Olhos de Água?
- How deep is the piezometric surface between Oura and Albufeira?

These questions are relevant to setup a variable-density groundwater flow numerical model and may have strong implications in the computing of its resultant water balance. To check the hydrostratigraphy, hydraulic relationships, depth of the water table and detection of the freshwater–saltwater interface (FSWI), we performed hydrogeophysical surveys between January 2013 and December 2013 composed by 18 TDEM soundings, 3 FDEM profiles, 11 CVES profiles organized in 5 transects transversal and longitudinal to the main groundwater flow (A, B, C, D and E in Fig. 2.19). The methods were used to detect the position and slope of the FSWI by surveys on the coastal cliffs (TDEM, CVES), along the beach (CVES) and in profiles perpendicular to the coast (FDEM). TDEM and CVES were also used to detect the water bearings formations, as well as the Cretaceous aquitard below the Miocene aquifer. For this last purpose, 2 CVES were realized using the Scintrex equipment to detect in depth the geological contact. CVES method was also performed to detect karstic structure and fresh water springs on the beach due to its relatively high-resolution and cross-sectional characteristics. Note that the high urban development in the study area constrained the use of hydrogeophysics (lack of extension to deploy CVES cables, electromagnetic noise limiting the use of TDEM and FDEM) in areas that we considered important.

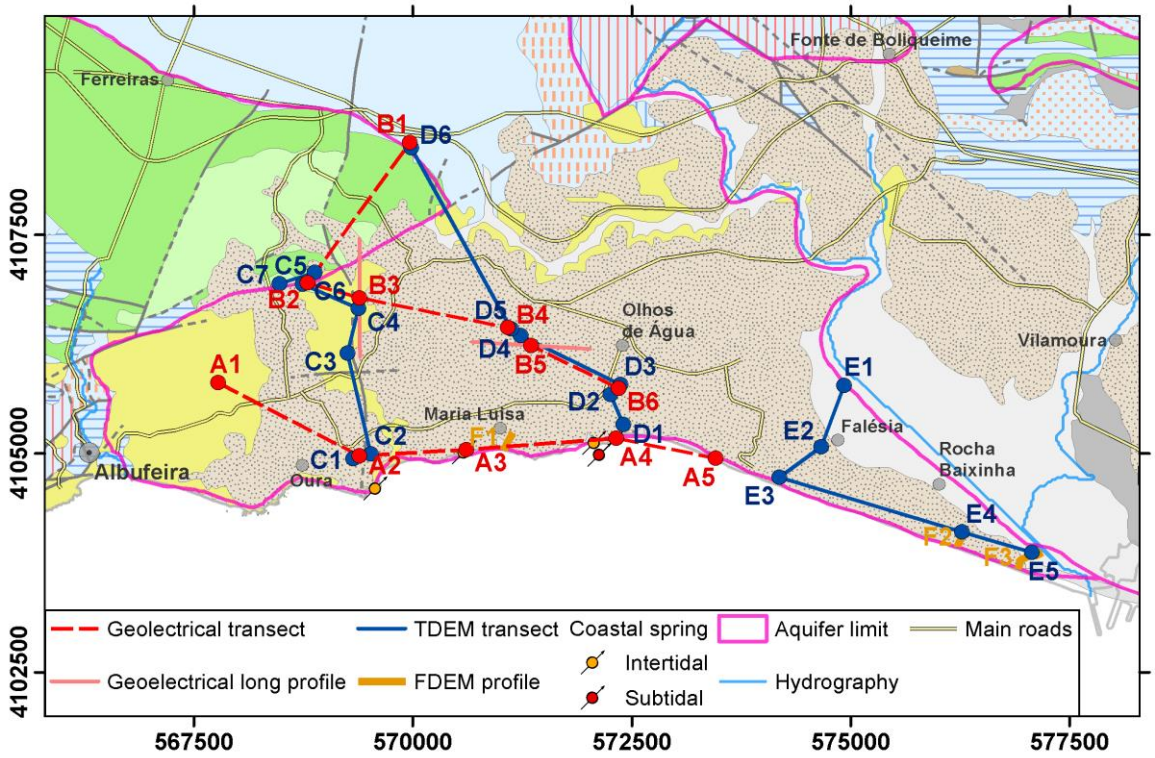

Fig.2.19 – Location of the hydrogeophysics surveys.

The CVES longitudinal transect A1 to A5 (Fig. 2.20) shows at A1 the water table at ~10m above sea level (m.a.s.l.). Above, it corresponds to unsaturated miocenic aquifer with resistivity between 75 and 200 ohm.m. The saturated zone shows a ~15 m thick layer of resistivity ~50 ohm.m above a layer of low resistivity (10ohm.m). As far as we know there is no clayey layer in the Lagos-Portimão formation, so we interpreted this result as fresh water above brackish-salt water. The saltwater is very shallow, i.e. -10 m.a.s.l., at ~1300 m from the coast. For comparison, the Glover model with highest K = 100 m.d-1 (plot not shown here) indicates the FWSI at ~-50 m.a.s.l. at this coastline distance. The shallow salt water observed in A1 CVES can be explained by two processes: (i) upconing; (ii) diapirism. Independently of the source of the salt water, the salinization is probably provoked by the large volumes of groundwater pumped by private boreholes belonging to the many Albufeira touristic installations (hotels and resorts). Indeed, the monitoring of the groundwater electrical conductivity in these private boreholes shows seasonal variations from 100 to 1000 µS.cm-1 (data gently provided by the Albufeira municipality).There is a slightly less resistive vertical structure at abscissa -80 that may be related to the extension of a W-E fault mapped eastwards.

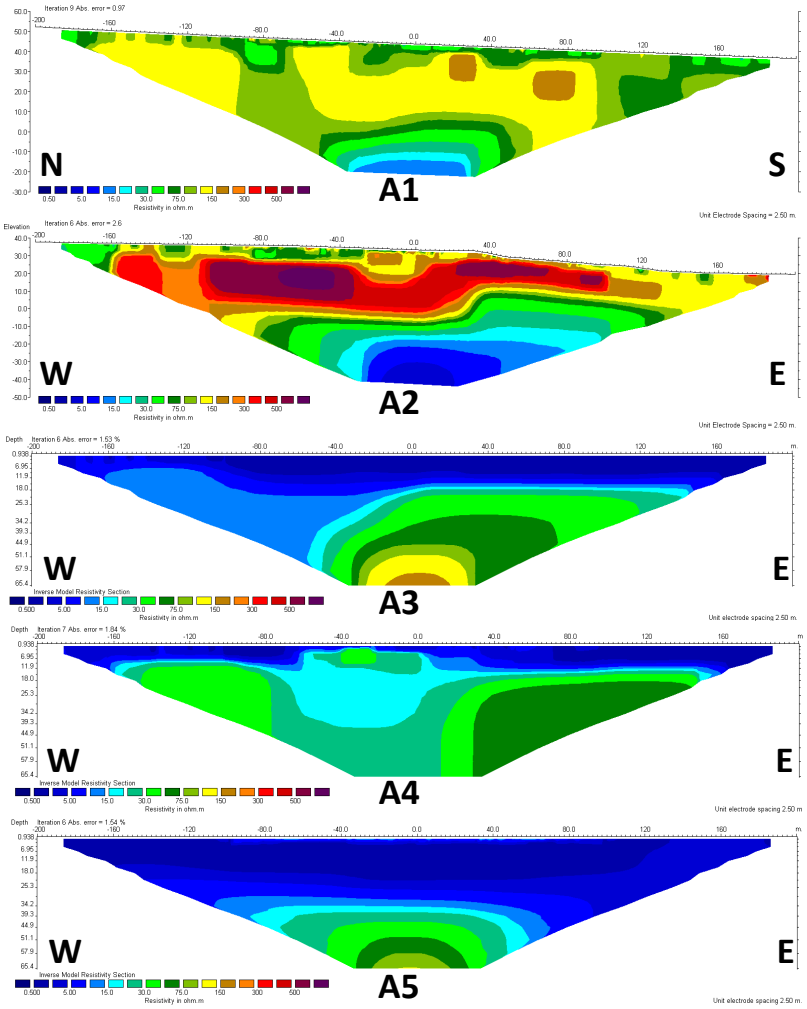

Fig.2.20 – Longitudinal transect A of geoelectrical profiles (see location in Fig. 2.19).

At site A2, located at ~400m from the coast, the highest resistive layer (100-700 ohm.m) corresponds to the Plio-Quaternary formations. Below, the ~50 ohm.m layer corresponds to saturated Miocene formations. As the Plio-Quaternary and the Miocene formations are outcropping on the nearby cliffs, we measure the elevation of this geological contact using a differential GPS. We found a very good agreement with the elevation obtained with the CVES. Moreover, the contact between the Plio-Quaternary and the Miocene formations shows an uplift on the right section of the CVES, i.e. between abscissa 30 and 100 m. The level change corresponds to the expression of the N-S Oura fault visible in Fig.1.1. The fact that the top of the saturated Miocene layer follows this uplift indicates that Miocene aquifer is confined by the Plio-Quaternary formations. The deepest layer is characterized by low resistivity (< 10 ohm.m) of saltwater, below a flat surface at -10m.a.s.l. Together with the

presence of an intertidal freshwater spring located E of the fault (Fig. 1.1), these settings are in agreement with the Glover model. West of the fault, the freshwater layer is very thin (~10m), which constitute a high risk of upconing. Indeed, the groundwater electrical conductivity measured from a private borehole located at the W edge of the CVES was between 2000 and 2500 µS/cm.

The beach CVES A3 to A5 present similar settings: low resistive layer (> 10 ohm.m) above a layer of resistivity ~20-100 ohm.m. The first layer corresponds to seawater in beach sands while the second to fresh groundwater in Miocene formations. This configuration is explained by coastal fringe processes, such as tidal dynamic and upper seawater recirculation zone (Werner et al., 2013). Karsts features, expressed by blocks of slightly different resistivity, are also visible on CVES A3 and A4. An intertidal freshwater discharge is visible at A4 between abscissa -60 and 0. Finally, the deepening of the top of the Miocene formation towards east is clearly visible from A4 to A5. However the Plio-Quaternary was expected between the sand beach and Miocene expression, but either it is not present or its resistive signature is similar to the sand beach, which is probable due to the presence of saturated clayey lithologies.

The FDEM profiles of Fig. 2.21 show at S formations with seawater, characterized by low resistivity (<15 ohm.m) and at N freshwater saturated formations with resistivity of ~30-50 ohm.m. At F1 the freshwater formations correspond to Miocene aquifer while at F2 and F3 they correspond to alluvium, dune and beach sands. The slope of the FSWI is clearly imaged, showing a steep inclination at F1 while at F2 and F3, located in the most oriental part of the AQR, the inclination is smooth. This geometry was expected and is in agreement with the Glover model, since the hydraulic heads are quite low in the oriental sector.

Below the Quarteira stream, at NE of the F3 profile, the ~30-50 ohm.m resistivity layer seems to indicate fresh groundwater. Above, the low resistivity layer indicates saltwater intrusion from the Quarteira stream inside the alluvium aquifer. This profile exemplifies the complex relationships between the Quarteira stream and the aquifers, with a temporal variation of influent and effluent characteristics at the same location.

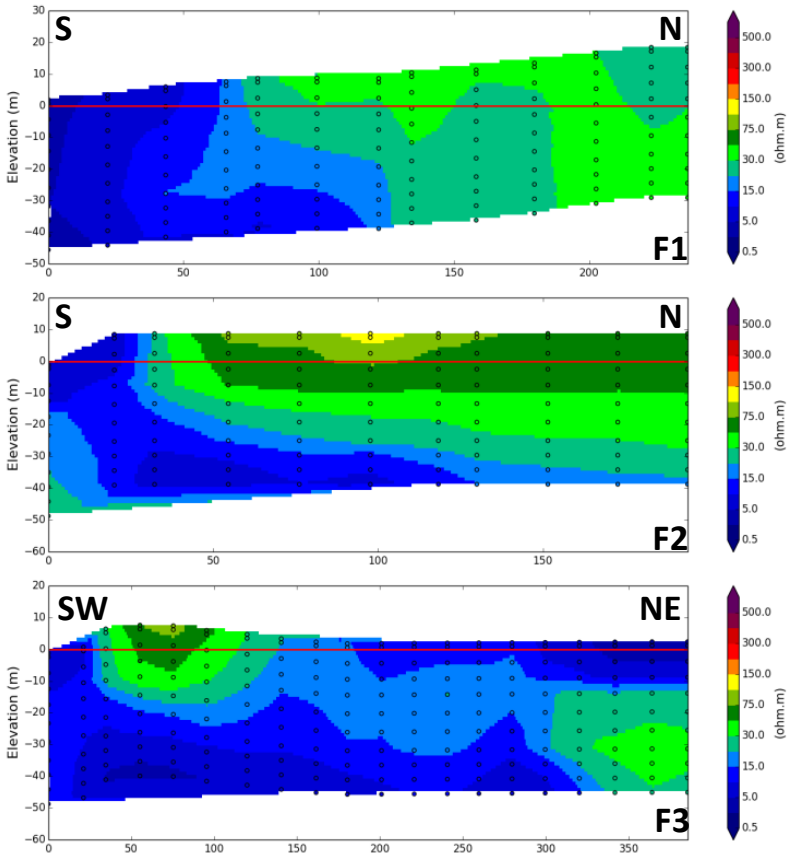

Fig. 2.21 – FDEM profiles (see location in Fig.2.19). These profiles show steep (F1) and smooth (F2 and F3) inclined freshwater-saltwater interface. All profiles were starting from the beach, located at South.

On transect B (Fig. 2.22, see location Fig. 2.19), B1 makes visible the contact diving towards S between Jurassic and Cretaceous formations (respectively resistivities of ~100-200 ohm.m and ~10-75 ohm.m). The Cretaceous formations have similar signature than saturated Miocene observed previously, although they show a larger range due to the presence of low resistive clayey/marly layers. At B2, almost made in Cretaceous formations, a fault diving towards NE, probably related with Mosqueira faults system, seems to separate a blocks of lower resistivity at S of 100 m abscissa. The long CVES B3, east of B2, identified clearly a vertical anisotropy between abscissa 525 and 565 m with resistivity ~150-200 ohm.m, corresponding to the interseption of Olhos de Água Fault. The Mosqueira fault is intercepted in the N part of the profile This reverse fault can explain the heterogeneous high resistivities pattern obtained in that area down to depths of about 140 m. Information from a borehole log located in Montechoro (Long. -08º 13' 18,157"; Lat. 37º 06' 07,621"), near the Oura fault, crossing Miocene and Jurassic formations, shows a strongly cemented carbonate fault

breccia below 113 m depth till the end. Similar rocks can be responsible for the high resistivity values detected in the profiles where faults interception occurs. The interpretation is difficult since the Plio-Quaternary is covering the underlain geological formations. The water table was measured at 5m.a.s.l in an abandoned borehole south of the B2 CVES. However, due to the coarse resolution, it is uncertain to recognize the water table on the B2 CVES. At B4, the interpretation is supported by a municipality's borehole 187 m deep. The surficial ~15m thick, resistive layer (~100-200 ohm.m) corresponds to Plio-Quaternary formations. Below, the Miocene formations show resistivity between 30 and 100 ohm.m. The water level measured in the borehole was -5m.a.s.l. but is not visible in the CVES profile, although a slight resistivity increase is observed below this depth. The long dipole-dipole B5 CVES represents better the geological layering despite the intersection of the Olhos de Água fault with resistivity of 100-200 ohm.m in the middle of the profile. The borehole logs shows, below a Plio-Quaternary layer 26m thick, typical Miocene lithology from 16 to -54 m.a.s.l., that we relate to the B5 horizontal stripe between 0 and -80 m, and marly limestones between -54 and -97m.a.s.l., probably Cretaceous, that we related to the low resistivity below -80 m.The very low electrical resistivity values of 0-5 ohm.m may be related to salt injection along faults, which is a common situation in the Algarve region due to diapiric tectonic. Between 97 and 146 m deep (bottom of the borehole), the log described grey and reddish hard limestones that may correspond to the Jurassic formations.

The differences in elevation between the borehole and the inverted resistivity profiles are due to the coarse resolution of the geoelectrical acquisition array (75m inter-electrode distance). Finally, B6, located ~1km to ~600 m from the coast and A4, show ~20 m of Plio-Quaternary (resistivity of 150-700 ohm.m) on top of Miocene formations (resistivity of 50-100 ohm.m). As in A2, the Miocene is probably confined. At abscissa 20 the Olhos de Água fault is intercepted.

The TDEM C2, D1, D2, D3, close to coast shore (Fig. 2.23), show low resistivity at their last layer, which depth increase from coast to inland. This contrast seems to indicate the FSWI. Above, the layer with resistivity between 20 and 75 ohm.m indicates the Miocene aquifer, in agreement with the CVES. The upper resistive layer (> 150 ohm.m) indicates the Plio-Quaternary unit. More inland, one can identify a low resistivity layer at C3, C4 and D5 (distance of ~2000 m from the coast) as well as in C7 (> 3000 m from the coast).

This low resistivity at a far distance from the coast, as observed in CVES profile A1, may correspond to groundwater salinization due to upconing and/or diapirism. Finally, the E profile indicates similar information as CVES A3 to A5. The low resistivity observed at E1

(~15-20 ohm.m) seems to indicate that the Quarteira streamis influent in the alluvium aquifer and causess groundwater salinization. E2 gives information that may help to interpret the CVES A5.

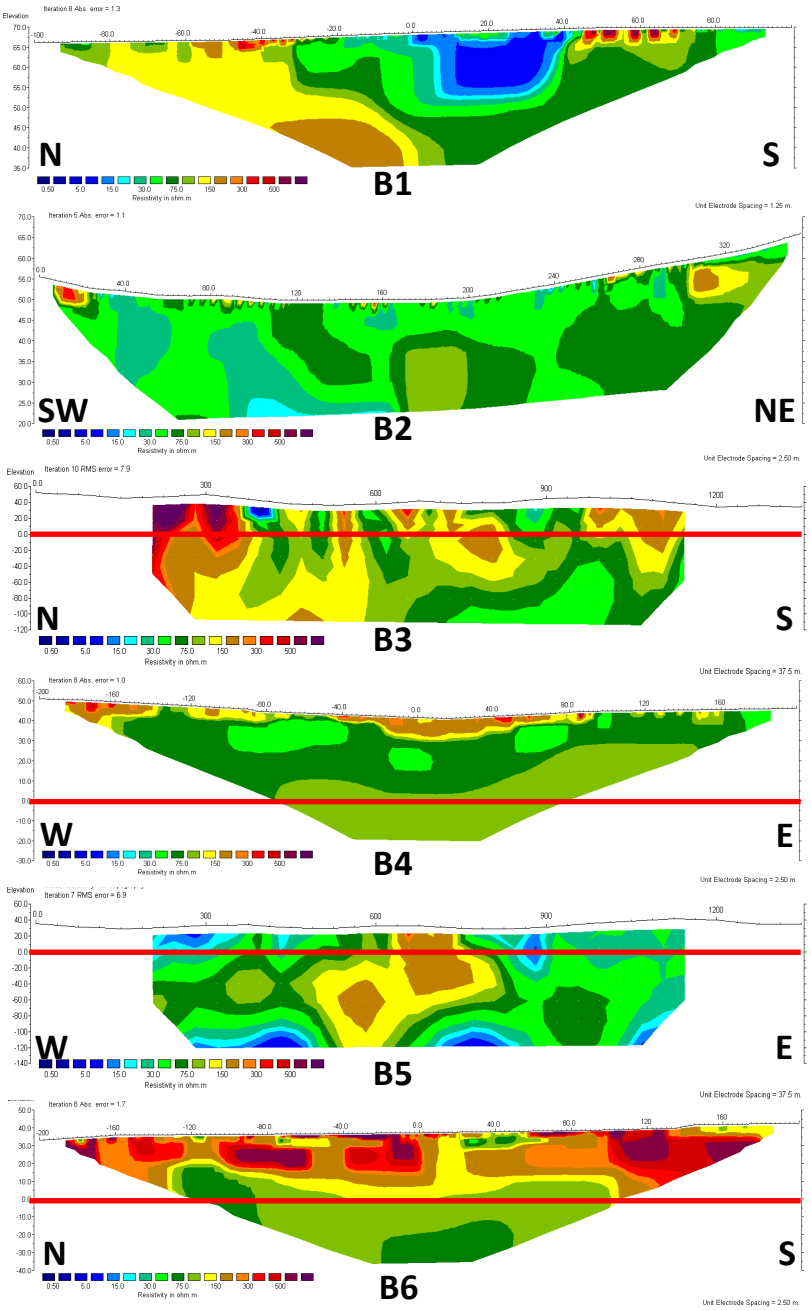

Fig.2.22 – Transversal transect B of geoelectrical profiles (see location in 2.16). Note that profiles B3 and B5 were ~1400 m long, reaching a depth of ~120 m, while the other ones were ~400 m long or less. Red line – 0 m.

Below a high resistive layer (>500 ohm.m) corresponding to unsaturated Plio-Quaternary observed on the cliff, a thin layer appears with very low resistivity, being above a layer with resistivity of ~30-50 ohm.m. The last one corresponds to fresh groundwater in the buried, confined Miocene aquifer, while the latter corresponds to saturated Plio-Quaternary that, due to its high clay content, shows very low resistivity similar to the resistivity of seawater saturated beach sand.

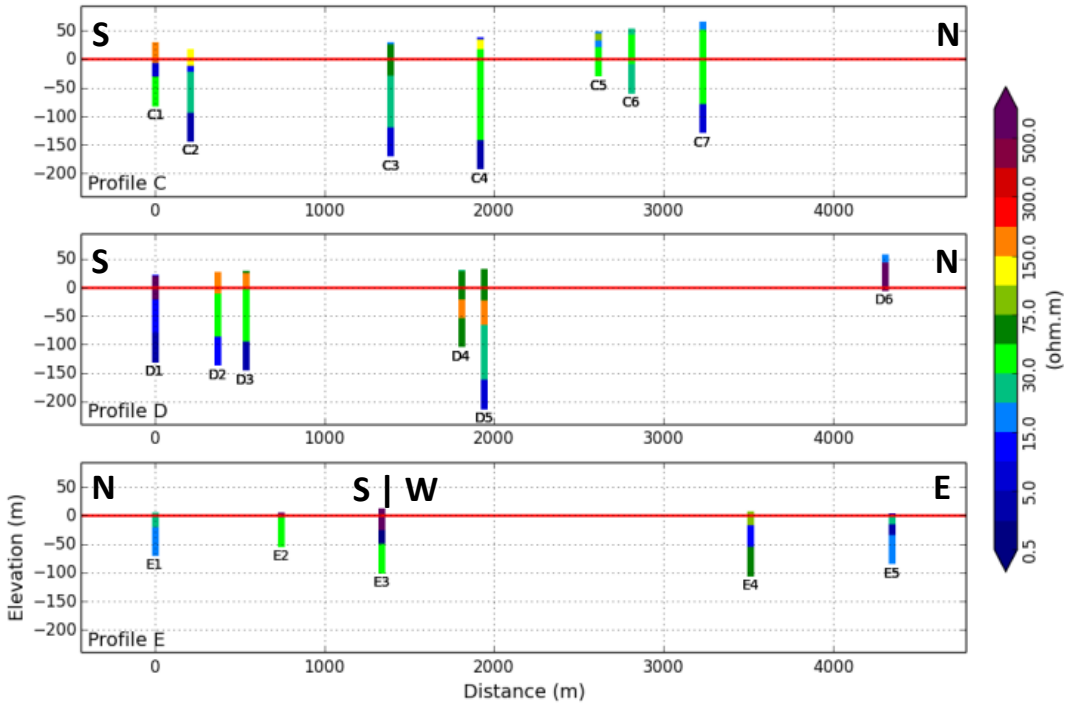

Fig.2.23 – TDEM transects C, D and E (see location in 2.16). Deepest layer arbitrarily set to 50 m thick.

2.4.3 Geoelectrical model

The resistivity ranges of the hydrogeological formations of the study area are presented in Table 2.2. It was observed a very good agreement between the 3 geophysics technics. TDEM is more expedite to perform in the field, although more sensitive to EM noise, while CVES gave a very good overview of the spatial relationship between the hydrogeological formations.

Layer	Resistivity range (ohm.m)	Profile
Sand beach (SW)	<10	A3-5
PQ unsat.	100-700	A2, B4, B6, A2
PQ sat.	10-15	A3
Mio unsat.	75-200	A1
Mio. sat. (FW)	20-100	A-5, B4, B6
Mio. sat. (S/BW)	< 10	A1-2
Cret.	10-100	B1, B2, B5
Jur. unsat.	100-200	B1

Table 2.2 – Geoelectrical range of the formations. PQ: Plio-Quaternary; Mio: Miocene; Cret: Cretaceous; Jur: Jurassic; FW: freshwater; SW: saltwater; BW: brackish water.

Our results are in agreement with previous geoelectrical surveys (unpublished work from the Amsterdam Free University). For instance, one of this study (Elsendoorn et al., 1982) presents a N-S geoelectrical profile made with 5 vertical electrical soundings (VES), located N to Olhos de Água and ~4 km long, in which the Plio-Quaternary has resistivity ~270 ohm.m, the saturated Miocene ~110 ohm.m, the upper Cretaceous (C2 in Table 1.1) ~25ohm.m, and the Cretaceous C1 60-100 ohm.m. The cross section presents a sub-tabular Plio-Quaternary above Miocene and Cretaceous formations diving towards S. The marly Cretaceous formations were also identified below the Miocene ones by other authors in the Quarteira region (Carvalho et al., 2012; Carvalho et al., 2006; Geirnaert et al., 1982).

The hydrogeophysical interpretation is still ambiguous due to two main reasons: (i) too shallow depth of penetration; (ii) overlap of resistivity ranges of geological formations. The use of a complementary method, such as seismic (Carvalho et al., 2012) or magnetic resonance soundings MRS (Legchenko et al., 2009; Vouillamoz et al., 2012), which targets to other material properties (seismic wave propagation and presence of hydrogen, respectively), may be of great use to solve the two enunciated limitations.

2.5 Contribution to the ARQ HCM

The presence of the Cretaceous between the Miocene and the Jurassic formations seems to be confirmed by the geophysics results of this study and the previously cited studies. As the cretaceous formations behave as an aquitard, it explains the hydraulic heads difference between Miocene and Jurassic aquifers. It is this probable that the Jurassic aquifer recharge the Miocene aquifer through the Cretaceous aquitard. However a few logs show the direct hydraulic connection between Miocene and Jurassic water bearing formations. Such hypothesis could be tested using numerical groundwater flow model. To do so, we propose to extend the current ARQ west boundary towards the Albufeira N-S fault, excluding Albufeira Diapir.

We also detected and confirmed several accidents affecting the Miocene and Cretaceous formations (CVES B2, B3, B5). These faults may have a strong influence in the hydrogeology and hydrochemistry of the groundwater, namely in groundwater salinization by diapir ascension. On other hand, seawater intrusion can occur very far from the coast. For instance, De Montety et al. (2008) showed than in a confined aquifer of the Camargue region (France), the proportion of saltwater reaches 98% in the aquifer at 8km from the coast. Several coastal aquifers in the mediterranean basin faces the problem of groundwater salinization, provoked in many cases by several sources (Mongelli et al., 2013; Trabelsi et al., 2012). To distinguish diapiric and sea origins, extensive hydrogeochemical and isotopic surveys must be done to complement previous work (Bronzini, 2011).

The concentration of inter and subtidal freshwater springs at Olhos de Água can be explained by the geological settings. Indeed, the submerse Miocene formations are confined by Plio-Quaternary at east of Olhos de Água. No SGD were detected in this area by off-shore surveys of electrical conductivity, temperature and depth in the sea, while between Albufeira and Olhos de Água there is clear indices of SGD (Sousa et al., 2014). With a groundwater flow towards S and SE, the groundwater is trapped in the submersed Miocene formations and the discharge must occur at Olhos de Água. Thesehypotheses also means that below the off-shore Miocene aquifer may store large groundwater resource, as it was recognized in recently in several world coastal aquifers (Post et al., 2013). Once again, variable-density groundwater flow numerical model may be crucial to test such hypothesis. Such model would have to integrate the off-shore geology, which requires costly off-shore geophysics surveys and interpretation. On other hand, it would be very important to optimize the monitoring

network, with at least one piezometer in each sector of the aquifer (unconfined Jurassic, unconfined Miocene, confined Jurassic below Cretaceous, confined Jurassic below Miocene and Cretaceous, confined Miocene below Plio-Quaternary). The spatio-temporal assessment of groundwater recharge using hydrometeorological network and distributed recharge model coupled with groundwater model (Francés et al., 2011) is also of crucial importance to constrain the groundwater model and reduce uncertainties.

2.6 Numerical Models

The following section descscribes two generations of numerical models of the Albufeira-Ribeira de Quarteira (ARQ) and Quarteira (QRT) aquifer system. The first generation is comprised of a regional 2D horizontal model, based on previous work by Monteiro et al. (2007). In a subsequent phase, 2D cross-section and regional 3D models of the system are develped taking into account new data on the system geometry and structure.

2.6.1 Regional 2D Horizontal Model

The model geometry takes into account the Albufeira-Ribeira de Quarteira (ARQ) and Quarteira (QRT) aquifer limits presented by Almeida et al. (2000). Constant head boundary conditions (BC) (1st kind/Dirichlet boundary condition) equal to 0 m above mean sea level were imposed along the coastline, representing the contact with the sea. A second BC was imposed along nodes corresponding to the lower reaches of the Quarteira stream, with constant heads equal to terrain elevation. A constraint was imposed on the stream BC so as to only allow water to exit the aquifer, thus ignoring any potential recharge from the stream.

Withdrawal rates for public water supply, determined from Municipal Council data, were imposed on nodes corresponding to the location of public supply wells. Additional abstraction rates for private use for each aquifer system, estimated by Almeida et al. (2000), were distributed uniformly over nodes corresponding to the location of private boreholes currently in use.

Recharge rates determined by Oliveira (2006), were applied to the spatial distribution of rainfall proposed by Nicolau (2002), resulting in 33.1 x106 m^3/year of average annual recharge.

Transmissivity (T) values were estimated through inverse modeling under steady-state conditions taking into account pumping for public water supply, using the Gauss–Marquardt–Levenberg method as implemented in the nonlinear parameter estimation software PEST (Doherty 2002).

The defined conceptual flow model was translated into a 2-D finite element mesh with 5453 elements and 2914 nodes. The following formula expresses the physical principles at the basis of the simulation of the hydraulic behavior of the aquifer system:

$$S\frac{\partial h}{\partial t} + \mathrm{div}(-[T]\cdot\overrightarrow{\mathrm{grad}}\cdot h) = Q \qquad (1)$$

where T is transmissivity [L2T-1]; h is the hydraulic head [L]; Q is the volumetric flux per unit volume [L3T -1L-3], representing sources and/or sinks; and S is the storage coefficient [-].

2.6.1.1 Results

The spatial distribution of discharge along the coastline reveals that although discharge along the QRT is relatively uniform, ARQ shows a more heterogeneous distribution. Higher discharge rates along the ARQ coast coincide with inlets at the coastline. Effectively this is due to the BC being further inland, and therefore there is a higher hydraulic gradient at these points. Curiously, the area with the highest discharge rate coincides with the Olhos de Água beach where many significant intertidal springs exist. In fact, between 30-35% of ARQ coastal discharge occurs along the inlet corresponding to Olhos de Água. Apart from coinciding with the most inland point of the coastline, it is also the most direct path between the high recharge Jurassic lithologies to the north and the discharge area. Although there is no definitive data on sub- and intertidal spring flow rates or distribution to confirm these simulations, the results do offer an explanation for the high concentration of springs at Olhos deÁgua. The model is an equivalent porous model and does not in fact represent conduit flow, characteristic of limestone areas. However, the dissolution process associated to karst conduit development accelerates along preferential flow paths (more water leads to more dissolution) (Groves and Howard 1994; Domenico and Schwartz 1997). Therefore, it is conceivable that the preferential flow suggested by the model could have favored karst development along the path to Olhos de Água.

On the other hand, this behavior may also just be an artifact of the conceptual model. Several authors suggest that the Jurassic lithologies may extend under the low permeability

Cretaceous formation in the west portion of the ARQ (see Fig. 1.1 and 1.2), and connect with the Miocene in the south (Bronzini 2011). However, due to the complex geological structure of the area it is unclear whether a hydraulic connection exists. Ongoing fieldwork is currently attempting to answer this question, applying geophysical methods to determine the thickness and angle of the overlying Cretaceous layer. Should these results show that there is a connection, overall groundwater budget values will not change, however the spatial distribution of discharge from the ARQ system will probably be different.

Spatial variation in discharge rates reinforces the need to take into account the location of abstraction when defining sustainable yields (Hugman et al. 2012). On one hand there is a greater likelihood of Seawater Intrusion if abstraction is located closer to low discharge rate areas, and on the other there will be a greater effect on intertidal springs and SGD (and subsequently any Groundwater Dependent Ecossystem) if pumping is closer to these areas. This is a highly complex matter and the available groundwater resources and the needs of the various water users have yet to be properly identified and quantified. Impact of SGD on the marine ecosystems has been demonstrated (Encarnação et al. 2013) but a quantifiable relationship has yet to be defined. Currently there are ongoing efforts to identify and measure SGD along the ARQ and QRT coast which should lead to a better comprehension of ecosystem variations between sites seen by Encarnação et al. (2013).

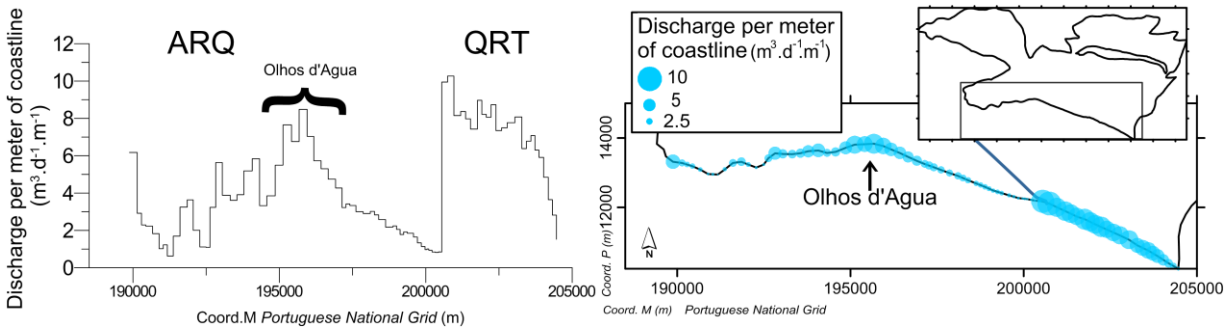

Fig. 2.24 - Calculated coastal freshwater discharge per meter of coastline (in Hugman et al., 2013, in review).

2.6.2 Regional 3D and 2D Cross-section Flow Models

The numerical model geometry is based on a simplified 3D hydrogeological model of the aquifer systems as described in Almeida et al. (2000) and shown in Fig. 1.1. From top to

bottom, the first aquitard is called PLIO, the first aquifer MIO, the second aquitard CRET and the second aquifer JUR. The following information was used to create the top and bottom of each layer:

1. Geological map and cross-sections (Fig. 1.1 and Fig.1.2);
2. log of boreholes information, essentially for the PLIO and MIO layers (Fig.2.1);
3. bibliographic compilation.

The top and bottom of the MIO and PLIO layers was calculated using a set of points coresponding to the geological contacts, boreholes and virtual boreholes (false boreholes defined by the operator to constrain the interpolation. At the geological contacts, a thickness of 1 m was assigned at the north boundaries and the thickness observed in the field (cliffs) at the lateral and south boundaries. At boreholes, thicknesses obtained from borehole logs interpretation were assigned. The thickness at the virtual boreholes was assigned arbitrarily following bibliographic information (Almeida and Lourenço da Silva, 1990; Almeida and Lourenço da Silva, 1992; Almeida et al., 2000; Lopes et al., 2006) and surrounding information (geological contact and borehole). Next, the thickness of the layers was obtained using natural neighbor interpolation on a 50x50 m raster. The top of the layer was extracted from the DTM when outcropping. When covered by another layer, the top was obtained after subtracting the thickness of the covering layer(s) to the DTM. The bottom of the layer was obtained by subtracting the layer thickness from the top.

To determine the top and bottom of the CRET and JUR layers, a net of points of virtual boreholes were defined. Based on the thickness at the northest points and on the slope of the layer at each point, thickness at each point was computed. A maximum thickness of 650 m and 250 m was defined for the JUR and CRET layers respectively. Following the bibliography and geological maps, we assumed a slope of these formations of 10º S for the west part of the study area, a slope of 35ºS for JUR between the north limit and the flexure Sto Estevão-MonteFigo-Vale de Judeu and a slope of 20ºS for JUR and CRET south of the same flexure. Next, the interpolation using natural neighbor interpolation on a 50x50 m raster was defined to obtain the thickness. The top and bottom was obtained as described previously for the PLIO and MIO layers.

Offshore, outcropping of the MIO layer was defined using the seafloor sediment distribution map presented in Fig. 3.12 (Teixeira and Macedo, 2001) and the interpretation of the seismic profiles. The interpretation of thees lines show that close to the shoreline the MIO is outcropping, since the contact between the PLIO and the MIO, called H1, is cutting the sea bottom. The thickness of these formation was defined following Lopes et al. (2006), the

seismic data (see Chapter 3.3.3) and Noiva (2009). After merging the on-shore and off-shore layers, smoothing filters were applied to remove incongruent values such as spikes.

2.6.2.1 2D Cross-Section Model

The finite element mesh was built using quadrilateral elements for greater numerical stability. The generated mesh is composed of 137610 elements and 69537 nodes. Constant head and constant mass (1st kind/Dirichelet) boundary conditions (BC) were set along nodes corresponding to the sea floor. Equivalent freshwater heads were assigned, based on the depth of the node below sea level. Recharge was simulated using imposed flux (2nd kind/Neumann) boundary conditions at nodes representing Miocene and Jurassic outcrops. Total recharge to the ARQ system was estimated by Almeida *et al.* (2000) as 8.7x10^{6} m^{3}.yr^{-1}. This value was divided by the length of the coast, resulting in 751 m^{3}.yr^{-1} per meter of coastline. 28.6% occurs on Miocene outcrops and 71.4% on Jurassic outcrops.

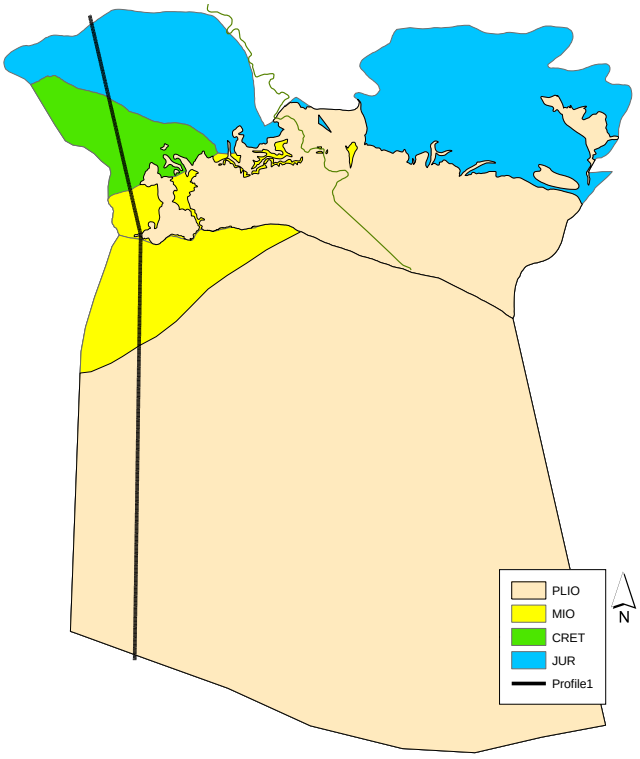

Fig. 2.25 Hydrogeological model and profile location of the cross-section.

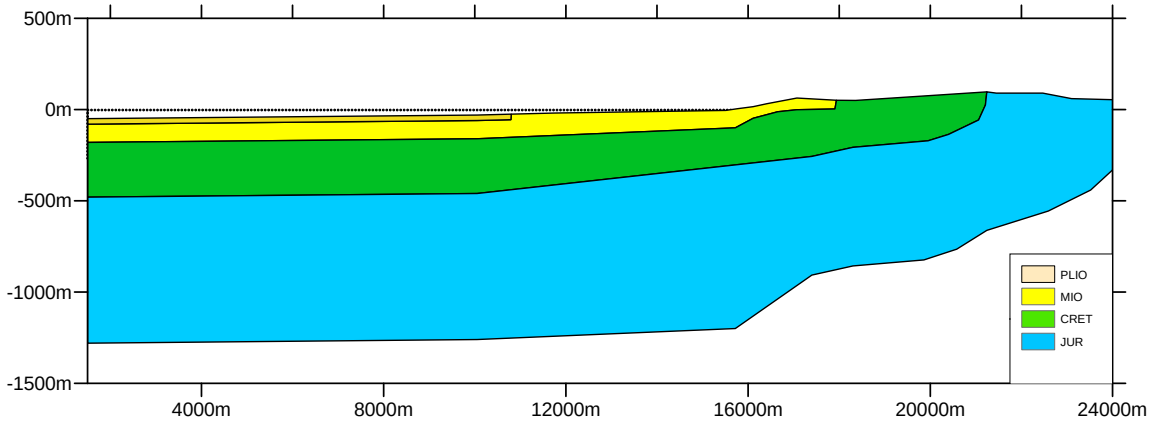

Fig. 2.26 - Cross-section model geometry.

Hydraulic conductivities (*k*) for the Pliocene, Miocene and Jurassic layers are based on average values reported for the area (Table 2.3). The value for *k* for the Cretaceous layer (k_{Cret}) was obtained by trial-and-error. Values were varied across orders of magnitude between 0.001 and 0.1 until acceptable values of hydraulic head were reached. Best fit was obtained with k_{Cret} = 0.01 $m.d^{-1}$. Porosity was set at 0.3 (Almeida 1985). Longitudinal and transversal dispersivity were defined as 5 m and 0.5 m respectively, according to the empirical relationship suggested by Neuman (2005). The model was constructed with the FEFLOW code (Diersch & Kolditz, 2002), and run until reaching quasi-steady state conditions.

Layer	Hydraulic conductivity ($m.d^{-1}$)			
	Max	Avg	Med	Min
PLIO	0.08	0.02		0.0001
MIO	30.80	5.40	2.35	0.84
CRET			-	
JUR	4.11	0.72	0.31	0.11

Table 2.3 - Reported values of conductivity (k) for the area (Almeida 1985, Almeida et al. 2000).

2.6.2.2 3D Regional Model

A 3D finite element mesh was generated with 84304 nodes and 142814 elements, distributed over 8 slices and 7 layers. Each slice coresponds to the top or bottom of one of the layers in the hydrogeological model (Fig. 2.27).

Recharge rates determined by Oliveira (2006) were applied, considering an average rainfall of 593 mm.yr^{-1} resulting in 33.1 x106 m^3.yr^{-1} of average annual recharge for the two systems. Constant head (1st kind/Dirichelet) BCs were set along nodes corresponding to the sea floor. Constant head BCs were set along nodes corresponding to the Quarteira and Algibre streams, equal to terrain elevation. Constraints were imposed on these BCs to only permit discharge from the aquifer to the stream. Hydraulic parameters are equal to those used in the cross-section model when applicable.

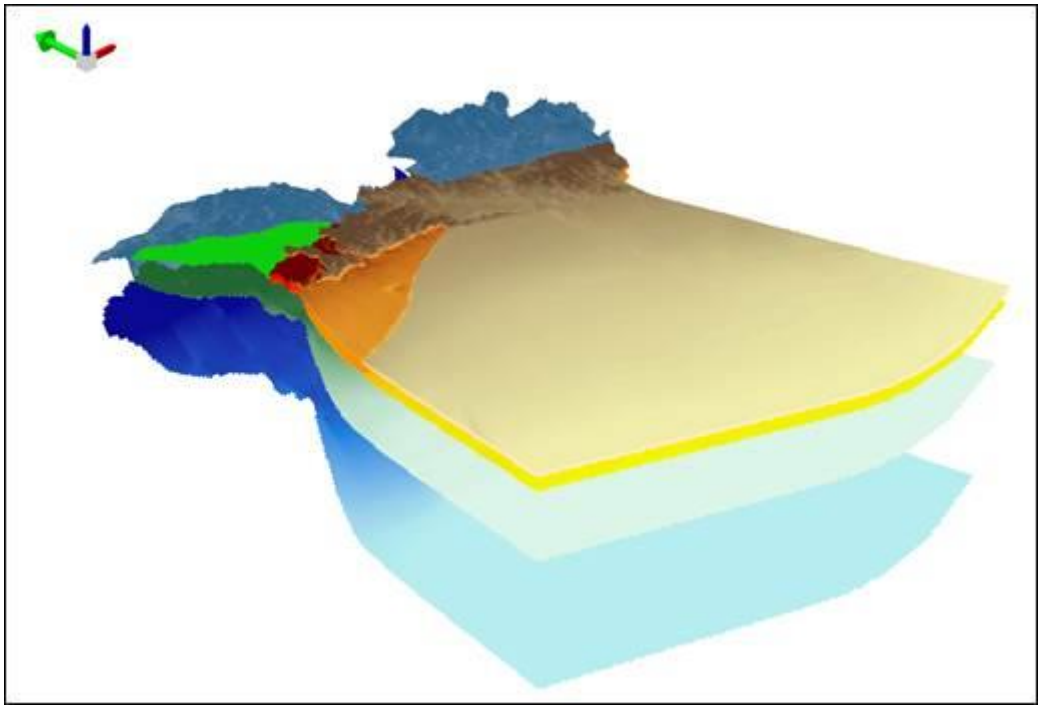

Fig. 2.27 – 3D view of the hydrogeological model (vertical exaggeration x5).

2.6.2.3 Results

Results from the cross-section model demonstrate the potential for brackish SGD up to 8 km from the coast (Fig. 2.28). Discharge is concentrated near the coast (with freshwater discharge up to 40 m offshore) and at the beginning of the offshore confining Pliocene layer. Results indicate that the saltwater wedge in the upper Miocene reaches approximately 300m inland, in agreement with the analytical solutions presented in Francés *et al*. (2014).

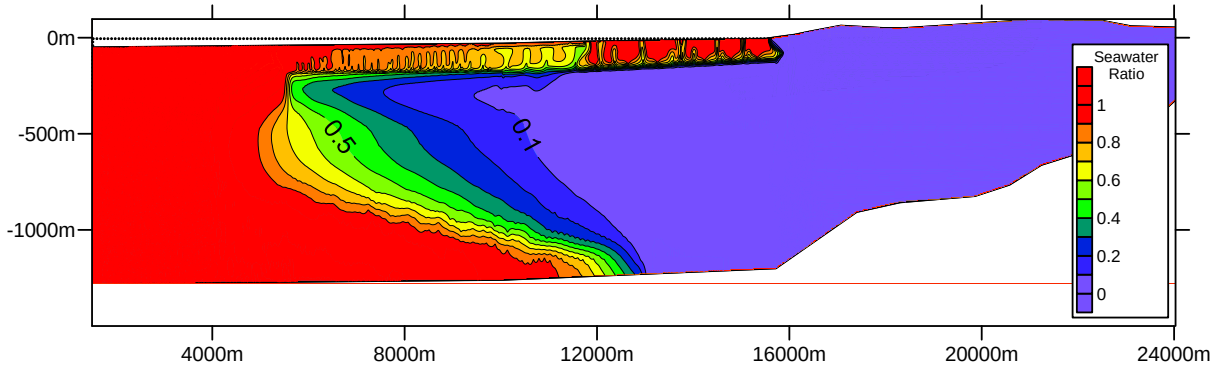

Fig. 2.28 - Simulated distribution of saltwater.

Depth and extent of the salt-water toe in the upper-Miocene layer are a similar to results from geophysical profiles taken perpendicular to the beach (Fig. 2.29). The Miocene formations with seawater are characterized by low resistivity <15 ohm.m, and by 30-50 ohm.m when saturated with freshwater (Francés *et al*., 2014). The presence of low resistivities below the beach slope can be explained by tidal and wave pumping effects which are not included in the simulation.

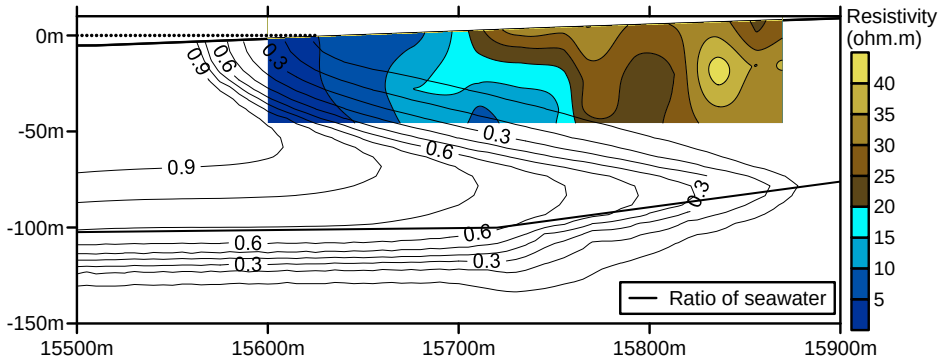

Fig.2.29 - Comparison between model results and FDEM resistivity profile.

Confirming the existence of the freshwater wedge in the Jurassic layer would be of significant interest from a management perspective, as it could represent a significant volume available at less risk from saltwater intrusion. Due to the significant lateral heterogeneity in the systems structure, cross-section model results are merely indicative and do not supply a precise representation of the system. Due to the confining nature of the Pliocene layer, it is likely that there is a significant lateral flow offshore from east to west. Due to the higher

conductivity of the Miocene layer, freshwater will tend to flow toward the area where this layer outcrops offshore, as this will be the path of least resistance. Thus, simulated SGD rates and offshore extent may in fact be underestimated.

Fig. 2.30 presents simulated distribution of hydraulic headsfrom the regional 3D model in the two main productive layers (Miocene and Jurassic). Values are slightly overestimated, and further work is necessary to obtain a more accurate distribution of hydraulic parameters.

Coastal discharge rates are highest in the area near Olhos d'Água (Fig. 2.31). As mentioned in the previous section, this is due to the confining Pliocene layers no longer extending offshore west of this location. The outcropping Miocene creates a path of least resistance, inducing lateral flow. Discharge from the offshore Miocene outcrop amounts to 9.38 x10^6 $m^3.yr^{-1}$. This corresponds to 52% of all offshore discharge. The absolute value is probably underestimated, due to the model simulating a large amount of recharge lost to streams, however the proportion is likely accurate. Once hydraulic parameters have been adequately calibrated, a more accurate value may be obtained.

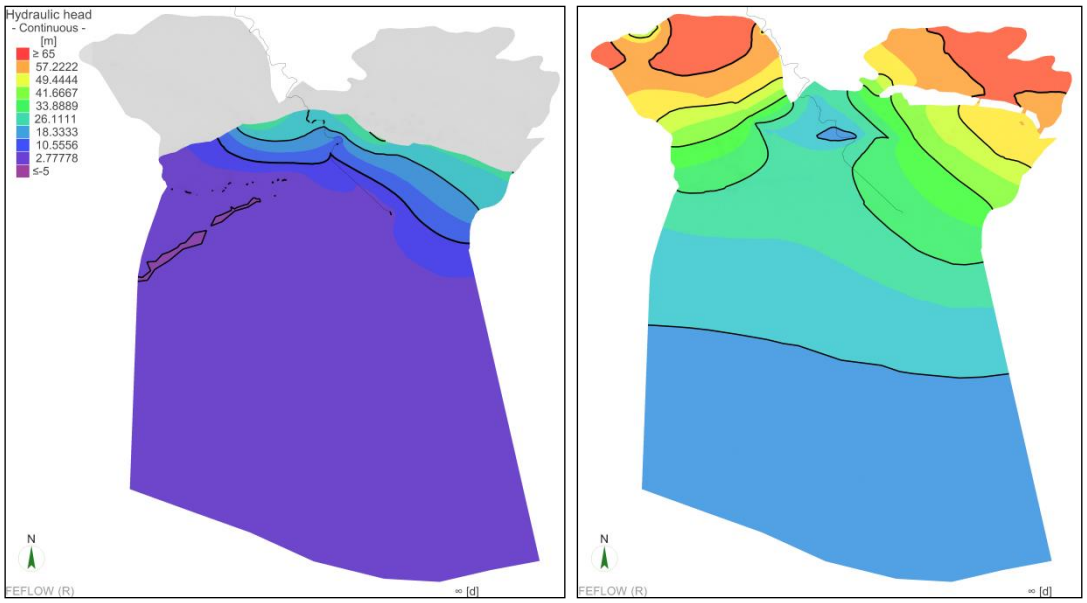

Fig. 2.30 - Simulated hydraulic head in Miocene (left) and Jurassic (right) layers.

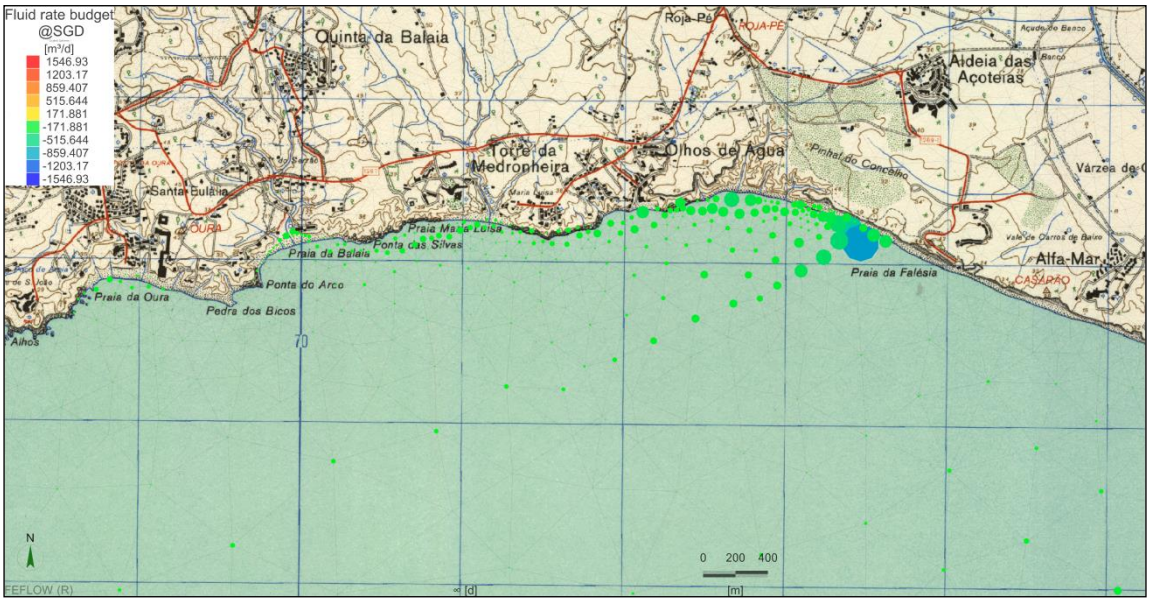

Fig. 2.31 - Simulated distribution of coastal discharge.

2.7 Hydrochemistry

Groundwater characterization of boreholes and costal springs in the study area classifies them mostly with bicarbonate-calcic and chloride-sodium hydrochemical facies, as seen in the Piper diagram from Fig. 2.32 (Left). The elements that are susceptible to a more intense variation are, progressively, SO_4, Na and Cl. A deeper analysis of major elements allows grouping groundwater into five major groups, mostly based on water mineralization (electrical conductivity and TDS) and the ions concentrations that may play an important role in groundwater chemical quality (especially Cl, Na, SO_4, NO_3 and HCO_3). They have the following main characteristics, supported by a major ions relation analysis (Cl/Br vs Cl, Na/Cl vs Cl, NO_3/Cl vs Cl and SO_4/Cl vs Cl, Fig. 2.33):

I. Group 1: Located near the coastline. Groundwater characterized by high electrical conductivities (between 4700 and 18500 µS/cm) and very high Cl, Na, K, Mg and SO_4 concentrations.

II. Group 2: Located between 700 and 2500 m from the coastline, near the Quarteira Stream. Groundwater is probably from Miocene formations, presents an important mineralization averagely 2000 µS/cm and is enriched in typical sea water elements (Na, Cl, Mg, SO_4, etc.).

III. Group 3: Located between 1 and 4 km away from the coastline, groundwater from Miocene and/or Cretaceous formations. Electrical conductivity is relatively important (between 948 to 1244 µS/cm) and sometimes SO_4 concentration is high denouncing evaporite dissolution.

IV. Group 4: Groundwater from the Jurassic aquifer boreholes, located in the southern Jurassic outcrops with electrical conductivity ranging from 1155 to 1380 µS/cm and chemical characteristics similar to Group 3.

V. Group 5: The least mineralized groundwater (electrical conductivity ranging between 582 and 1016 µS/cm) from all the previous groups. Groundwater from the main Jurassic aquifer in the most upstream region, more than 4 km away from the coast.

The geographical correlation with groundwater hydrochemistry allowed the definition of these five major groups, and can be seen in the Piper diagram represented in Fig. 2.32 (Left) and the borehole location, highlighting each defined group Fig. 2.32 (Right).

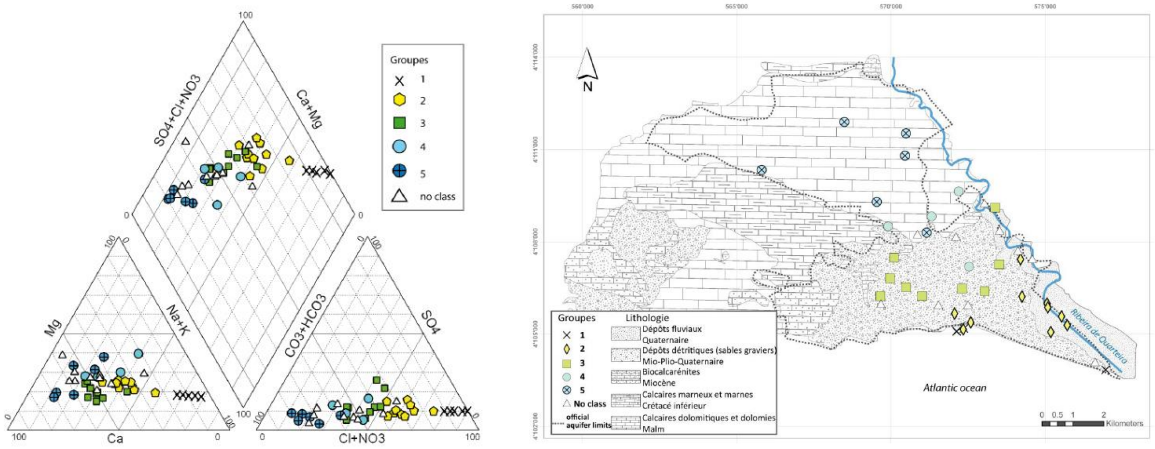

Fig. 2.32 – (Left) Chemical characterization of the different groundwater groups, using a Piper diagram. (Right). Spatial distribution of groundwater as function of the defined groups. No class means groundwater doesn't respect the classification characteristics either regarding their location either different chemical characteristics (Bronzini, 2011).

In the northern part of the aquifer, groundwater dominant is HCO_3. Cl and SO_4 increase progressively towards south, following groundwater circulation pathway. Spatial distribution of these elements is rather similar, being also similar to the electrical conductivity. This fact

suggests that sea water plays an important role in most mineralized waters. Groundwater located upstream in the system present a carbonate-calcic dominant facies, as a reflection of the geological support of the system. Towards the coast, groundwater progressively increases in Na-Cl.

Cl/Br ratio distribution highlights evaporite dissolution processes in group 3 (ratio 800-950) (Fig.2.33). These samples are spacially distributed nearby or over the uplift zones and faults with evaporites injection. They can be distinguished from the other goups 1 and 2 (ratio 488-613), representing repectively the springs located near the shoreline and water points near the Quarteira stream that are affected by the tide influence (Fig. 2.33). They can also be distinguished from group 4 (ratio 620-730) whose values correspond to groundwater circulation in Jurassic limestones.

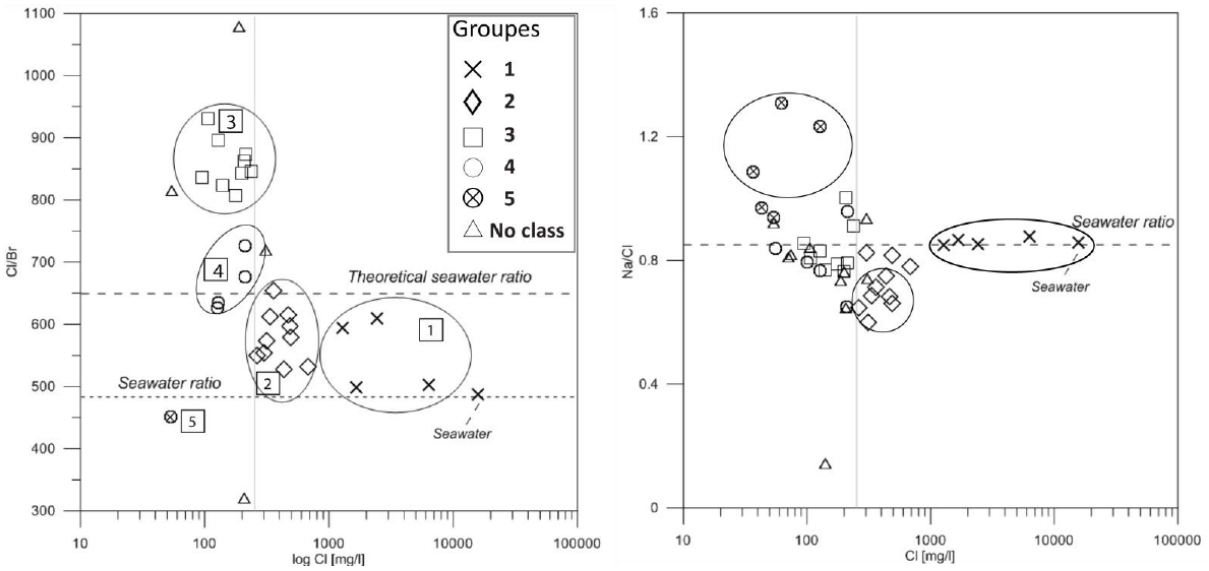

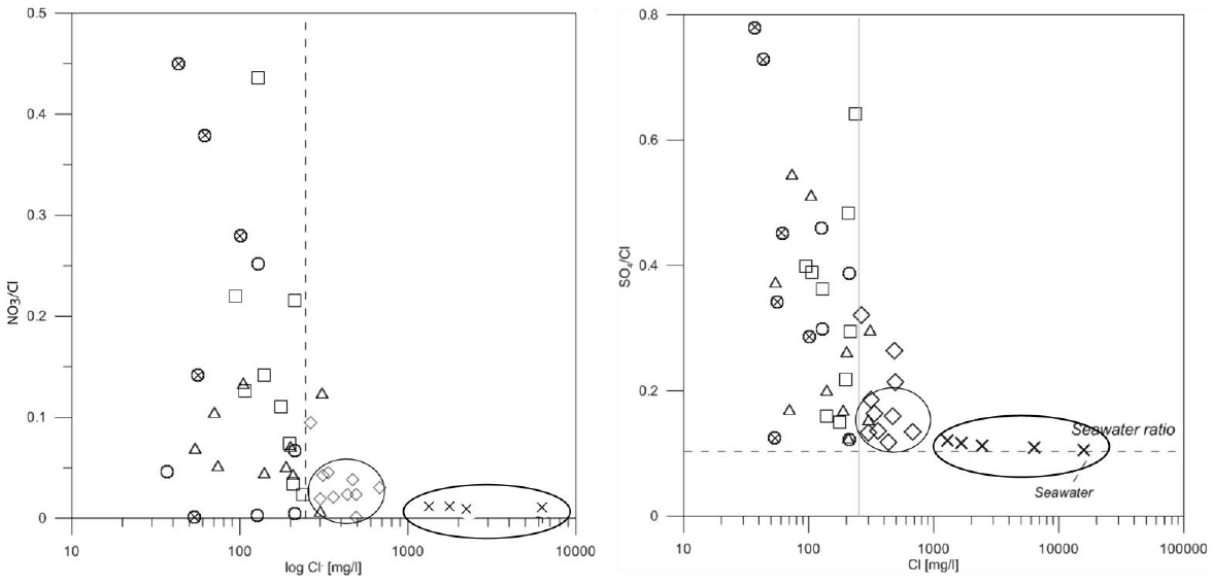

Fig. 2.33 – Chemical characterization of the different groundwater groups, Relation between ionic ratios (Cl / Br; Na / Cl; NO_3/Cl; SO_4/Cl) and concentration of Cl (Bronzini, 2011).

Isotopic analysis values range approximately from -25 to -30 to Deuterium and -4.6 and -5.5 to Oxygen. Groundwater isotopic signature appears to be rather constant with absence of continental effect, even at 8 km distance. The exceptions are related with sea water contamination. The more enriched isotopic signature in relation to groundwater is located above the Olhos de Água beach. Since the continentally effect doesn't explain this variation in the isotopic signature, this isotopic enrichment may be related to sea water contamination, as explained by the following isotopic relations:

i. Relation Cl/ δ18O

Used as an indicator to evaluate the hypothesis of a direct contamination from sea water in the aquifer, it seems that Group 2 is mixed water. Group 5 appears to have the least mixture, increasing progressively in Groups 3, 4 and 2 (Fig.2.34, left).

ii. Relation NO_3/ δ18O

Useful in the impact evaluation of agricultural activities and effects of irrigation practices. These last show an isotopic enrichment and an increase in dissolved elements, but the correlation between these two parameters is very weak (Fig.2.34, right).

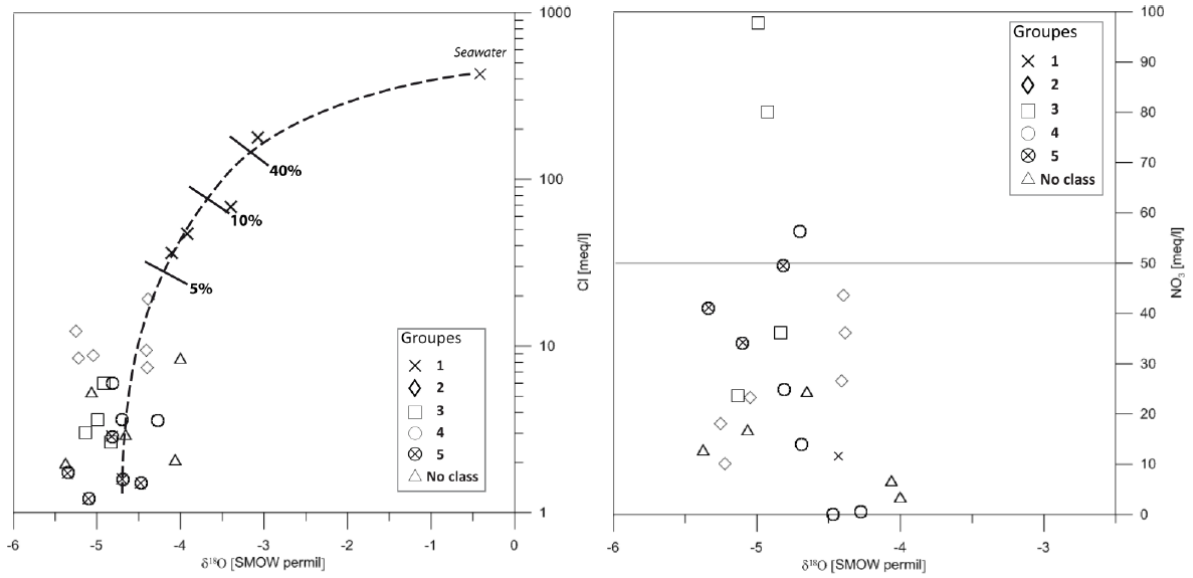

Fig. 2.34 – (Left) Relation between isotope ^{18}O and concentration of Cl; (Right) Relation between isotope ^{18}O and concentration of NO_3 (Bronzini, 2011).

The salinization mechanisms were studied considering either ionic ratios or relations between ion concentrations and isotopic signatures. Their interpretation confirmed the dominant influence of sea water through several mechanisms like the salt wedge, estuary effect, sea spray and rain containing dissolved elements. However, ionic relations such as SO_4/Cl and NO_3/Cl showed evidence of other salinization processes defined by water-rock interaction, especially evaporites dissolution and anthropic activities, namely agriculture. All these processes probably play a role in groundwater salinization can be resumed schematically in such way that different zones in the hydrogeological system regarding water quality and processes affecting groundwater can be identified.

Groundwater was therefore divided into four major groups (see Fig. 2.35), based on the physical-chemical parameters and location and also according with the dominant geochemical processes:

i) A coastal zone, defined by a potential risk of direct sea water infiltration in the aquifer, according with piezometer data and proximity of sea level.

ii) A zone located along the last section of Quarteira Stream, characterized by high salinity (average 2000 µS/cm) and typical sea water ratios, with influence estimated as 1% and 3%. Dominant salinization mechanism is probably defined by an estuary effect.

iii) An intermediate zone characterizing groundwater from the Miocene aquifer and part of the Jurassic, although with salinity (around 1200 µS/cm) will probably be related with sea spray and recharge water enriched with its infiltration in soil, by the effect of evapotranspiration. Moreover, these waters are characterized by SO_4/Cl and NO_3/Cl ratios more important than sea water, indicating local influence of agriculture activities and/ or evaporite dissolution.

iv) A zone located upstream, characterizing recharge water of the Jurassic aquifer, with low mineralization (500-1000 µS/cm), with a bicarbonate-calcic dominant facies.

The most vulnerable zones to salinization processes are considered to be the coastal zone and the zone near the Quarteira Stream. On the other hand, the northern region is not very touched by the salinization phenomena. Karstification processes affecting the main Jurassic aquifer could however interfere with microbiological pollution, due to the soil filtration time reduction due to a very fast groundwater infiltration in the aquifer.

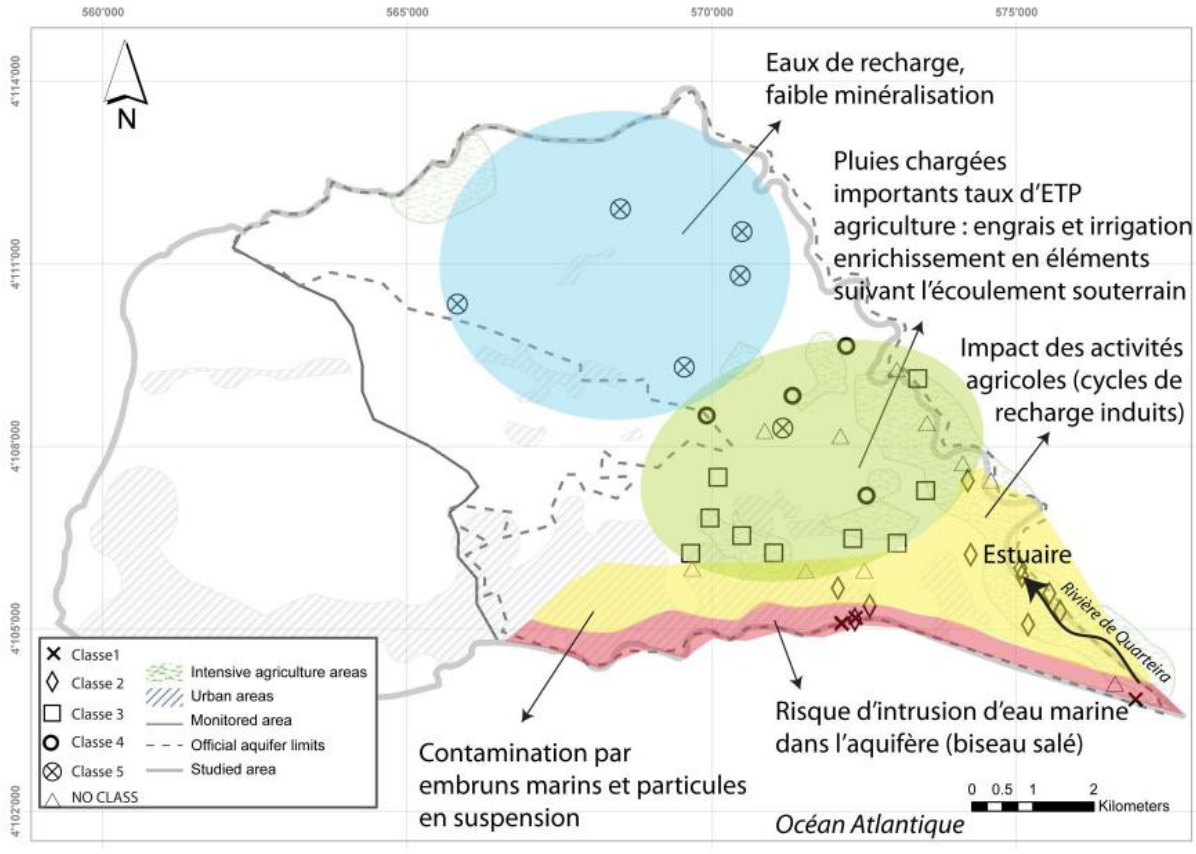

Fig. 2.35 – Conceptual scheme of the main geochemical phenomena (Bronzini, 2011).

The analysis of physical-chemical and isotopic parameters allowed groundwater characterization and its quality. There is a chemical evolution according with the direction of groundwater flow, towards the coastline, characterized by bicarbonate impoverishment and the progressive enrichment of the Cl, Na, SO_4, Mg and K major ions. A good correlation between electrical conductivity and their concentration suggests the sea influence in groundwater. Other sources of salinity are also recognized considering soil occupation, the geological support of the aquifers and evaporite dissolution.

.

3. TASK 2 - Geological setting and sediment distribution offshore the Albufeira-Quarteira costal aquifer system

3.1 Objectives

Along the Algarve coast important aquifers systems are present and previous studies on the groundwater flow reveal a regional southwards direction of flow which favors the occurrence of SGD. Our case study was the Olhos de Água SGDs in central Algarve. These SGDs have been known to be present in the intertidal and sub-tidal zones since historical times. They occur on a sub-horizontal karstified limestone of Miocene age that crops out on the coast and represent only one of the possible discharges of the Albufeira-Ribeira de Quarteira aquifer system. As a matter of fact, the existent hydrological data relative to this aquifer system let us presume the existence of additional SGDs further offshore. The marine areas offshore the Albufeira-Ribeira de Quarteira aquifer system were poorly known until now because of the lacking of detailed bathymetric and geophysical data. Task 2 aimed to cover part of this gap.

Fig. 3.1 - FREEZE project study area (modified from Bronzini, 2010).

The main goals of Task 2 were addressed to:

- define the geological structure (faults, fractures and sedimentary architecture) offshore Albufeira-Quarteira aquifer;
- understand the extent of the SGD bearing strata;
- characterize the morphological expression of the inferred submarine springs and finally
- map the precise position of existing SGDs.

This task produce results such as: i) a detailed bathymetry map of the investigated sector, ii) a reflectivity map of same sector, iii) integration of the on-shore structural map produced by Task 1.

3.2 Offshore Surveys

Task 2 extended offshore the geological investigation of the Albufeira-Quarteira coastal aquifer system. The marine areas offshore the Albufeira-Ribeira de Quarteira aquifer system were poorly known until now because of the lacking of detailed bathymetric and geophysical information. Thus to accomplish the task's objectives more than 200 km of high resolution seismic profiles have been acquired off Olhos d' Água in 2010 and 2011. Figure 3.2 shows the area covered by the high resolution seismic and bathymetric surveys (FREEZE-2010, dashed green; TOPOMED-FREEZE-2011, dashed red; high resolution bathymetry 2010, dashed blue).

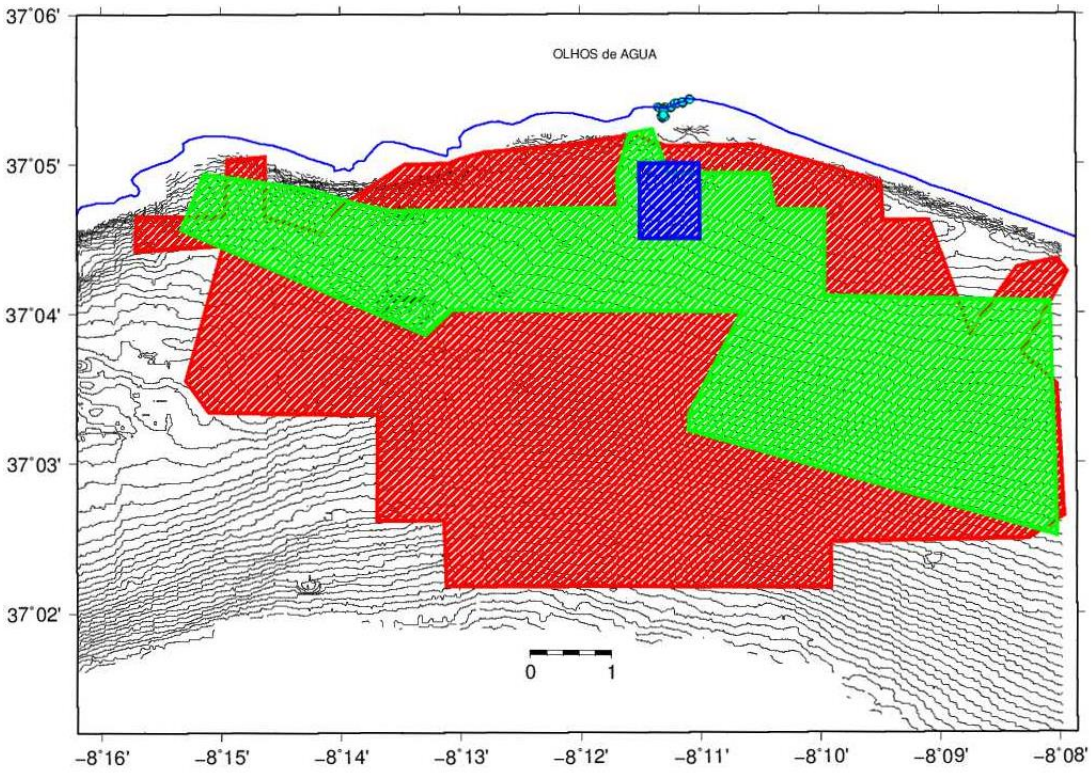

Fig. 3.2 - Freeze2010 (green) and Topomed-Freeze 2011 (red) surveyed areas with high resolution seismic. High resolution bathymetric survey (light blue area).

3.2.1 FREEZE-2010 Geophysical Survey

Since 10 to 16 May 2010 a geophysical cruise off Olhos de Água has been carried out on board of the 18 m length catamaran XUNAUTA vessel by SUBNAUTA s.a. (Lisboa). The survey is fully described in the attached survey report (http://geoportal.lneg.pt/Freeze).The bathymetric survey was planned using the dedicated software PDS2000 – Reson and the data were acquired using a multibeam probe Reson Seabat 8125 loaned by IST – Instituto Superior Técnico to the project and operated by the BlueEdge private company. The high-resolution seismic and the reflectivity datasets were acquired using an integrated combined system of sub-bottom profiler and Side Scan Sonar EdgeTech 2000-CSS, operated by the Aveiro University team. The survey was initially planned as a combined bathymetric and high resolution reflection seismic acquisition but due to equipment safety reason, the acquisitions were carried out separately. So a couple of days were entirely dedicated to the bathymetric acquisition and the rest of the survey to seismic acquisition. The bathymetric survey target was a tiny area in very shallow water (8 meters max depth, Fig 3.3) just in front of the intertidal SGDs laying on the Olhos de Água beach. The purpose was to find clear SGD

evidences on the seafloor using the high lateral resolution of the SEABAT 8125 multibeam probe (~ 10 cm for depth less than 10 meters). Bathymetric data have been processed using both PDS2000-Reson (Fig. 3.4) and Caraibes–IFREMER packages and the grids produced using GMT 4.5.11 package. During the cruise ~75 km of high resolution seismic lines and 12 km^2 of Side Scan Sonar data have been acquired as shown in Figs.3.5 and 3.7 respectively.

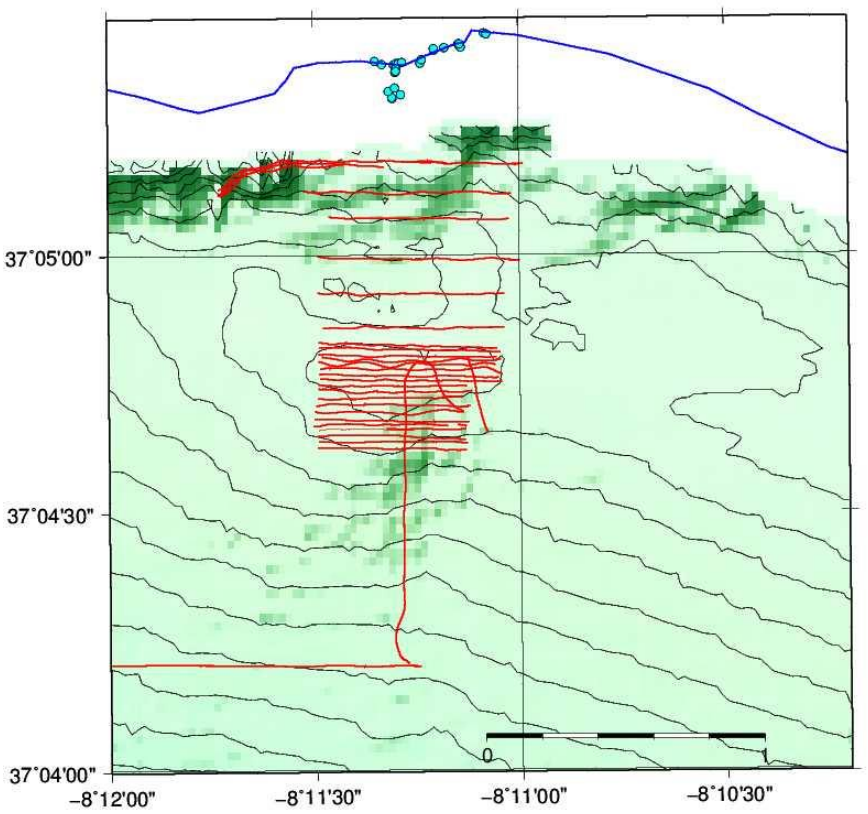

Fig. 3.3 - Detailed bathymetric survey performed during the FREEZE-2010 survey off Olhos de Água.

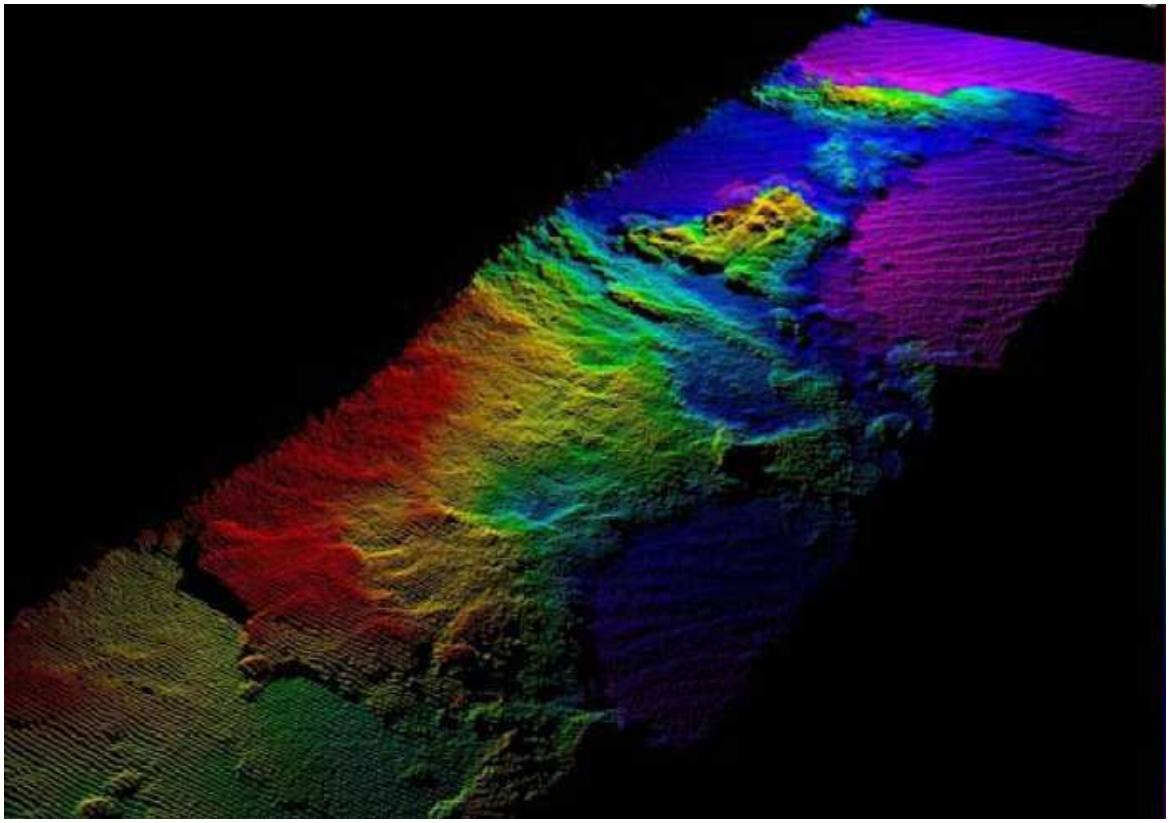

Fig. 3.4 - Example of high resolution bathymetric data acquired during Freeze2010 survey.

Seismic data were acquired between 10 and 15 of May 2010. Navigation was operated in DGPS mode with RTK correction and is shown in Fig 3.5. The high resolution seismic profiles (sub-bottom-chirp) were acquired using a frequency of 0.5-7kHz in order to obtain a good compromise between high resolution and an adequate penetration (~ 20 msec TWT) as shown in Fig 3.6.

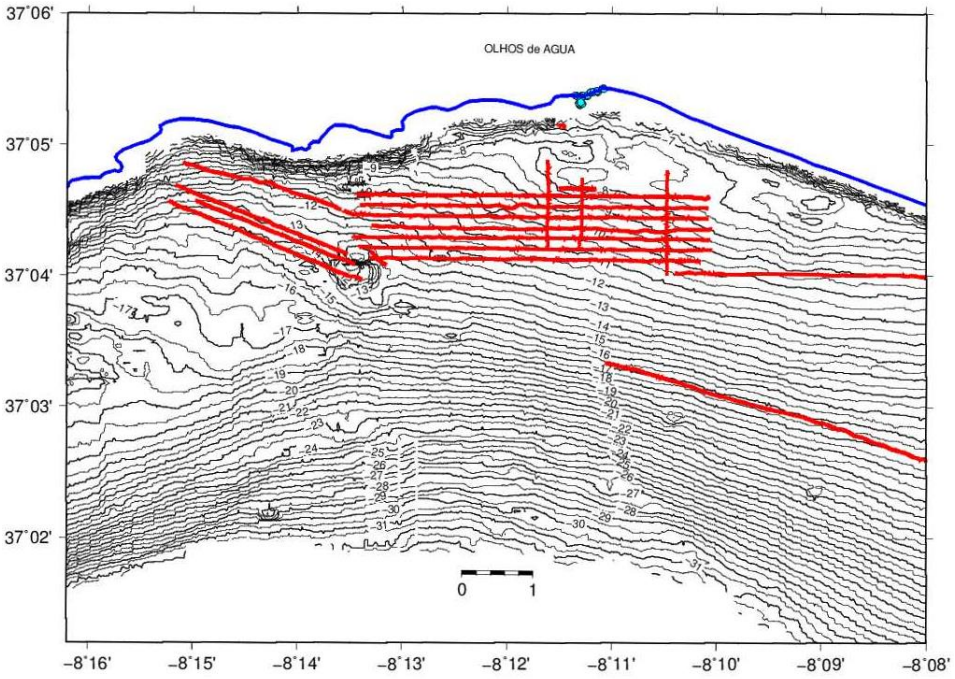

Fig. 3.5 - FREEZE-2010 Sub-bottom Chirp and SideScanSonar positioning.

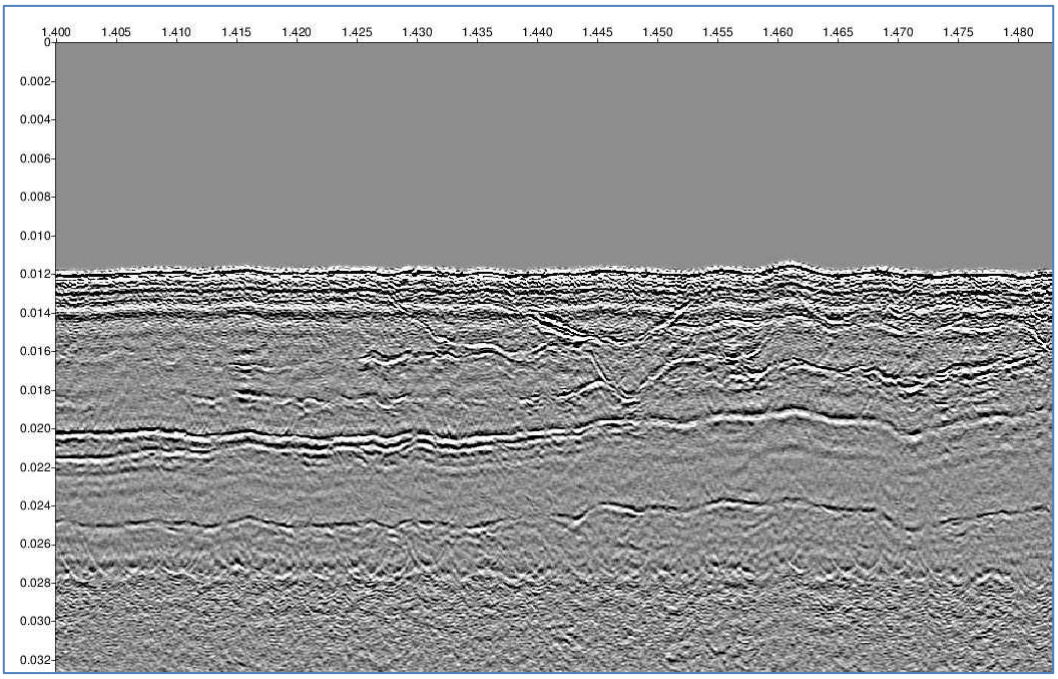

Fig. 3.6 - Example of CHIRP profile acquired during FREEZE-2010.

Seismic processing was conducted using SPW (Seismic Processing Workshop) package and side scan sonar data have been elaborated using PRISM (Processing of Remotely-sensed Imagery for Seafloor Mapping) software at Aveiro University.

The side scan sonar data was acquired along the seismic lines using a double frequency, 100k Hz and 400k Hz, with a line spacing of 120-160 meters. An overlap of 40 to 80% was obtained in order to allow the processing and mosaicking with results shown in Fig 3.7.

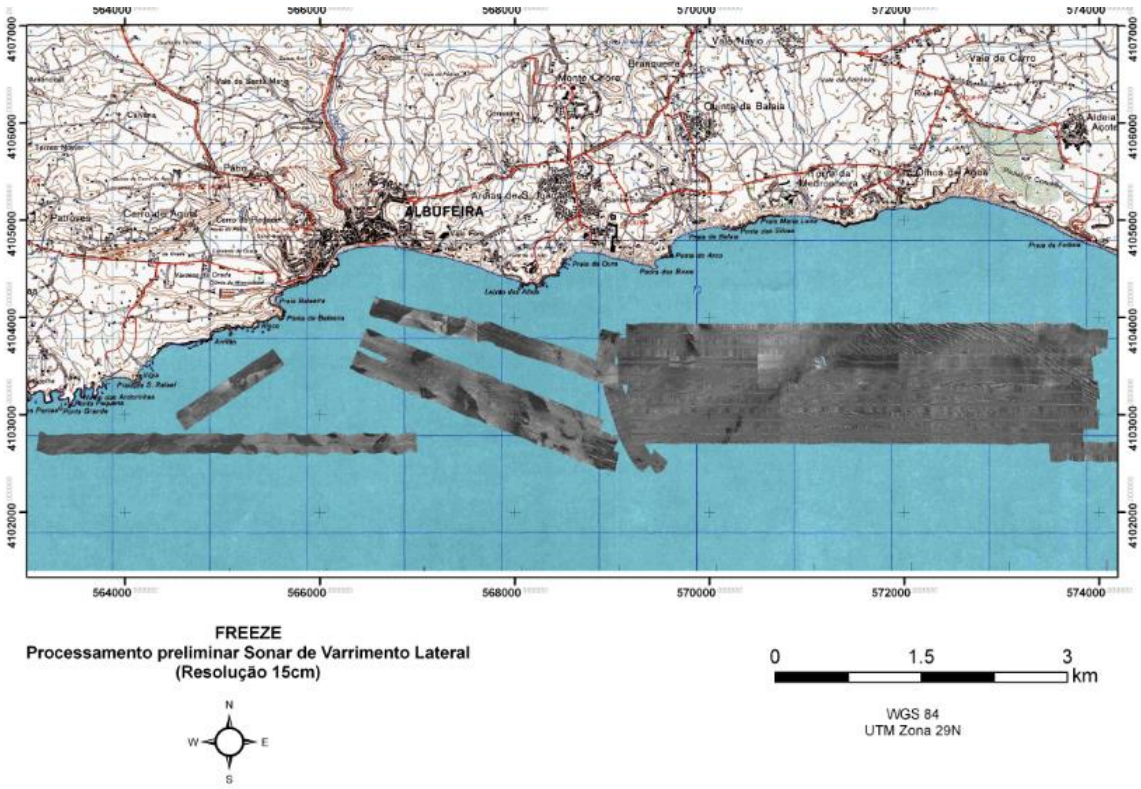

Fig. 3.7 - Side Scan Sonar mosaic.

3.2.2 TOPOMED-FREEZE-2011 Geophysical Survey

A second geophysical cruise off Olhos de Água was performed in April 2011 (since 4 to 15), in cooperation with the European project TOPOMED that had already planned an investigation in offshore Quarteira and Faro. The survey was carried out on board of the 18 m length catamaran XUNAUTA vessel by SUBNAUTA s.a. (Lisboa) and is fully described in

the attached survey report (http://geoportal.lneg.pt/Freeze). This new medium-resolution seismic survey (SPARKER) was necessary to complete the previous seismic coverage and investigate the deepest sector where the satellite images (analyzed in TASK 4) shown the presence of a suspect “slick” possibly related to SGD activity.The Sparker source was a 200 tip, Geo-Source 200, used with a Geo-Spark 1000 pulsed power supply. During the surveymore than 130 km of seismic lines were acquired for both the investigated areas.The profile’ tracks acquired off Olhos de Água are shown in Fig. 3.8 and an example of acquired profiles is shown in Fig 3.9.The seismic processing was performed both at Aveiro University and UGM-LNEG, with different seismic platforms and different processing flowsand. All the final data were loaded on a LANDMARK seismic system platform to be interpreted.

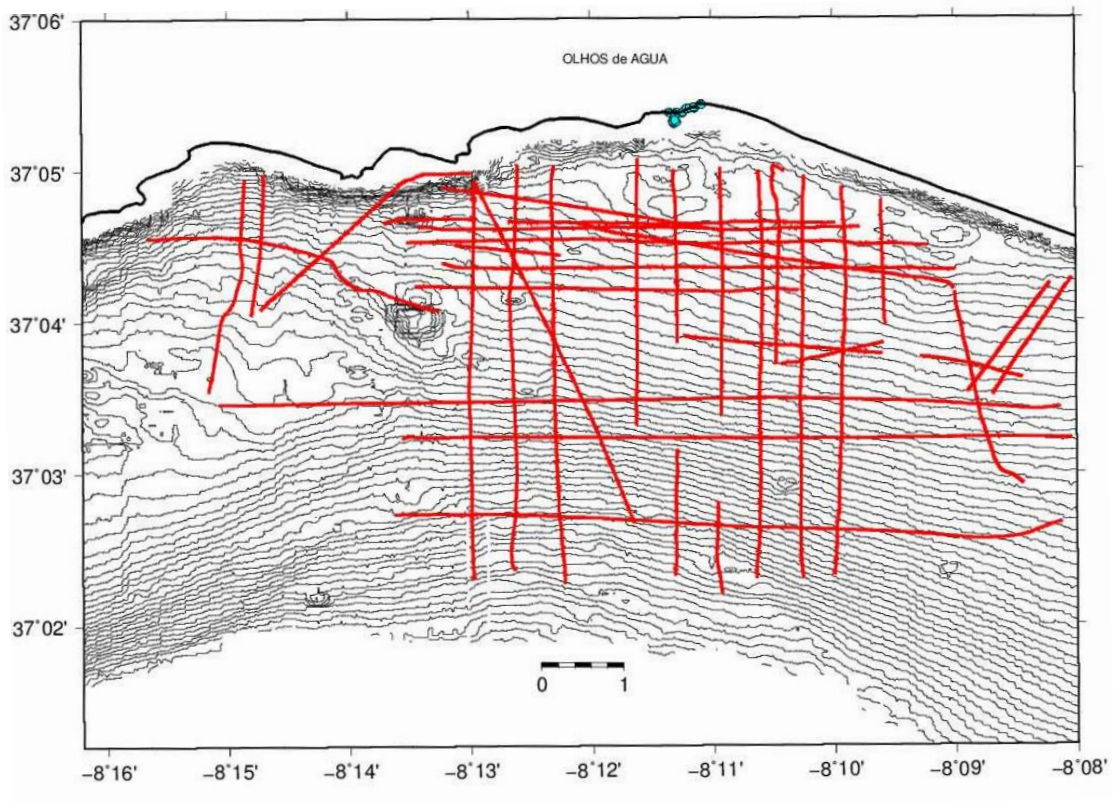

Fig.3.8 - Survey 2011:SPARKER lines locations.

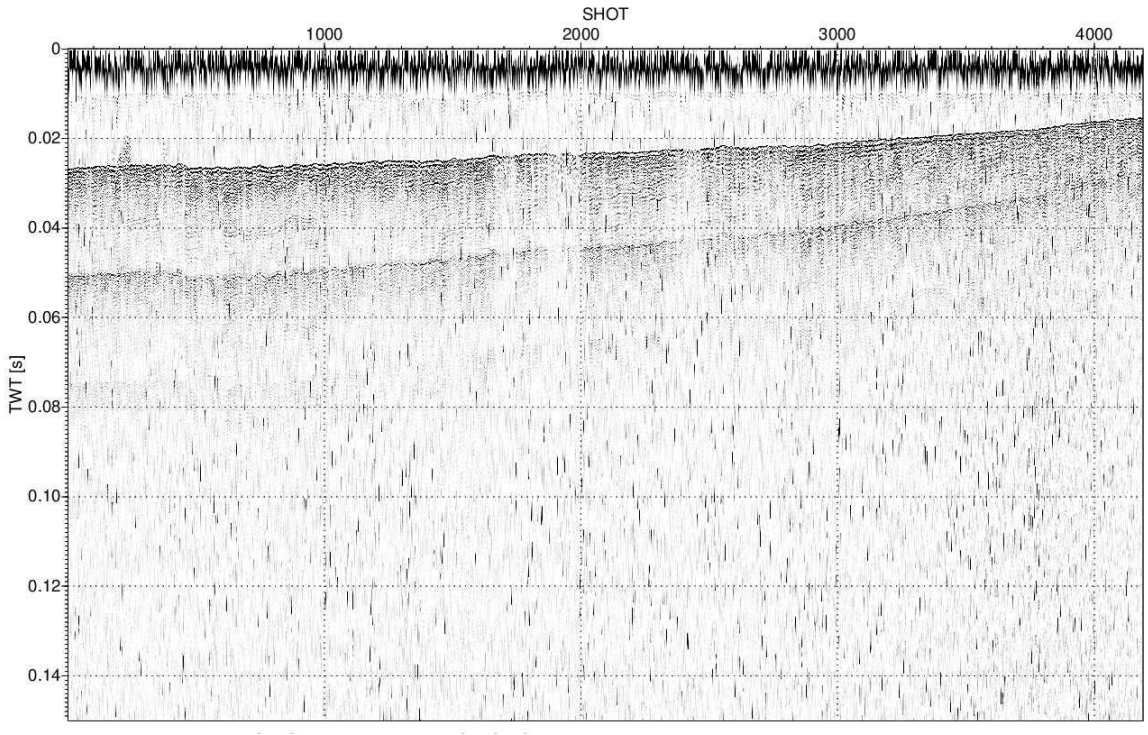

Fig. 3.9 – Example of Sparker data acquired during TOPOMED-FREEZE 2011 survey.

3.3 Results

3.3.1 Bathymetric data description

The tiny bathymetric dataset acquired during 2010 geophysical survey (see Figs.3.3 and 3.4) didn't allow a "regional view" of seafloor morphology of the area and its possible relationships with the surrounding structural setting. To accomplish this purpose a 50 m bathymetric grid was gently shared to the project by Prof. Joaquim Luis (Algarve University) and is available on MIRONE web site (http://www.es-loule.edu.pt/biogeo/mirone_en.html). This bathymetric grid (Fig. 3.10) was also used for TASK 3 oceanographic surveys positioning planning (see TASK 3 of this report).

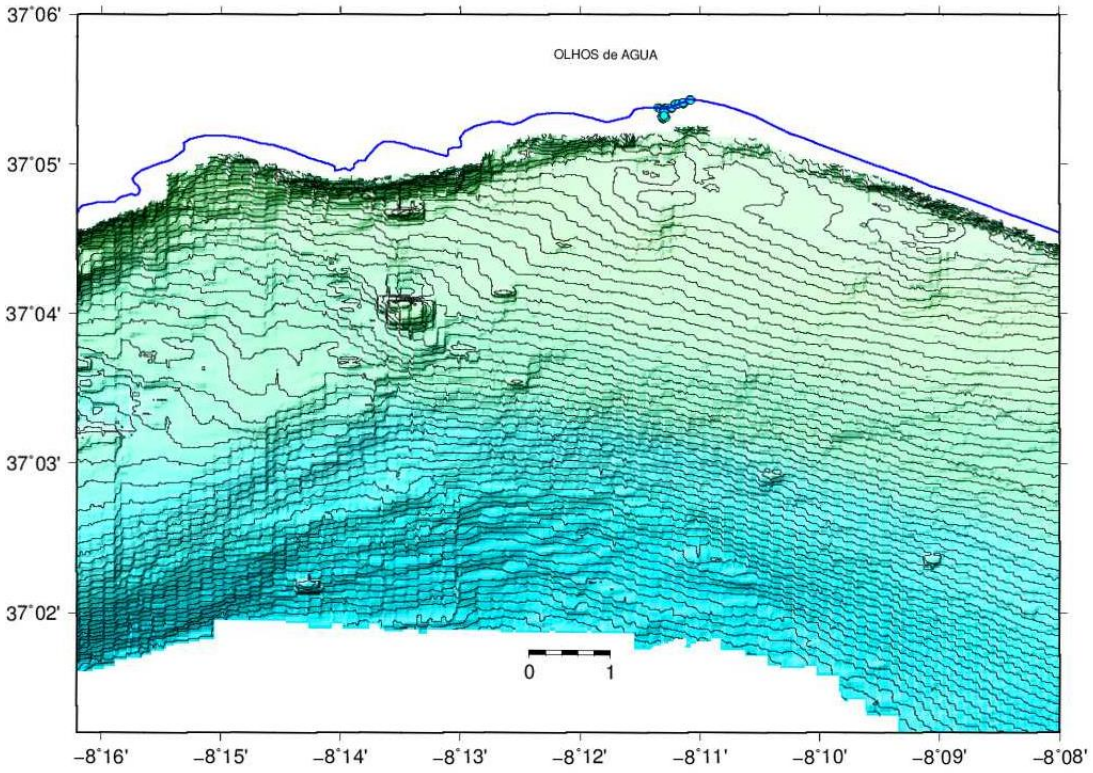

Fig.3.10 - Shaded relief of Algarve 50m grid. Contour interval is 1 m. The grid was visualized using GMT 4.5.11 software (Wessel and Smith, 1991, 2013).

Bathymetric data show two distinct sectors a western and an eastern one. On the western side the seafloor is quite irregular with some circular rocky outcrops (mainly sandstone) as mentioned in literature and confirmed by our Side Scan Sonar data. The biggest one, known as Pedra dos Arrifes (Teixeira, 1998 and Teixeira and Macedo, 2001), represents the remnant of theHolocenepaleoshore.The Pedra dos Arrifes is composed by medium to coarse calcarenites, with subhorizontal attitude, anddevelops between -6 and -12 m (ZH) depthwhereits base lies.Moving to E and SE, the seafloor forms a little NE-SW oriented scarp dipping toward SSE.In the eastern sector of the analyzed area the seafloor gently dip toward SW between 8 m and 32 m depth as shown by the quite regularly spaced bathymetric contour. Between 0 and 8 m depth the data show a relatively flat area with the presence, at 8m depth, of supposed sand ripple of 35-40 m wave-length partially highlighted by side scan sonar data.

In the eastern sector some little circular highs are present, aligned in NW-SE direction and are probably rock outcrops as evidenced in some places by seismic lines (Fig. 3.11), and by Teixeira (2000). In fact he described that the limit between the Algarve windward rocky and

the sandy coast leeward internal platforms has a generic NE-SW trend and the coast anchor point is located near Olhos de Água (Fig. 3.12). This alignment is the cartographic expression of the rocky formations interseption that generically dive towards SE, under the overlaying sedimentary coverage (Teixeira, 2000).

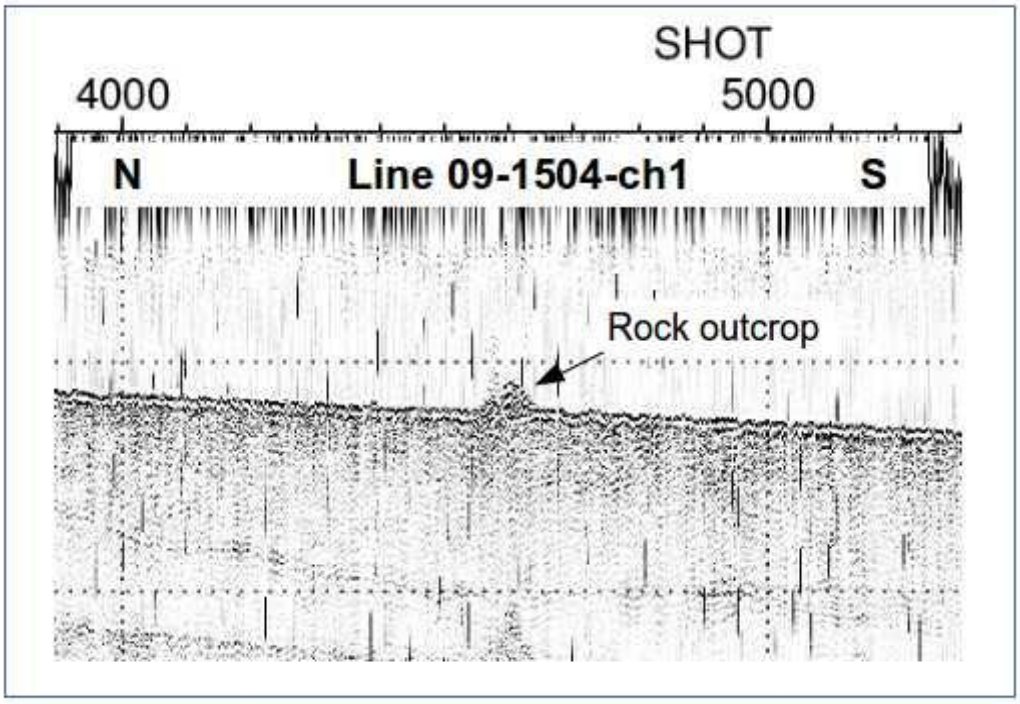

Fig. 3.11 – Seismic evidence of a rocky outcrop.

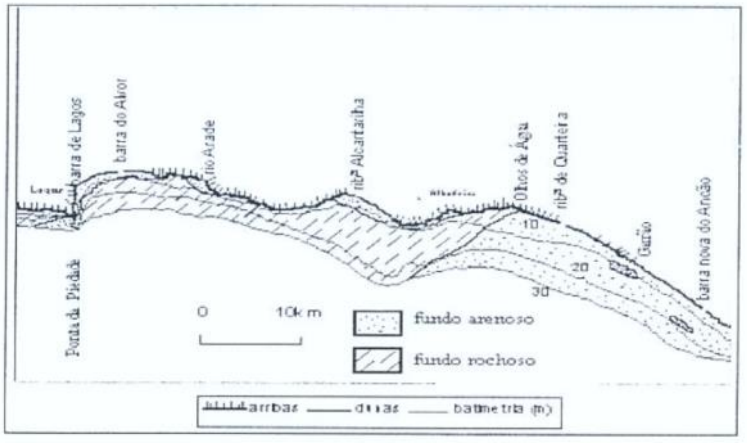

Fig. 3.12 – Southern Algarve internal platform. Generic distribution of sediment types from the coast to 30 mt depth (extract from Teixeira, 2000).

3.3.2 Side scan sonar data interpretation

The Side Scan Sonar data gave acoustic information of submarine rock outcrops and sediment distribution. In the western sector of investigated areathey confirm the presence of hard/rocky outcrops visible in the bathymetry (Figs. 3.13 and 3.10, respectively) as well as the presence of a well-developed area of (probably sandy) ripples just in front of Olhos de Água beach. We don't know if those features represent a stable ripple field or are merely the instantaneous image of a previous storm. What is really curious is the geometrical path of the boundary with the surrounding sediments and its very sharp character (Fig. 3.14). Anyway this kind of data represents an initial patrimony that could increase with new future acquisitions allowing an improvement of our knowledge of this very dynamic environment.

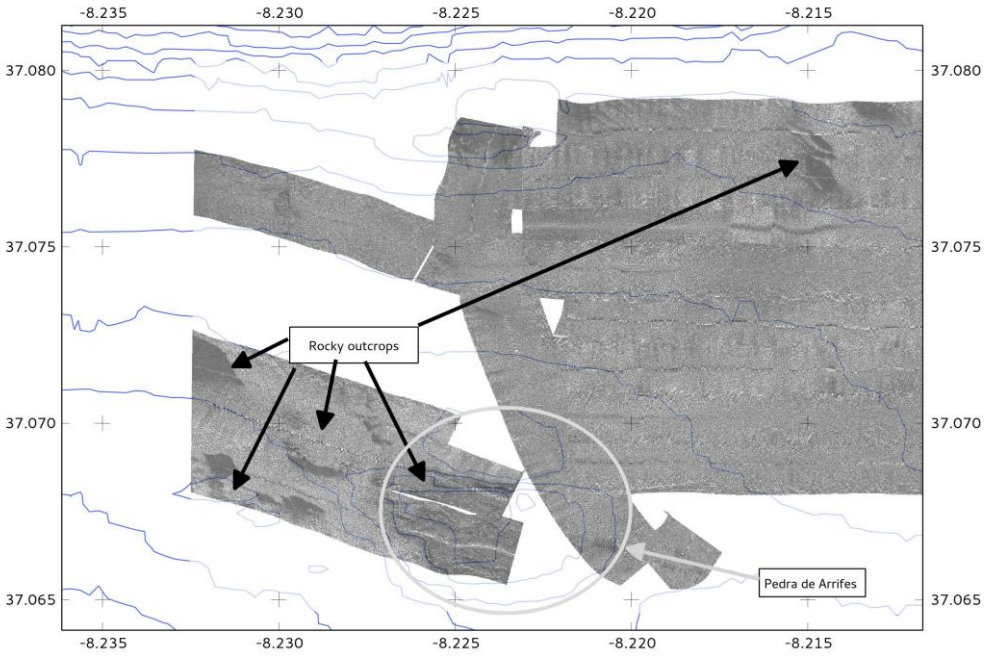

Figure 3.13 – Side Scan Sonar data showing rock outcrops in the western sector of investigated area. The circle surrounds the so called Pedra de Arrifes as indicated by Teixeira (1998),

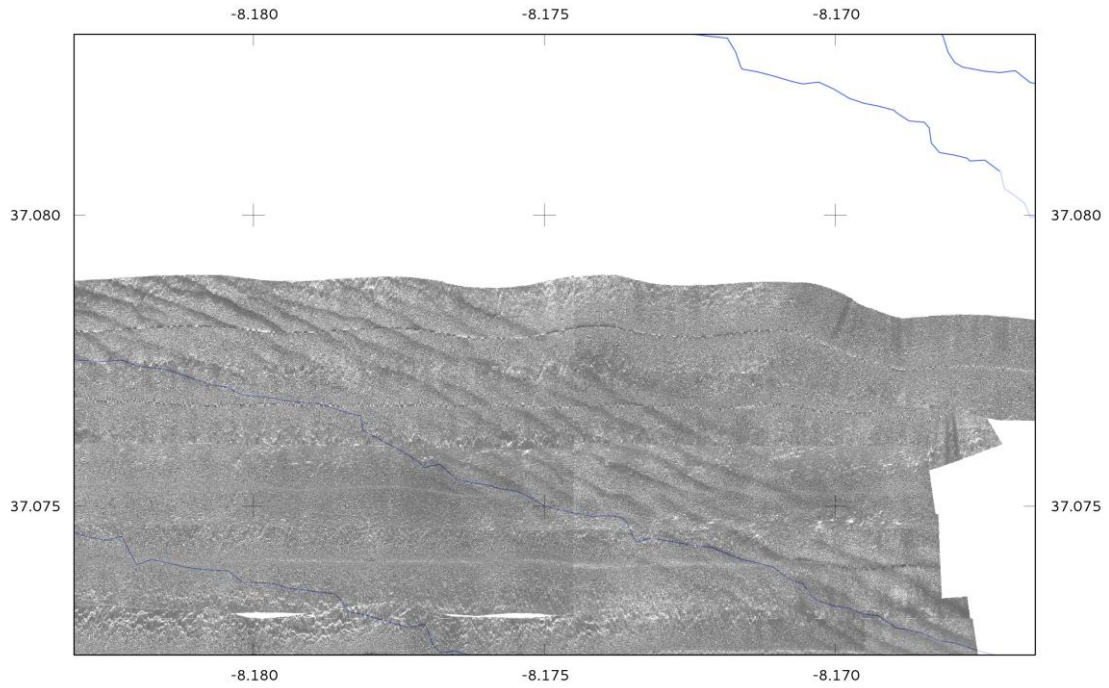

(a)

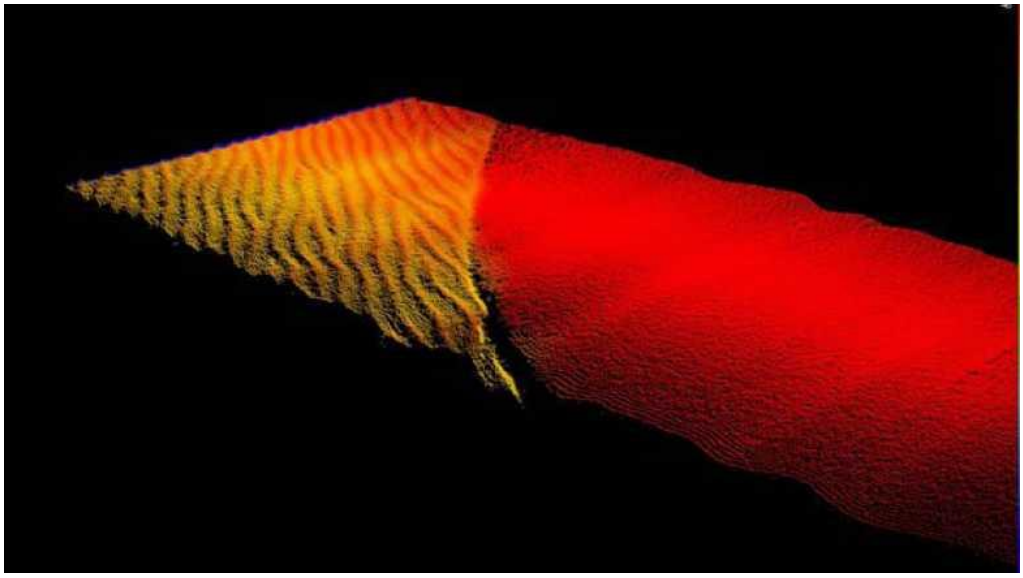

(b)

Fig.3.14 – Side Scan Sonar (a) and high res bathymetry data (b) show the ripple marks area and its sharp contact with the surrounding seafloor.

3.3.3 Seismic data interpretation

The main objectives of the seismic data interpretation were the following: i) establish the stratigraphic onshore-offshore correlation of the study area, ii) understand the environmental modifications that occurred during the Quaternary, iii) map and describe the neotectonics tectonic features, their origin, iv) relationship between neotectonics, sedimentary regime and environmental changes and v) understand the geologic control on the submarine freshwater discharges of Olhos de Água.

3.3.3.1 Offshore stratigraphic model

2011 seismic data have been integratedwith the 2010 ones because, despite their different resolution, are complementary: the high resolution CHIRP dataset highlighted the stratigraphic architecture of the Quaternary/Holocene formations; Sparker dataset, with lesser vertical resolution but deeper penetration, allowed the visualization of the upper portion of Miocenedeposits.

The interpretation shows that acomplex Quaternary/Holocene drainage system (highlighted only partially by the bathymetric data) is imposed on slightly deformedMiocene unit.

Seismostratigraphic interpretation of CHIRP profiles (FREEZE_2010 cruise) allowed the identification of four seismic units (U1 to U4), which correspond to ~12 m of sedimentary record, probably of Late Pliocene (?) and Quaternary age (Fig. 3.15 and 3.16):

- **Seismic unit U1** - This unit is bounded at bottom by the acoustic basement and truncated at top by horizon bc1 that records the first phase of channel incision. Internal configuration of the unit is stratified with parallel discontinuous high amplitude reflections, suggesting deposition in a low energy environment. This is the oldest unit imaged and could be tentatively correlated with Late Pliocene (?) and Early Quaternary siliciclastic sediments

- **Seismic unit U2** - This unit is bounded at its bottom and top by horizons that testified the beginning of two major phases of channel incision, respectively horizons bc1and bc2. Internal reflections are very discontinuous due to channels erosion and migration. Since the basal boundary of this unit, horizon bc1, is an erosional surface marked by channel incision, it could be correlated with a major sea-level fall and

consequent aerial expose of the inner continental shelf and erosion during the Late Pleistocene.

- **Seismic unit U3** - This unit is bounded by horizon bc2 at base and horizon R at top and shows a succession of several episodes of channel erosion, migration and filled-up by fluvial and/or littoral sediments. These episodes suggests interaction through the Late Quaternary and Holocene of estuarine and wave/tidal environments.

- **Seismic unit U4** – This unit is bounded at base by horizon R, a very continuous high amplitude reflection that truncates unit U3, and at top by the present-day sea-floor. Unit configuration is aggradational showing alternating parallel high- and low-amplitude reflections. Horizon R can be interpreted as a *ravinement* surface, probably Holocene, covered by marine/littoral sediments.

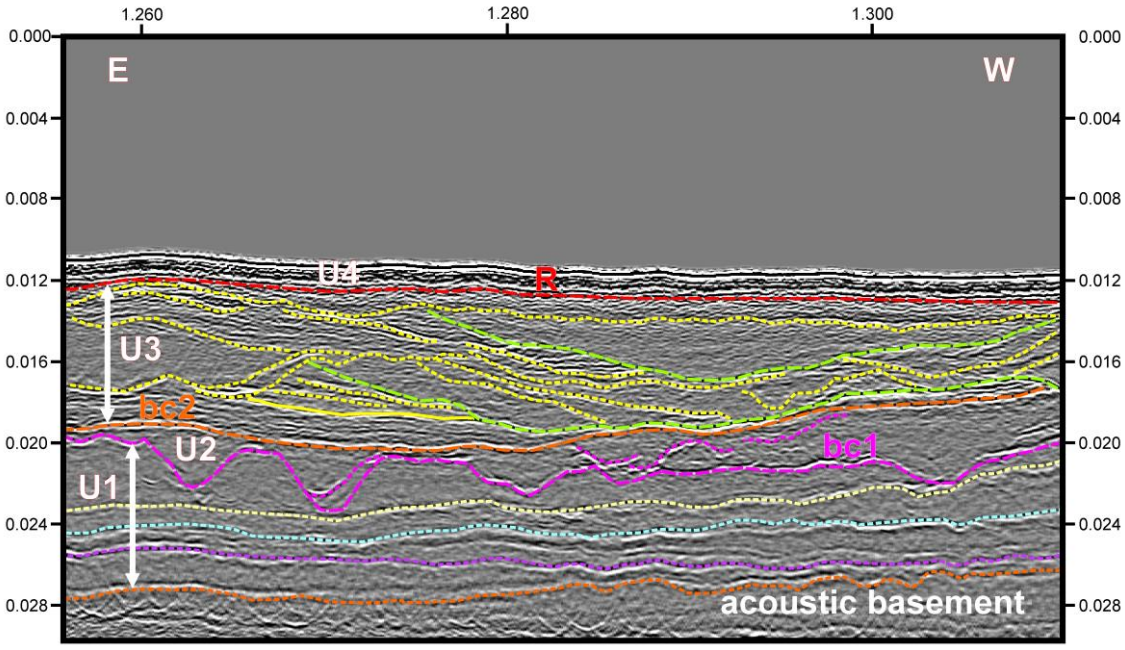

Fig. 3.15 – Section of interpreted seismic line Freeze_2010_L9. The sedimentary succession overlying the acoustic basement is about 12 m thick and composed of four seismic units (U1 to U4). The beginning of two phases of channel erosion is recorded by horizons bc1 and bc1. Horizon R can be interpreted as a ravinement surface. Vertical scale is in seconds TWT.

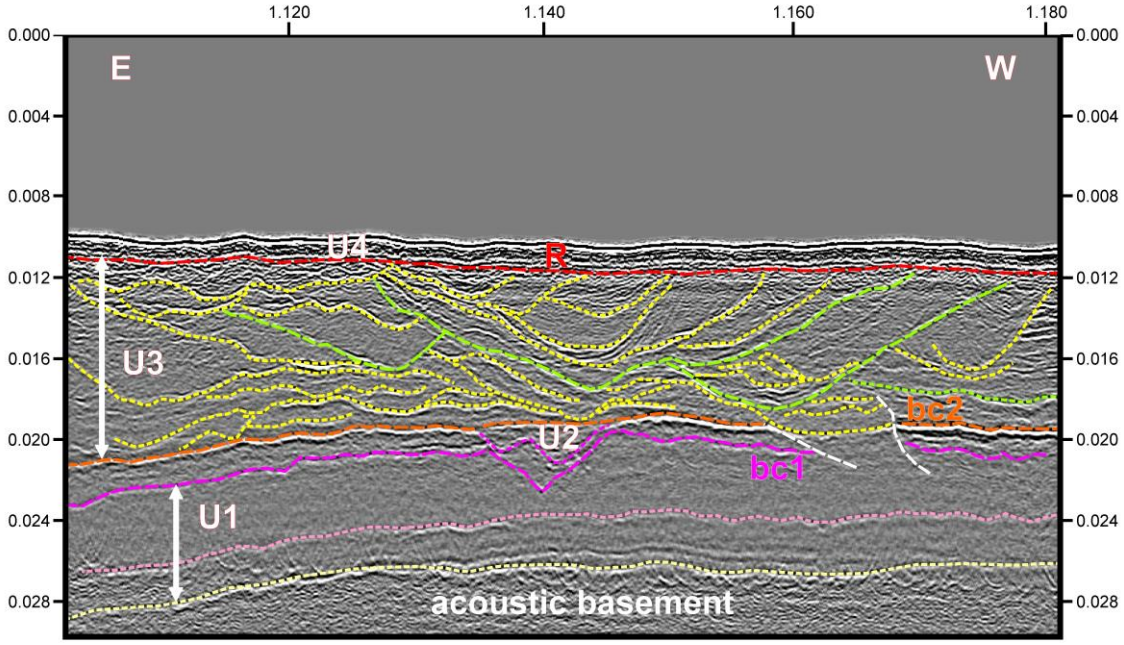

Fig. 3.16 – Section of seismic line FREEZE_2010_L9 showing detailed interpretation of seismic unit U3. This unit presents a complex geometry due to the succession of several episodes of channel erosion, migration and sediment-fill. Vertical scale is in seconds TWT.

Seismostratigraphic interpretation of SPARKER profiles (FREEZE_2011 cruise) allowed the identification of three seismic units (Ua to Uc), bounded at base, respectively by horizons H1 to H3 (Fig. 3.17).

- **Seismic unit Ua** – This unit overlies horizon H1 and shows progradational configuration. It is truncated by horizon H2, a lower amplitude and discontinuous reflection.

- **Seismic unit Ub** – This unit overlies horizon H2 and as the previous one shows progradational configuration.

- **Seismic unit Uc** – This unit is bounded at base by horizon H3, a low amplitude and very discontinuous horizon. No internal reflections are clearly identify, except in the seaward part.

The oldest horizon identified is horizon H1, which is high amplitude discontinuous reflection showing evidences of erosion. Considering the regional lithostratigraphy it could be correlated with the top of Miocene karst. The overlying seismic succession probably is of Pliocene through Quaternary age.

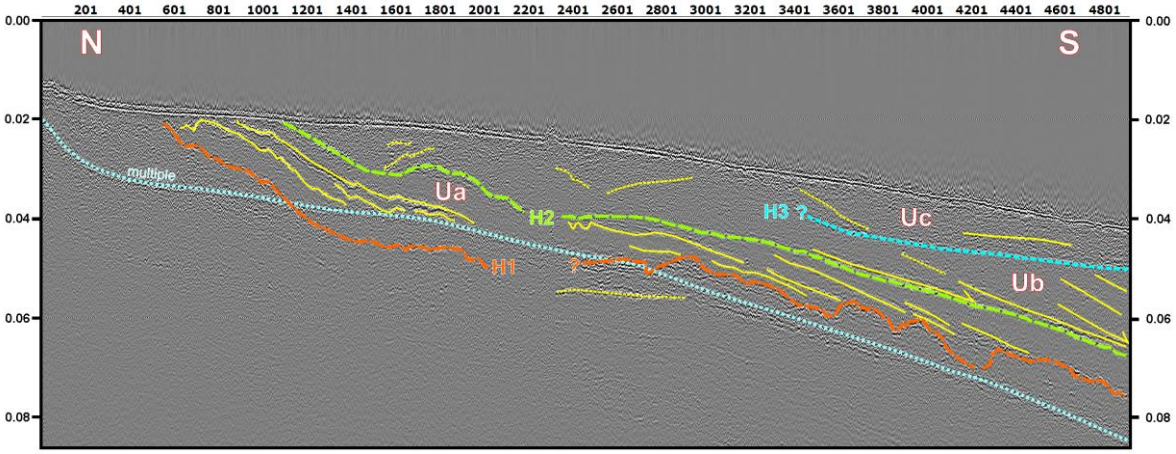

Fig. 3.17 – Interpreted seismic line FREEZE_15_2011. The sedimentary succession overlying the multiplereflector is about 32 m thick and composed of three seismic units (Ua to Uc). Vertical scale is in seconds TWT.

A tentative correlation between the seismostratigraphic models of Freeze_2010 and Freeze_2011 datasets is presented in Fig. 3.18. A more accurate correlation can only be done with strong age control of seismic horizon and/or seismic units based on coring and dating of sediments.

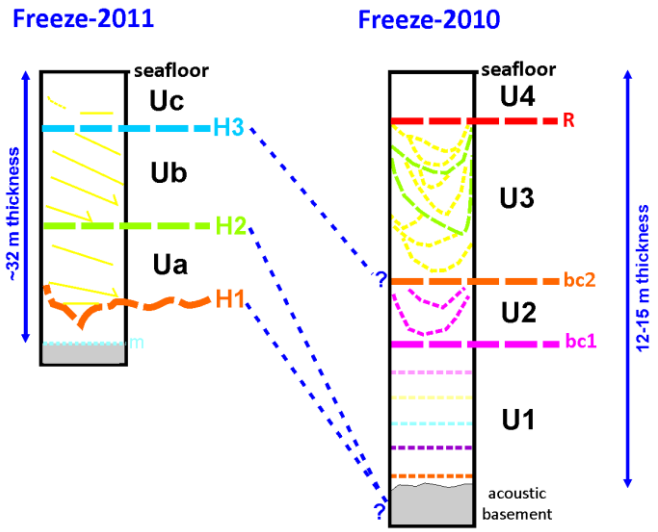

Fig. 3.18 – Seismostratigraphic columns for FREEZE_2010 and FREEZE_2011 surveys. A tentative correlation between horizons is presented.

Seismic data analysis reveal, between 10 and 30 m water depth, the presence of a complex depositional morphology and erosive features overlying locally karsted and/or deformed Miocene deposits.

The sedimentary architecture shows the presence of a very articulated drainage system with the presence of migrating paleochannels and characterized at its base by an erosional surface marked by channel incision. This erosional surface could be correlated with a major sea-level fall and consequent subaerial exposure of the inner continental shelf and erosion during the Late Pleistocene. In addition the beginning of Quaternary coincided with global thermal cooling and the occurring of important sea level changes. As a consequence of that, hydrographic networks have been heavily changed and rivers cut deeply the morphology during low-stand stages. Mean sea level during last maximum glacial (LGM) (19.3 and 18.3 Ky, Shanfeld et al 2003) was 120-140 meters below the present one. Ocean water temperature at the end of Pleistocene was lesser than 5-12ºC respect the Holocene mean temperature that was 27ºC approximately (Abreu et al., 2003).

The rising temperature after the LGM caused the retreat of ice sheets to higher latitudes and the sea-level rised very quickly (1,2 m/century) at about 15 Ky. A cooling episode and associated sea-level of fall occurred during the Younger Dryas at 13-11Ky (Dias J. et al., 2000).

Late Quaternary sea-level changes acted as the main control and modeling factor for the development of most depositional and erosional morphologies of Southern Portugal proximal continental margin (Roque et al., 2010) as Olhos de Água offshore shows.

3.3.3.2 Seafloor sediment distribution model

Taking into account the complex sedimentary architecture highlightedby seismic interpretation, the side scan sonar evidences of high variability in sediment distribution and integrating the seafloor lithological mapping presented by Teixeira & Macedo (2001), an hypothetical profile from the shore towards south in Pedra dos Arrifes longitude would show the following main features:

i) the presence of the actual abrasion platform modeled in Miocene rocks (up to 4-5m depth);

ii) the presence of an extensive abrasion platform modeled during the late Pleistocene and retouchedin the Holocene, with conglomeratic and coarse

calcarenites outcropswhich tend to become fine grained calcarenite for depths deeper than 8-10 mt;

Despite the lacking of sediment cores and grabs the info deriving from Teixeira & Macedo (2001) work allowed the following proposed the sediment distribution reconstruction:

iii) 5-18 mt depth (Pleistocene abrasion platform) the sediment cover is made by discontinuous deposits of uncalibrated calcarenite gravel and of fine grained sand. The first ones originated by adjacent rock blasting and the second resulting from scattered accumulations of sediments transported in suspension.

iv) 18-30 mt depth (Pleistocene abrasion surface sliced in medium and fine calcarenites), the sediment cover is made byrelic coarse reddish and brownish sands with 25 % bioclastic fraction and 0.5 to 2.5 m thickness. Relic sands form ripple marks trending NW-SE, have wavelengths between 50 cm and 1 m and 10-20 cm height, with coarser material located in the depressions and thinner sediments in the crests.

v) > 30 m depth the first muddish sand spots appear.

vi) The sedimentary cover is made by fine to medium sand deposits that constitute the most recent sedimentary coverage. They occur in small discontinuous spots in the entire area and correspond to transition sediments towards submarine beach fine sands.

3.3.3.3 Offshore tectonic model

Erosive features and complex depositional stacking patterns are clearly shown in the seismic lines. Structural discontinuities and, in few places, faults are also recognized even if, sometimes, the dipping of the faults plains could not be detected by our very shallow seismic. Here we propose the possible correlation between the offshore and the onshore structural settings.

Miocene tectonics probably associated with diapirism are shown (faulting and synformal folding due to salt withdrawal) as well as important intra-Miocene erosive discontinuities between Albufeira and Olhos de Água. Some of these fractures may control the Olhos de

Água freshwater submarine discharges. In addition thrust faulting in the Carcavai fault and Ribeira de Quarteira has been also identified.

To better constrain the offshore tectonic examination the study area has been extended toward east where major regional faults are present and have been investigated in cooperation with the European Project TOPOMED.

This work would deserve further investigations but here the main obtained results are summarized as follows (see Fig. 3.19):

i) the stratigraphic interpretation of Albufeira-Olhos de Água shows a great deal of internal erosion within the Miocene formations, with a larger degree of incision than was expected or described by the onshore previous works;

ii) the tectonic deformation by folding visible in the seismic profiles is compatible with salt withdrawal at the Albufeira diapir;

iii) the Ribeira de Quarteira estuary prolongates to the southeast which means it has been submerged.

iv) the prolongation of the Carcavai fault Carvalho, Matias et al. (2012) was mapped and is considered active as reported by Noiva, Duarte et al. (2010);

v) despite no clear evidence of tectonic control from field work, inspection of the seismic lines, let us presume the existence of a transfer fault in the Miocene formations in the area of Olhos de Água (Terrinha et al., 2014); whether this fault controls the location of the submarine freshwater discharges is not known.

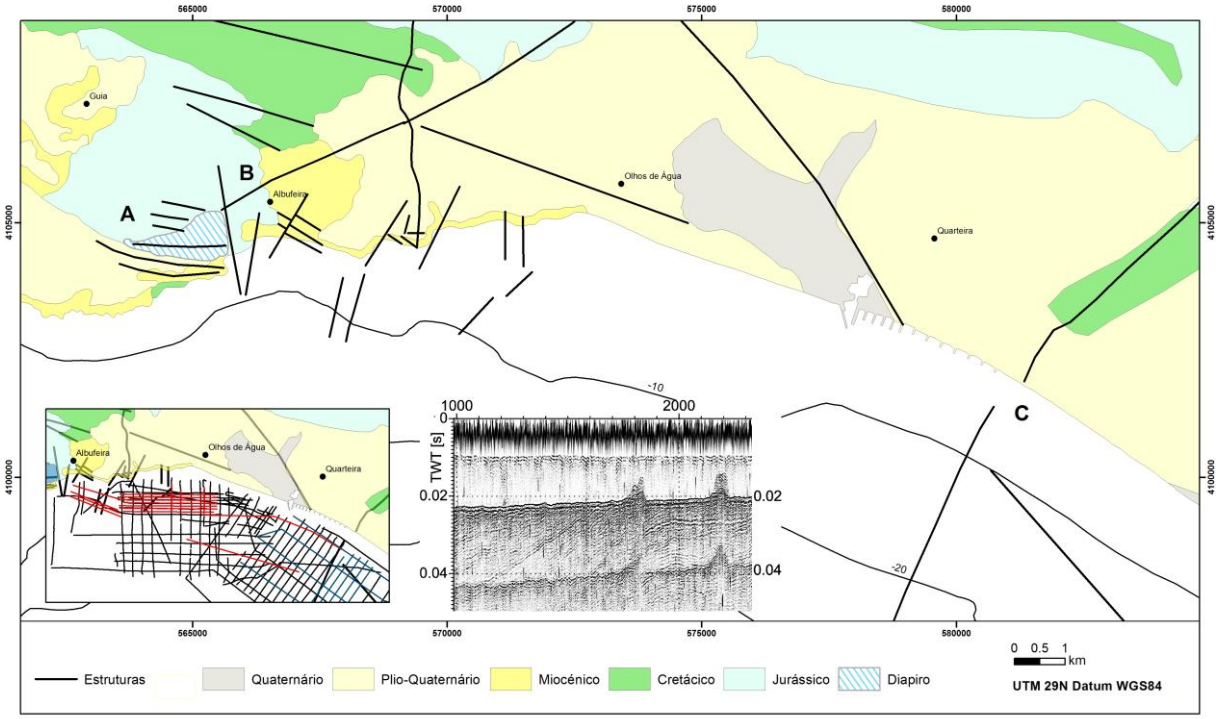

Fig.3.19 – Integrated onshore-offshore structural map of the study area. The main features are: i) the west region of Albufeira shows the pre-Miocene compression (A); ii) the Albufeira strike-slip fault in Quaternary was a transfer fault during the Miocene inversion and works as a normal fault during Mesozoic extension (B); iii) the Carcavai strike-slip fault during the Miocene inversion is in Quaternary a thrust fault (C). The inset map shows the seismic surveys done in the study area: blue lines are Sparker single channel profiles from ERSTA-SANDEX 2008 cruise, red lines are CHIRP single channel profiles from FREEZE 2010 cruise and black lines are Sparker single channel profiles from FREEZE-TOPOMED 2011 cruise.

3.3.4 Water column perturbation: possible SGD signatures

Additional information comes from the analysis of water column seismic images available on raw seismic data. We observe, in some places, an alteration of the seismic signal starting from seafloor bottom and rising toward the sea surface forming a sort of plume.

These signals are sometimes scattered along the same profile and sometimes form little clusters. Their presence and shapes could reveal the action of fluid escapes from the seafloor and in our perspective could be related to SGDs activity.

The signature visible on raw data (both chirp and sparker) presents the following characteristics:

- Possible plume (A): isolated strongand sharp perturbation made by a lot of diffraction hyperbolae inside water column. The signal starts from seafloor and ends in the middle of water column resembling a whale blow. This kind of signals is present on both CHIRP and SPARKER profiles. (Fig. 3.20).
- Suspect plume (B): sharp perturbation with diffraction hyperbolae, weaker respect the previous, and usually forming clusters. Sometimes those signals cross the whole water column. The signal is present on CHIRP profiles only (Fig. 3.20).
- Acquisition/environmental noise (C): sharp signals that cross the whole seismic section. This signal is present with this aspect on CHIRP profile only. On SPARKER profiles the noise is represented by scattered spikes. (Fig. 3.20).

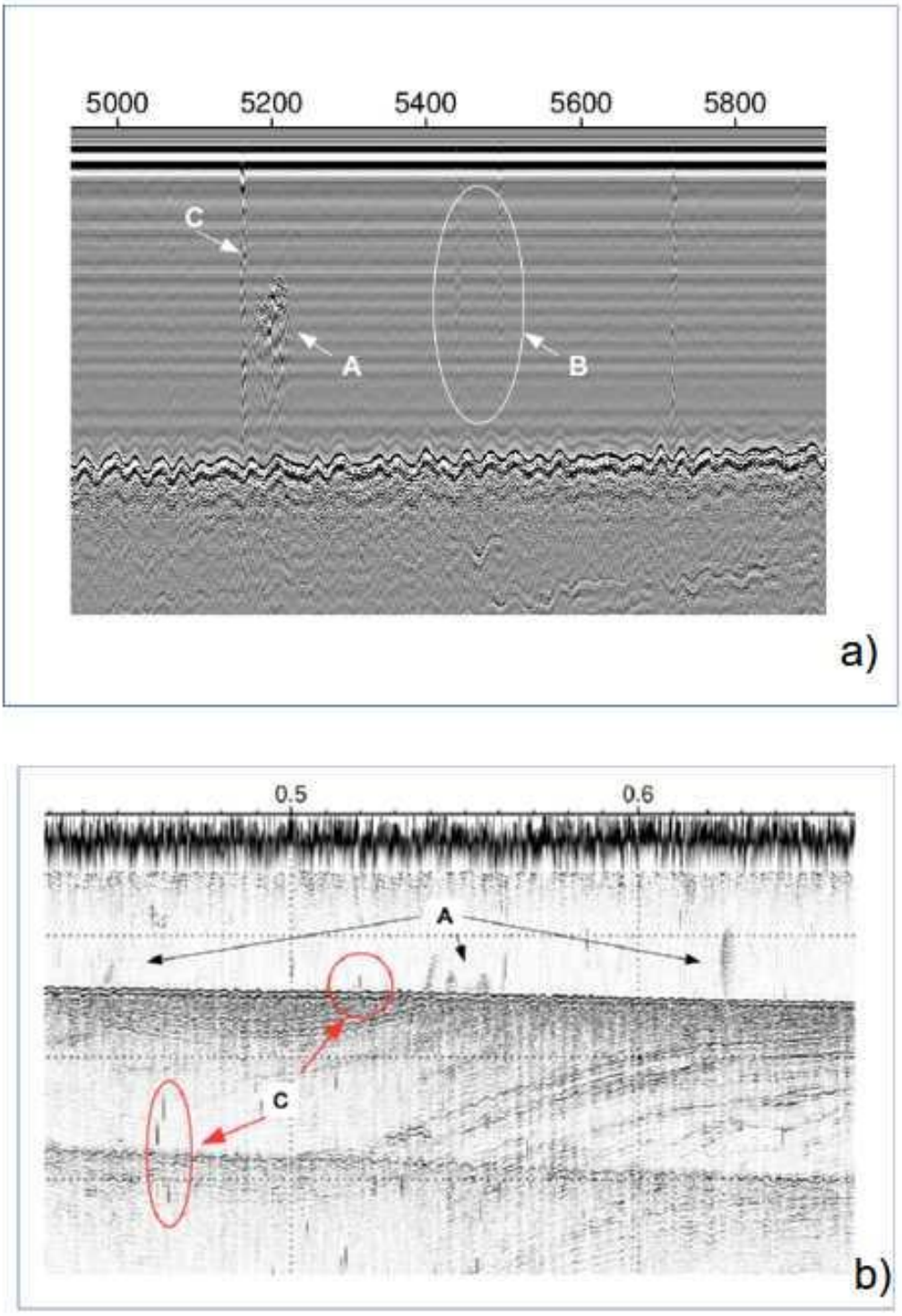

Fig. 3.20– Examples of different acoustic signals present on the analyzed seismic data.

(a) CHIRP data (FREEZE-2010). (b) SPARKER data (TOPOMEDFREEZE-2011).

After an accurate analysis of all available seismic profiles we present hereafter the possible SGDs' location in the study area (Fig 3.21).

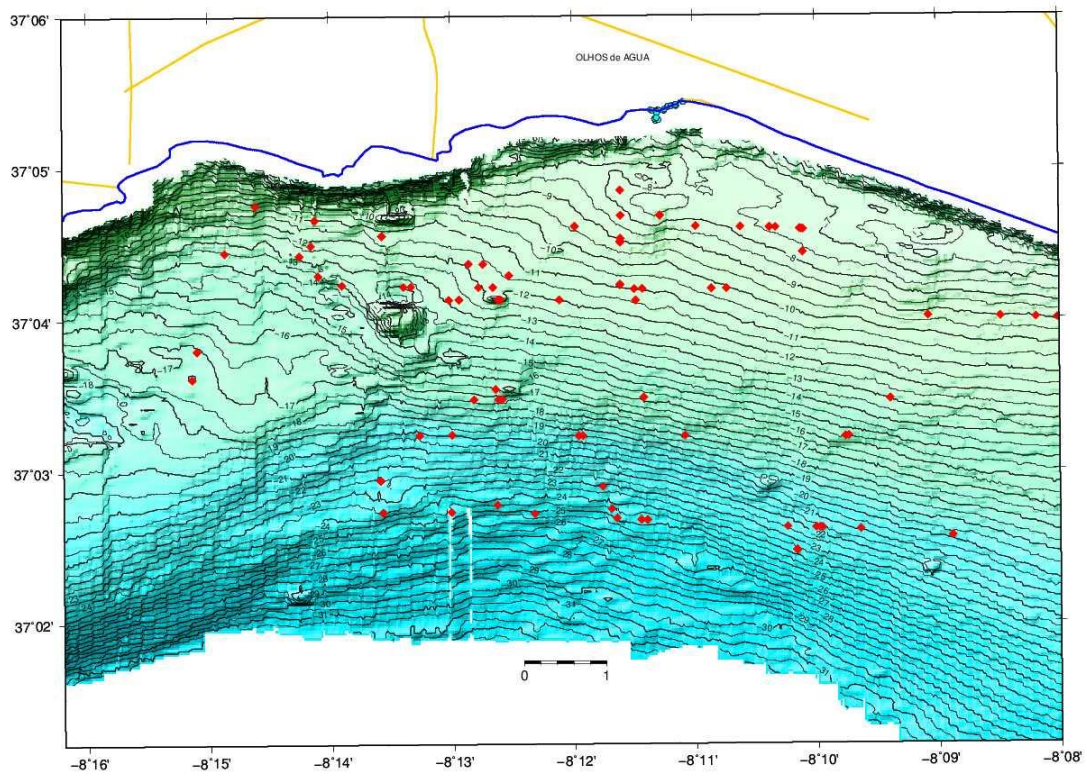

Fig. 3.21 – SGDs´ location offshore Olhos de Água derived from the seismic datasets. The yellow lines onshore indicate the neotectonic faults in the area.

SGDs are mainly distributed along two bathymetric corridor: between 7 and 12 mt depth and between 15 and 25 mt depth.

Local hydrogeological and geomorphologic characteristics are favorable to DAS existence since water-bearing formations composed by detritic-carbonate rocks from Miocene (visible on beach outcrops where are located the Olhos de Água springs), which gives support to groundwater flow, extends to the continental shelf with a slight slope towards S-SE, which also corresponds to the direction of groundwater flow.

After the cool period called Younger Dryas (13-11 ky BP) a period of fast sea level rise initiated around 10 ky to 8000 yearsBP (before present), when the relative mean sea level (RMSL) approached -20 mt depth (Dias et al. 2000). This transgressive regime forced the coastal line to retreat from 60 mt depth to actual position, when mean sea level is the same since ca 3500 y B.P. (Dias et al. 2000). Between present 60 and 40 mt depth, submersed

morphologies such as (abrasion platforms, beaches and isthmuses) indicating the presence of a paleocoast line, have been detected by Dias et al. (2000). Teixeira (1998) described a series of aligned submersed shore scarps along the southern coast of Algarve. One of those, located in front of Olhos de Água and called “Pedra dos Arrifes” at -13 mt depth, could evidence an Holocene paleocoast line existing when mean sea level lay 20 mt depth at 8000 years ago. Since 3500 years BP Holocene geological setting, hydrography distribution and hydrogeology conditions have been supposedly similar to the present ones. Also the paleosurface and groundwater flow would have been toward south as observed in seismic profiles, with preferential water flowpaths up to 60-40mt depths, and most recently, of 20 mt depths, where springs occurred probably close to the paleocoast lines.

This paleocirculation is still active and is more significant as recharge on land increases with the subsequent increasing of the aquifer potential, the permeability of water bearing formations and the highest concentration of the flow of the DAS.

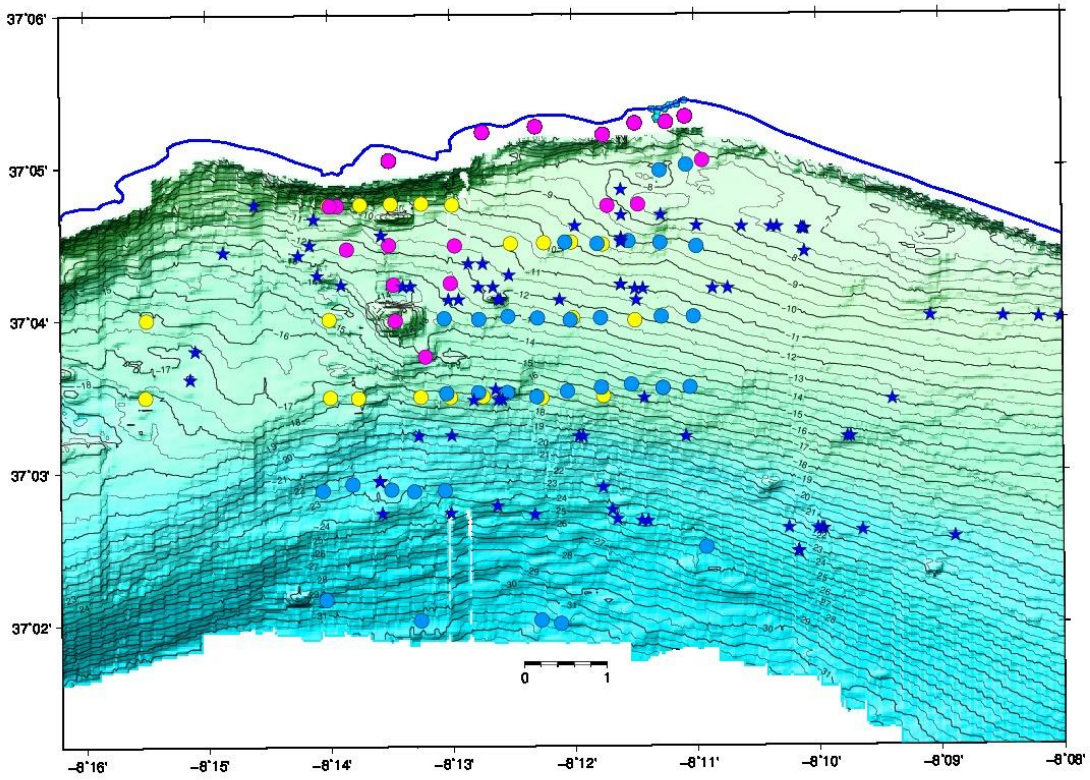

Fig. 3.22 – SGDs occurrence derived from the seismic datasets and CTD data. Blue stars indicate possible SGDs detected along seismic profiles; light blue, violet and yellow circles indicate low salinity values detected in CTD surveys (Nov2012, April2013 and Nov2013 respectively).

The main control for SGDs presence seems to be geomorphological and linked to the paleocoastal lines existing in the study area. What is permitting this mechanism to be continue and active? Probably similar lithological sequences are repeating through geological time and are present along the older and submersed coastlines. In addition some possible tectonic lineaments depicted in seismic data and bathymetric evidences could control SGDs location and their discharge flow rate (see Fig. 3.23).

This last topic constitutes a work in progress.

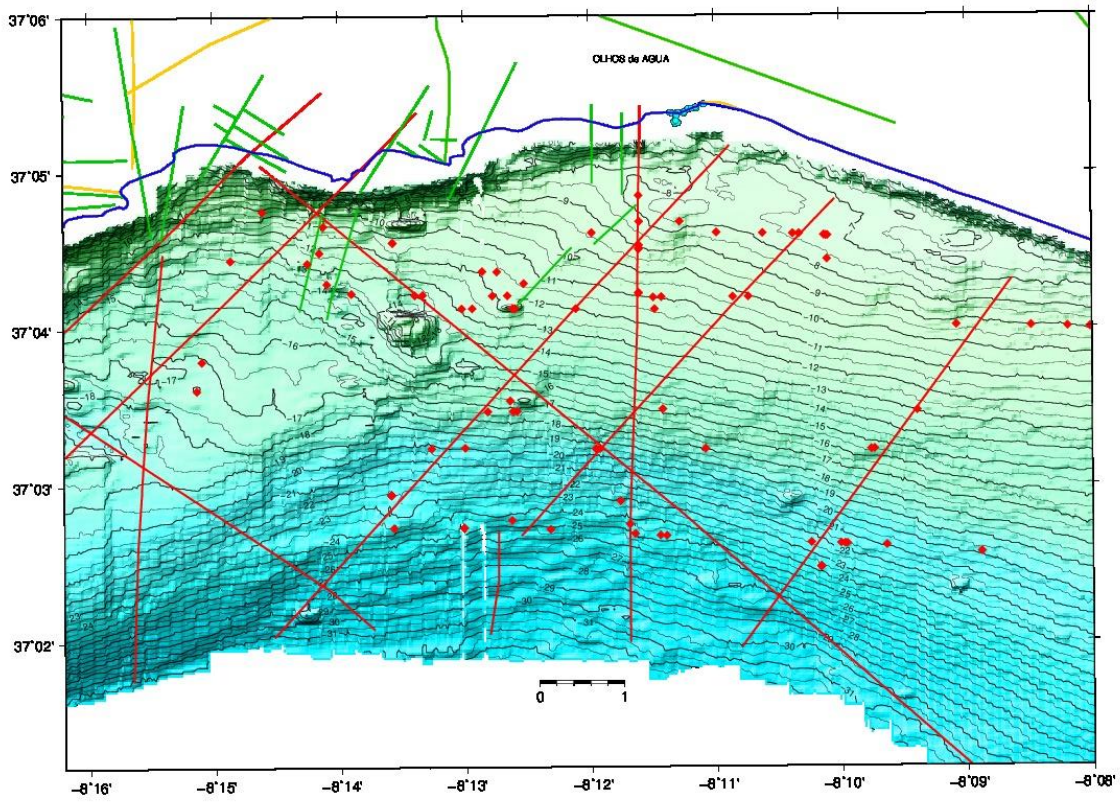

Fig. 3.23 – SGDs occurrence derived from the seismic datasets (red dots), 2 lineaments sets parallel to the onshore joints direction (NE-SW and NW-SE) and 1 N-S lineaments set parallel to the N-S main faults (red lines) and onshore/offshore main faults (green lines).

4. TASK 3 – Oceanographic setting of the submarine groundwater discharges

4.1 Objectives

The objective of this task consisted in the identification of the submarine groundwater discharges (SGD) over the continental shelf in the region of Olhos de Água, Algarve, and the characterization of the physical properties of the waters coming from the submarine springs.

To achieve the aforementioned objectives, an oceanographic campaign in the region of Olhos de Água was planned, and the location of that campaign was based on the geographical location of the slick identified on the SAR image obtained on 9 February 2010, at 10:43 UT (see Fig. 5.2 on Task 4). The region where the campaign should take place would cover the area where the potential SGDs could be found, but also in the surrounding waters with coastal oceanic thermohaline properties.

4.2 Oceanographic Surveys

Since November 2012 through November 2013, three CTD surveys were conducted in the Olhos de Água area, on board the "ECORECURSUS I" boat belonging to the Centro de Ciências do Mar da Universidade do Algarve (CCMAR/UAlg). The small size of the boat forced to operate inside the limit of 3 nautical miles (≈ 5.6 km) from the coast, thus restricting the area under study in the initial plan. A new acquisition work plan had to be established, with a much narrower net of CTD stations than the previous plan.

During the first survey, which took place on 6-7 November 2012 (from now on identified as 11/2012 survey), 59 CTD stations were carried out over the continental shelf off Olhos de Água, with depths ranging from 8 to 30 m. The whole station plan was not completed on the first day of the survey, and the bad weather conditions and increasing wave heights on the following day, did not allow covering the area nearer the coast. These 59 CTD stations are represented by yellow marks on Fig. 4.1.

The second campaign, planned with the scope of completing the previous survey, took place on 9-10 April 2013 (from now on identified as 04/2013 survey). 42 CTD stations were carried out in a very shallow area, with depths ranging from 2 to 14 m. These stations are

represented by light blue marks on Fig. 4.1. The location of the 101 (59+42) CTD stations carried out in the Olhos de Água area, during both surveys is presented in that figure and the area covered by the slick, identified on the SAR image (see Fig. 5.2 on Task 4) is also represented in Fig. 4.1 by a red circle.

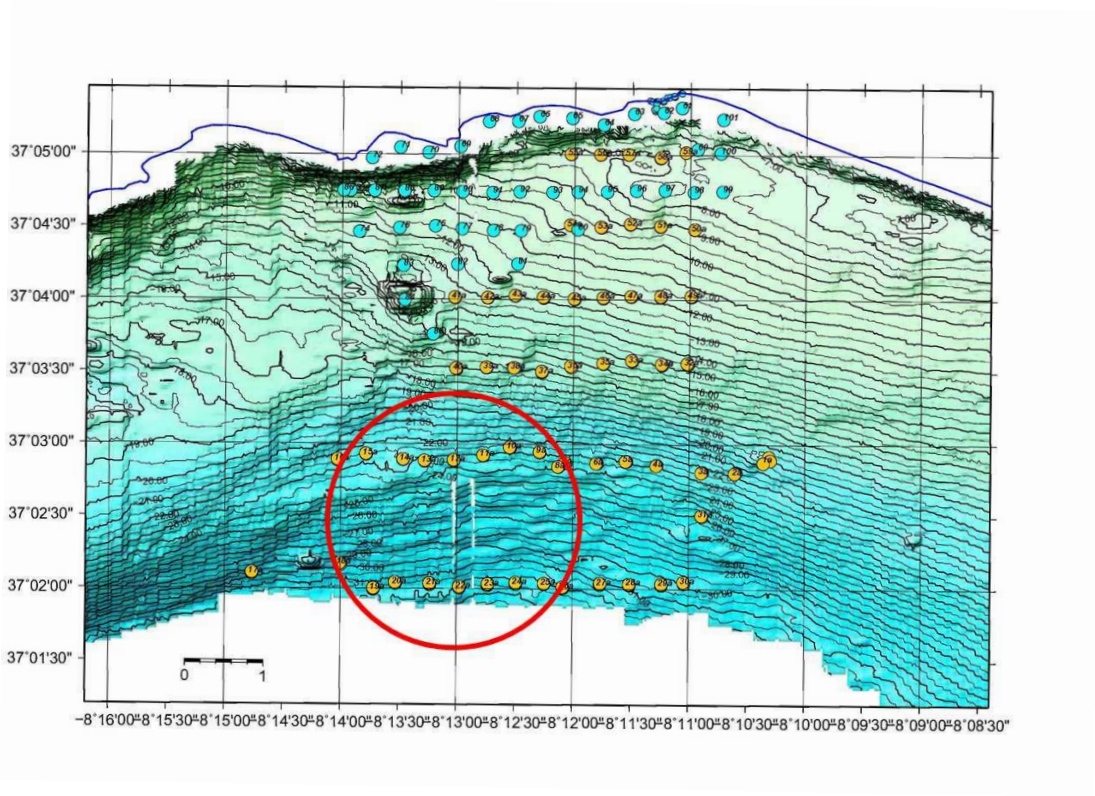

Fig. 4.1 - Location of the 101 CTD stations carried out in the Olhos de Água area, during the 11/2012 and 04/2013 surveys, represented as yellow and light blue marks, respectively. The red circle represents the area covered by the slick identified on the SAR image obtained on 9 February 2010.

On 11-12 November 2013, a third oceanographic campaign (from now on identified as 11/2013 survey) was carried out aiming to repeat the stations where the analysis of the CTD data from the two previous surveys, revealed the presence of salinity minima in the water column, thus indicating the presence of SGDs. In this third CTD survey, 95 stations were carried out: 65 in the Olhos de Água area (the same area covered in the previous surveys), 20 stations located to the west, just in front of the Albufeira Marina (or the Albufeira diapir) and 10 more stations located to the east, in front of the Falésia beach (between the Alfamar Hotel and the Vilamoura Marina). All these stations are identified as red marks in Fig. 4.2.

The “Albufeira Marina” and “Falésia beach” areas were chosen as locations where supposedlythere are no submarine springs, constituting then “non-SGDs referee places”. These non-SGDs areas will help in the identification of waters with a coastal oceanic origin in contrast with the waters influenced by submarine springs over the continental shelf off Olhos de Água.

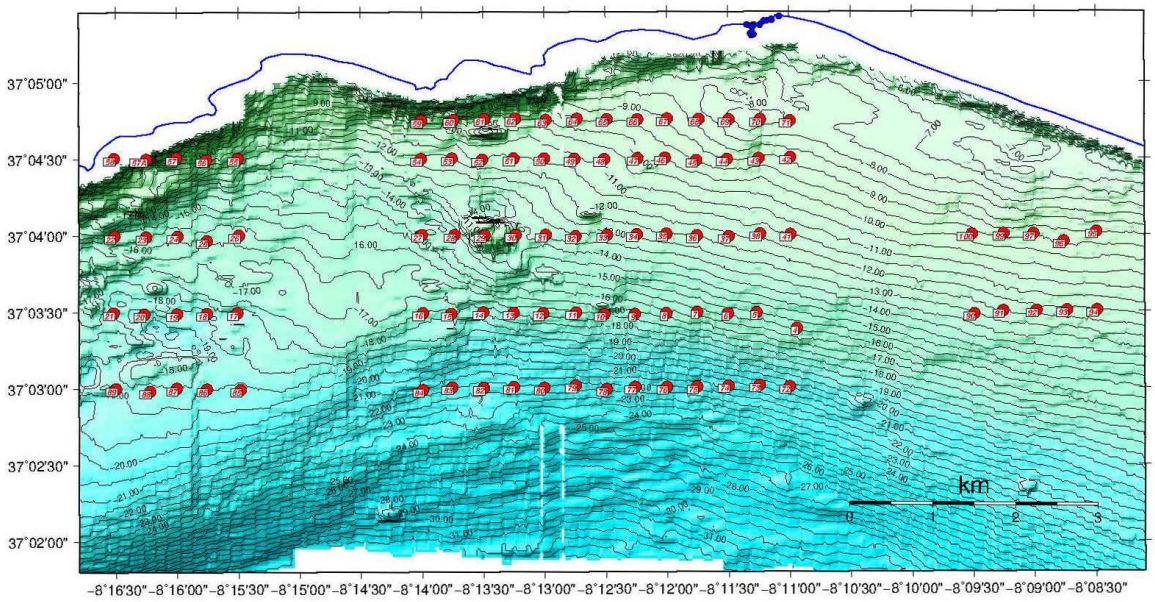

Fig. 4.2 - Location of the 95 CTD stations carried out during the 11/2013 survey (65 stations in the Olhos de Água area, 20 stations in the Albufeira Marina area and 10 stations in the Falésia beach area).

The positioning system used during the first survey was a Garmin GPSMAP® 60CSX without differential correction. In the second survey, a combined GPS positioning system and depth controller (GPSMAP® 421s) was installed on board for the first time and was successfully tested during the campaign. This equipment was also used in the third survey.

In the three campaigns temperature, pressure and conductivity data were collected with a NXIC (Non-eXternal Inductive Conductivity) CTD of Falmouth Scientific, Inc. (FSI, EUA). The analysis of the aforementioned parameters allowed the identification of places on the continental shelf with influence of waters coming from submarine springs, which present hydrological characteristics different from the ones from coastal oceanic origin.

4.3 Results

The observations carried out during the 3 surveys constitute the first CTD data base gathered on the continental shelf off Algarve, in an area very close to the coast, reaching the maximum depth of 30 m.

The CTD data gathered during the first two surveys was processed and analyzed and very interesting results were achieved. The temperature, salinity and sigma-t (density) profiles as well as the temperature-salinity (T/S) diagrams were drawn for each one of the 101 CTD stations carried out during the 11/2012 (59) and the 04/2013 (42) surveys. The scatter T/S diagram with all the stations of both surveys is presented in Fig. 4.3.

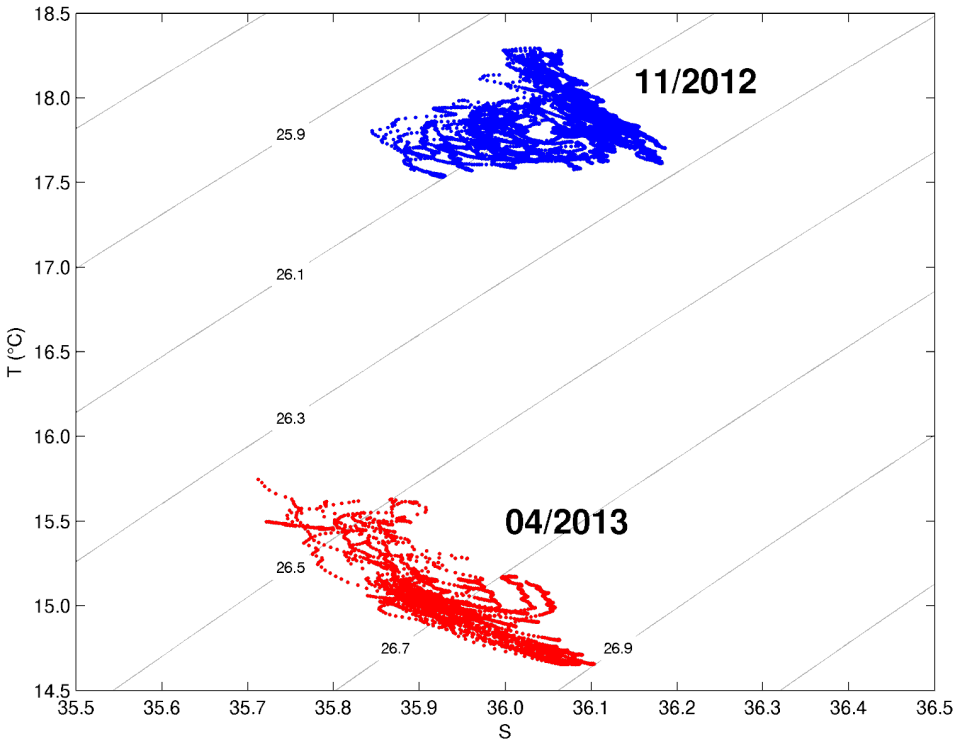

Fig. 4.3 – T/S diagram with all the 101 (59+42) CTD carried out during the 11/2012 and 04/2013 surveys.

The analysis of Fig. 4.3 shows that the salinity values are practically the same in both surveys, being the salinities found in the 11/2012 survey, 0.1 higher than the ones observed in the 04/2013 campaign. The difference between the temperatures observed during the two campaigns is about 3.0ºC. The survey 11/2012 took place during a summer-winter transition

situation of a relatively dry and hot year, with sea water temperatures ranging from 17.5 to 18.5ºC. The 04/2103 survey took place immediately after the oceanographic winter, and the sea temperatures show low values, ranging from 14.5 to 16.0ºC, probably reaching the lower sea temperatures all year around.

The data gathered during each survey will be analyzed separately.

4.3.1. Survey 11/2012 and Results

The scatter T/S diagram with all the 59 CTD stations carried out during the 11/2012 survey is presented in Fig. 4.4.

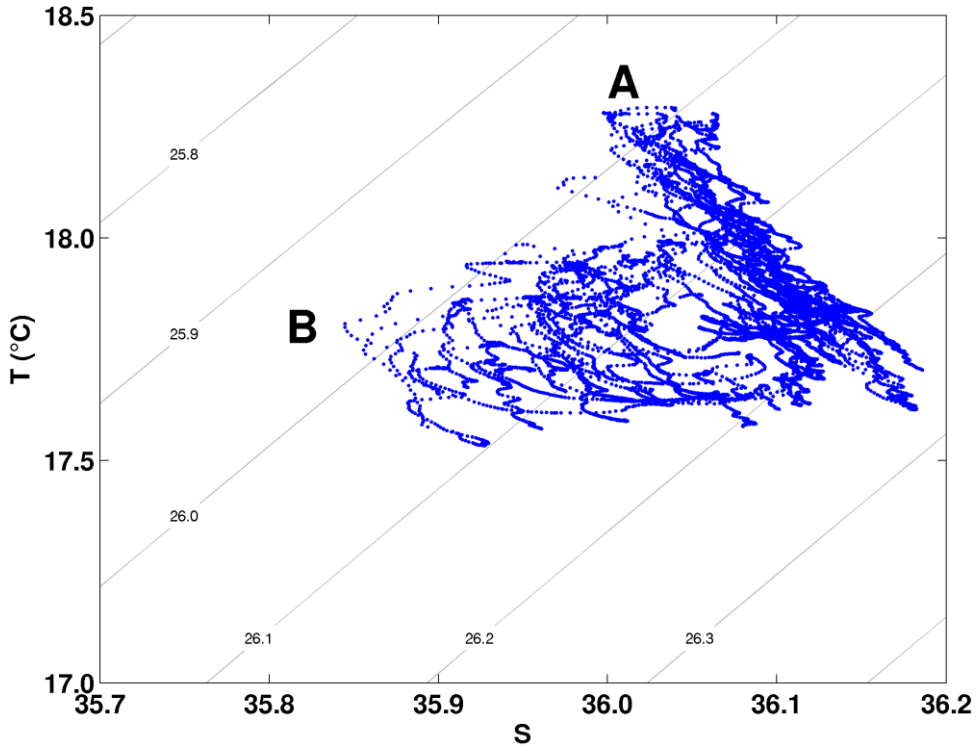

Fig. 4.4 – T/S diagram with all the 59 stations carried out during the 11/2012 survey.

It is interesting to note that the T/S diagrams are grouped in two distinct patterns. The stations refereed with an A on Fig. 4.4 present the highest salinity values in the whole water column, with sigma-t values slightly increasing with depth, they correspond to the stations located in the two more offshore sections (37º 02' 00 and 37º 03' 00 N – see Fig. 4.1 for location) and they have characteristics of coastal ocean stations.

The other stations, identified with a B on Fig. 4.4, present T/S diagrams completely different from the ones mentioned above, with instabilities in the water column (showing sigma-t inversions) probably associated with vertical mixing with submarine spring waters. The lowest salinity values were observed on these stations, thus reinforcing the influence of less saline waters coming from the submarine groundwater discharges.

Fig 4.5 shows an example of the behavior of the temperature and salinity along the water column for one station classified in the group A, with coastal oceanic characteristics (blue profile, depth of about 30 m – stn. 22) and another one belonging to group B, with influence of water coming from submarine springs (red profile, depth of about 10 m – stn. 43).

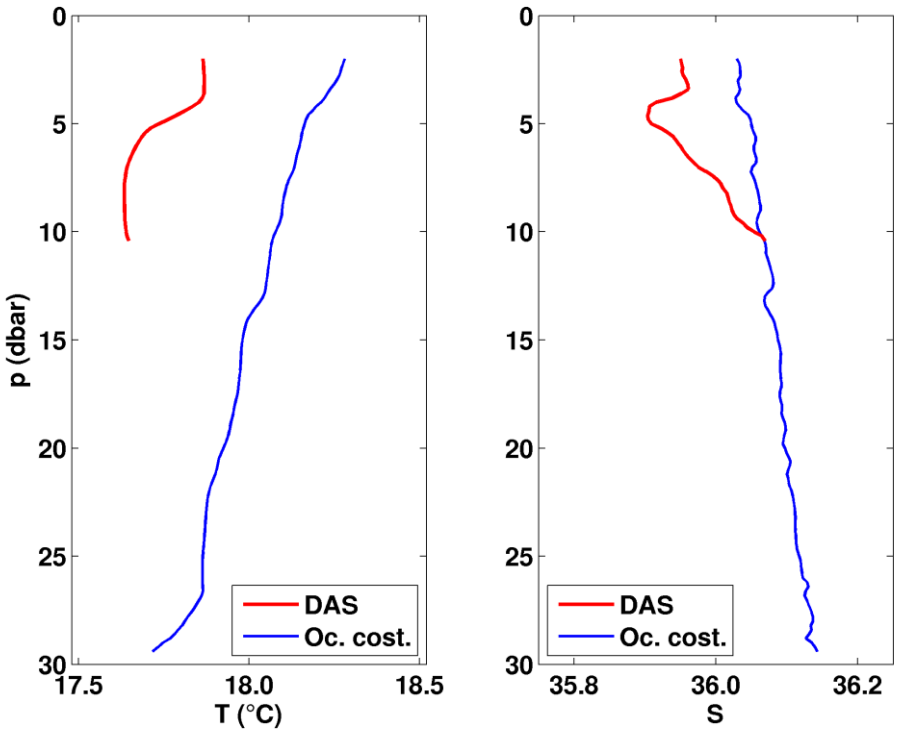

Fig. 4.5 – Temperature and salinity profiles obtained in an oceanic coastal station (in blue) and in another station influenced by submarine groundwater discharges (in red) during the 11/2012 survey.

Fig. 4.5 shows a small decrease in the temperature and a slightly increase in the salinity from surface to bottom in the coastal oceanic station (blue profiles), but in the shallow station (red profiles) it should be noted the presence of a salinity minimum at 5 m depth, with a

correspondent decrease in temperature. This could be a consequence of mixing with waters coming from SGDs.

Profiles with salinity minima were recurrent in all the stations with T/S diagrams referred with B in Fig. 4.4. Salinity variations of $\Delta S \geq 0.03$ were found in 33 stations with the salinity minimum located between 3 and 12 m depth.

4.3.2. Survey 04/2013 and Results

The T/S diagram with all the CTD stations (42) carried out during the 04/2013 survey is presented in Fig. 4.6.

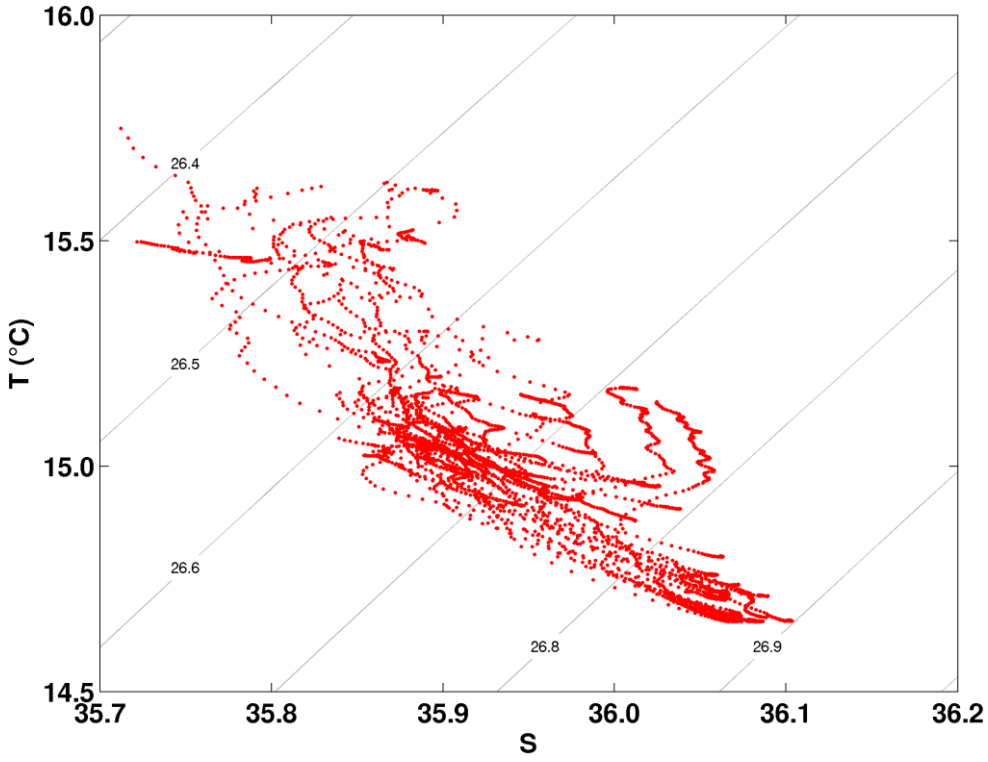

Fig. 4.6 – T/S diagram with all the 42 stations carried out during the 04/2013 survey.

It should be mentioned that all the stations carried out during the 04/2013 survey are very shallow, the maximum depth is 14 m, and the locations are very near from the coast (see the light blue marks in Fig. 4.1).

The T/S diagrams presented in Fig. 4.6 show a similarity with the patterns revealed in the previous survey (see Fig. 4.4), being evident that the coastal oceanic stations present the lowest temperatures (14.5-15.0ºC) and, as a consequence, the highest values of sigma-t. The stations where the lowest salinities were reached also show instabilities in the water column, and inversions in the density field (see Fig. 4.6).

Fig. 4.7 presents the temperature and salinity profiles obtained in one station with influence of submarine groundwater discharges (stn. 84 in red) and in another station with coastal oceanic characteristics (stn. 91 in blue) during the 04/2013 survey.

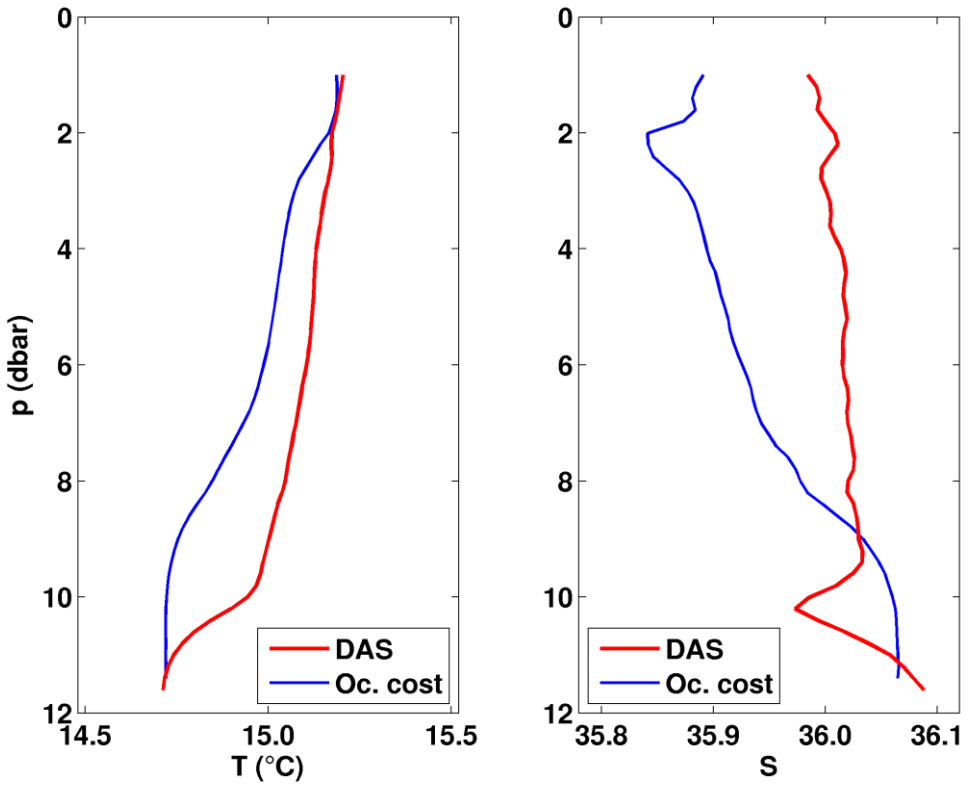

Fig. 4.7 – Temperature and salinity profiles obtained in an oceanic coastal station (in blue) and in another station influenced by submarine groundwater discharges (in red) during the 04/2013 survey.

The coastal oceanic station presents a small decrease in temperature and a slightly increase in salinity from surface to bottom (blue profiles in Fig. 4.7) as happened in the first survey. In

the station with influence of water coming from submarine springs (red profiles in Fig. 4.7) there is a salinity minimum at 10 m depth with the correspondent temperature decrease.

The analysis of the profiles presented in Fig. 4.7 shows that the temperature and the salinity values obtained in the coastal oceanic station are lower than the ones obtained in the station influenced by the SGDs, which seems a bit contradictory, especially in the salinity field.

The temperature values being higher in waters influenced by SGDs is reasonably as very often the submarines springs present higher temperatures than the surrounding coastal oceanic waters, mainly if the observations were conducted in winter, when the lowest temperature values are reached. It is interesting to note that the water temperature measured at the submarine springs located at the beach, presented a constant value of about 19.0ºC all year round.

The salinity values being lower in the coastal oceanic station could be explained through mixing processes occurring not only in the vertical (water column) but also in the horizontal. Submarine groundwater discharges occurring in very shallow places over the continental shelf, could be advected in the horizontal as plumes (see the schema in Fig. 4.8) thus affecting the physical parameters in the whole water column in the stations located in the trajectory of that plume.

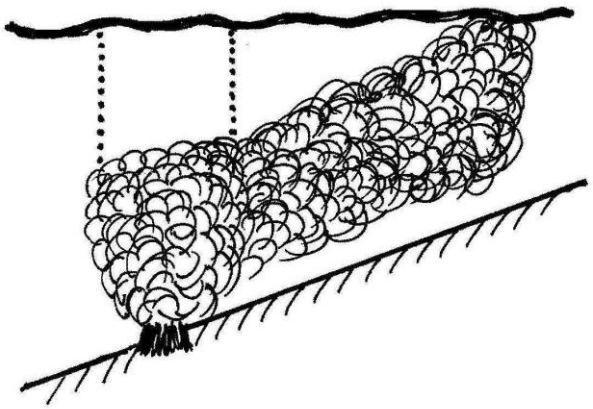

Fig. 4.8 – Scheme of the trajectory of a plume of waters with submarine groundwater origin over the continental shelf.

A carefully analysis of the profiles of the coastal oceanic station, represented in blue in Fig. 4.7, also reveals one salinity minimum at 2 m depth with a slightly temperature decrease,

showing characteristics of the influence of the SGDs. The presence of this minimum at such depth could be the result of the horizontal advection of a plume of waters with SGD origin.

Salinity variations of $\Delta S \geq 0.03$ were found in 20 stations with the salinity minimum located between 2.5 and 12 m depth. These 20 stations with influence of the SGDs are represented in pink in Fig. 4.9, as well as the 33 stations from the 11/2012 survey, also influenced by the SGDs, which are represented in yellow.

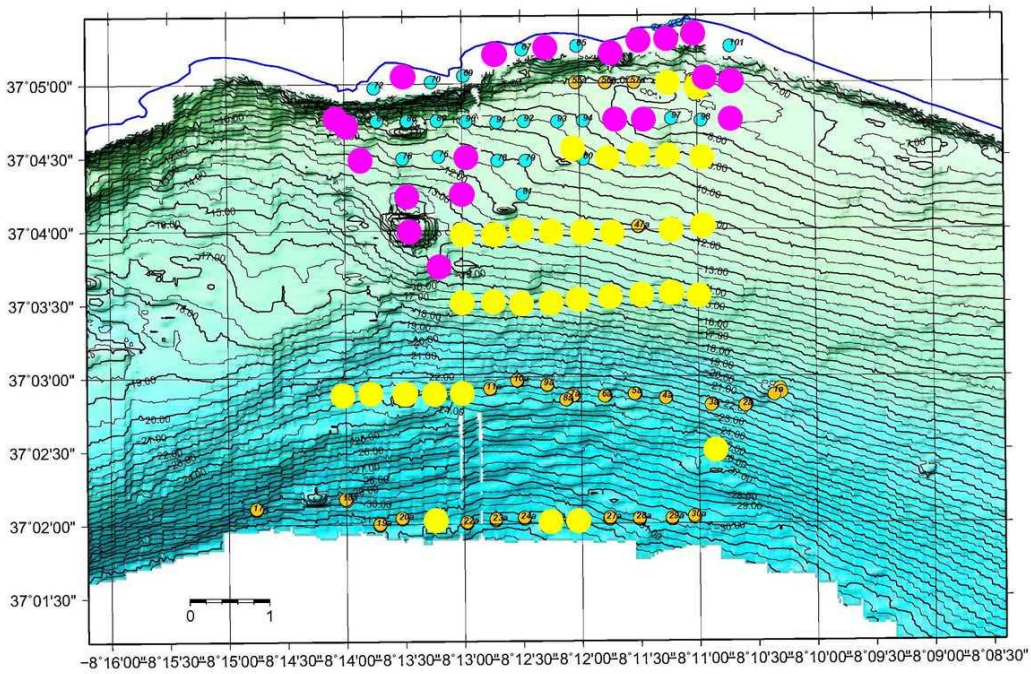

Fig. 4.9 – Location of the stations influenced by the SGDs: 33 stations (in yellow) in the 11/2012 survey and 20 stations (in pink) in the 04/2013 survey.

4.3.3. Survey 11/2013 and Preliminary Results

The data gathered during the last campaign (11/2013) is still under processing.

The CTD was calibrated in the end of all surveys and there is a new curve of calibration for the conductivity parameter. The new calibration curve must be applied to all the conductivity data gathered during the 11/2013 survey, and then the salinity values must be recalculated. Although the salinity values are not the final corrected ones, the figures from now on are only to show the behaviour of the T/S diagrams and the temperature and salinity profiles compared with the ones obtained in the two previous surveys.

Fig. 4.10 shows the T/S diagrams of all the 65 CTD stations carried out during the 11/2013 survey (in pink) in the Olhos de Água area, compared with the ones obtained during the 11/2012 and 04/2013 surveys, represented in blue and red in the same figure, respectively.

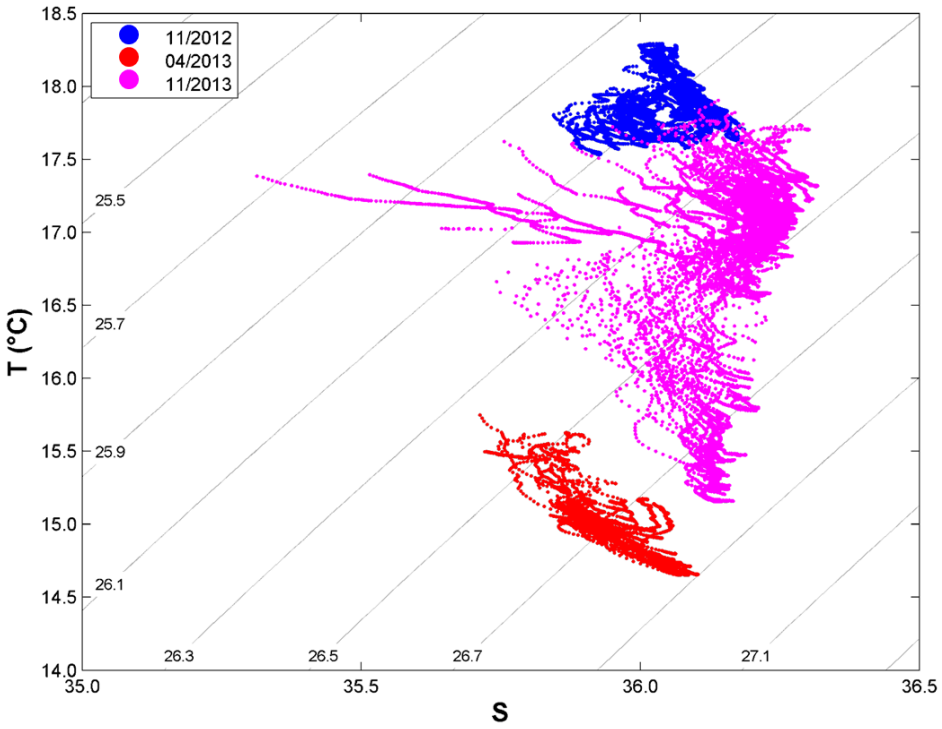

Fig. 4.10 – T/S diagram with all the 166 CTD stations carried out in the Olhos de Água area during the 3 surveys: 11/2012 (59 stations in blue), 04/2013 (42 stations in red) and 11/2013 (65 stations in pink).

It is interesting to note that the temperature values observed during the last survey vary in the range 15.0º-17.7ºC (lower than the ones obtained also in the beginning of November but one year before) and the salinities are slightly higher than the ones observed in the 2 previous surveys. A comparison between the new salinity values (after calibration) and the ones without calibration for one station, showed that the new salinity values are lower than the ones represented in the T/S diagram, which is in agreement with the salinities acquired during the previous surveys.

The T/S diagram with all the 95 CTD stations carried out during the 11/2013 survey is represented is Fig. 4.11: 65 stations represented in blue carried out in the Olhos de Água area, 20 stations represented in red in the Marina de Albufeira area and 10 stations represented in green in the Falésia beach area.

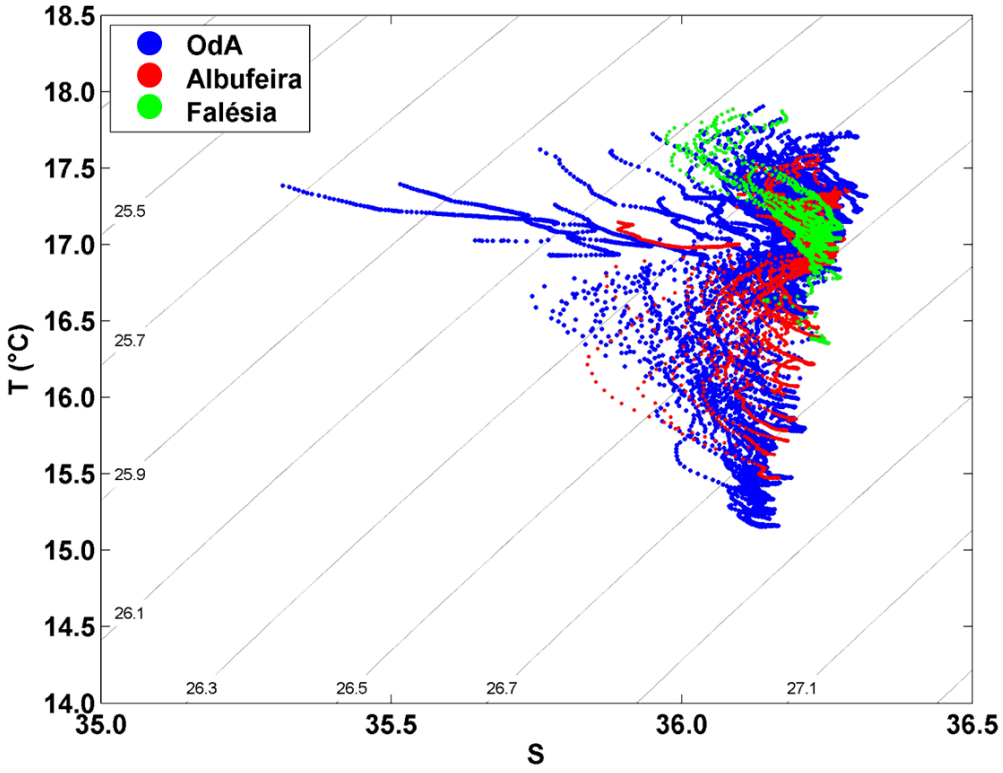

Fig. 4.11 – T/S diagram with all the 95 CTD stations carried out in the 11/2013 survey: 65 (in blue) in the Olhos de Água area, 20 stations (in red) in the Albufeira area, and 10 stations (in green) in the Falésia beach area.

The analysis of the T/S diagrams of the stations carried out in the Marina de Albufeira area, represented in red in Fig. 4.11, shows that this area, chosen as a non-SGD area, has a similar behaviour of an area influenced by SGDs, thus contradicting the previous idea. The stations carried out in the Falésia beach (represented in green in Fig. 4.11) do show a costal oceanic behaviour.

Fig. 4.12 presents, as an example, the temperature and salinity profiles obtained in one station with influence of submarine groundwater discharges (stn. 37 in red) and in another station with coastal oceanic characteristics (stn. 42 in blue) during the 11/2013 survey.

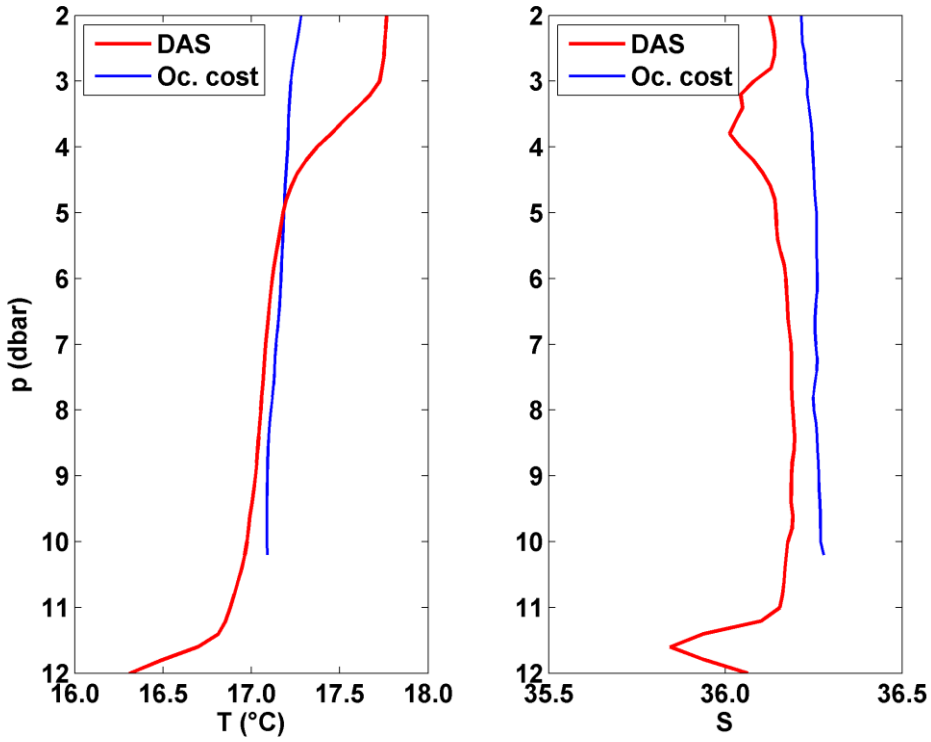

Fig. 4.12 – Temperature and salinity profiles obtained in an oceanic coastal station (in blue) and in another station influenced by submarine groundwater discharges (in red) during the 11/2013 survey.

The coastal oceanic station presents a very small decrease in temperature and a slightly increase in salinity from surface to bottom (blue profiles in Fig. 4.12) as happened in the two previous surveys. In the station with influence of water coming from submarine springs (red profiles in Fig. 4.12) there is a salinity minimum at about 11.5 m depth with the correspondent temperature decrease. There is another salinity minimum located at 3.5 m with the correspondent temperature decrease.

It is interesting to note that the salinity variation in station 37, represented in red in Fig. 4.12, is ΔS = 0.35, much higher than the salinity variations obtained in the previous surveys, their location is shown in Fig. 4.13.

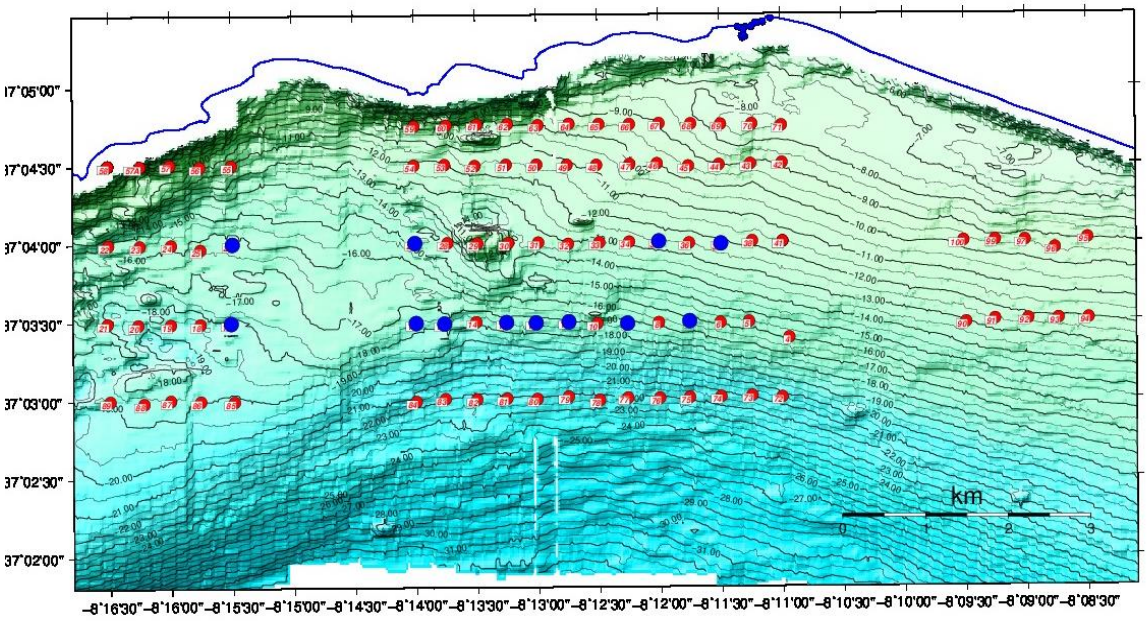

Fig. 4.13 – Location of the stations influenced by submarine groundwater discharges (in blue) during the 11/2013 survey.

The occurrence of such high salinity variations could be explained with high submarine discharges in this particularly rainy winter, such as the year 2012-13, when the last survey took place.

5. TASK 4 - Hydrological remote sensing survey offshore Albufeira-Quarteira

5.1 Objectives

The objective of this task consisted in the using of satellite imagery to look for patterns that could be associated with the surface signature of submarine groundwater discharges (SGDs).

5.2 Remote Sensing data analyses

The investigations have been addressed to the analyses of winter periods considering that the precipitations are in general more abundant in that season, the SGD activity stronger and the temperature contrast should also be more evident due to the lower temperature of the sea water.

To accomplish this goal different kinds of satellite imagery have been investigated:

- Radar images (SAR) to detect roughness contrast between sea water and fresh water lens created by SGD.
- Infrared images obtained with the sensor AVHRR on board NOAA-n satellites and infrared and visible images obtained with MODIS-AQUA and MODIS-TERRA satellites
- Images obtained with the thermal band of LANDSAT-7 and 8satellites to detect a temperature contrast between see water and SGD fresh water lens.

The values of the monthly accumulated precipitations obtained during the winter months in the climatological station of São Brás de Alportel (located at about 30 km far from Olhos de Água) were analysed during the period 2000-2011. Data have been downloaded from http://snirh.pt and are presented in Fig. 5.1.

Hydrologic years 2000-2001, 2001-2002, 2002-2003, 2005-2006, 2007-2008, 2009-2010 and 2010-2011 show high yearly rainfall with winters with monthly accumulated precipitations exceeding 700 mm (winters of 2001, 2002, 2003, 2006, 2008 and 2010, see Fig. 5.1). Those

periods seemed to be the most suitable ones to look for high submarine groundwater discharges (SGDs), which could be easily identified by their ocean surface signature on satellite imagery.

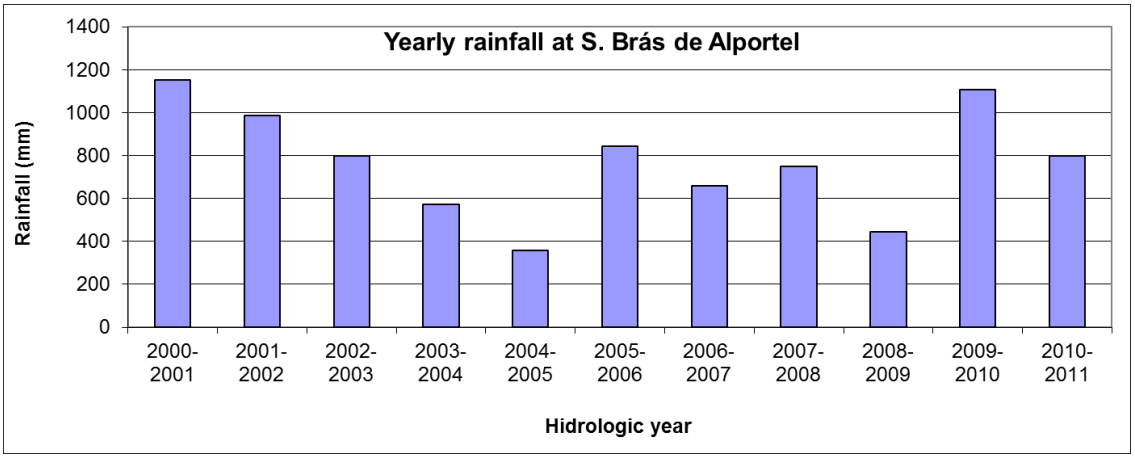

Fig. 5.1 – Rainfall data(unit mm or l/m^2) from São Brás de Alportel climatological station (source: snirh.pt)

5.3 Results

5.3.1 SAR imagery

Ten SAR (Synthetic Aperture Radar) images obtained during those particularly rainy winters were processed and analysed in order to look for patterns of sea surface roughness that could be associated with the presence of SGDs. These patterns, usually called *slicks*, identify areas where capillary waves are attenuated, and the surface roughness is reduced. The smoothed areas appear darker on SAR imagery compared with the usually wind-roughened surrounding ocean, which appears brighter on those images. These slicks could represent the surface signature of the SGDs, where less dense water discharging from the submarine springs reach the surface. Due to this smooth aspect of the sea surface, the submarine springs at the Avola site, in SE Sicily, are locally called “bubbles” (*bugli*in Povinec *et al.*, 2006).

Some SAR images analysed in this study revealed slicks in areas where the local geology and hydrogeology could justify the location of the potential submarine springs. One SAR image obtained on 9 February 2010, at 10:43 UT, during a particularly rainy winter, is

presented in Fig. 5.2. This image, with a 75 m ground resolution, shows an excellent example of a slick, thus indicating a potential location of SGDs. The slick presents an almost circular shape, with a diameter of about 3.5-4.0 km, and is identified by a white circle on the aforementioned figure.

The geographical coordinates of the slick were evaluated and then plotted on a nautical chart of the study area, and its location was just in front of Olhos de Água. This was very important for the planning of the CTD campaign to be conducted not only in the area occupied by the slick but also in the surrounding waters with oceanic thermohaline properties (see Task 3).

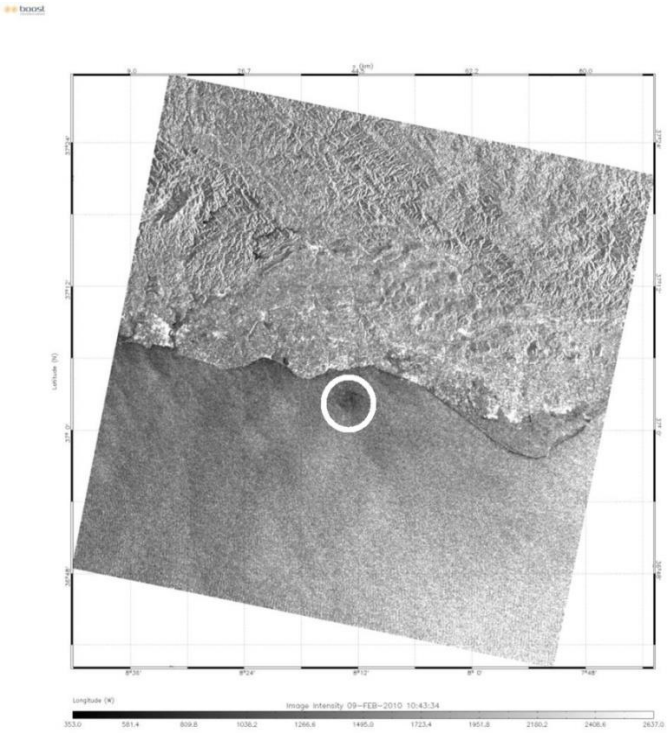

Fig. 5.2 – SAR image obtained on 9 February 2010, at 10:43 UT, showing a slick offshore Olhos de Água, encircled in white.

5.3.2 Infrared and visible imagery

Sea surface temperature (SST) distributions obtained with thermal infrared sensors (AVHRR) on board NOAA-n satellites were also analysed, for the same period (2000-2011), and in particular for the rainy winters mentioned above. The ground resolution of these images (1.1 km x 1.1 km) is very broad for such studies, but it was also interesting to verify if the SGDs could have their own thermal surface signatures on satellite imagery.

In a general way, the SST distributions did not show any particularly pattern on the continental shelf, which could be associated with the presence at the sea surface of submarine groundwater discharges.

On the day the first oceanographic campaign took place (6 November 2012: 11/2012 survey) two images from MODIS-AQUA satellite were available at the http://oceancolor.gsfc.nasa.gov/ (level 2 data). The location of Olhos de Água (OdA) is identified in both images.

Fig. 5.3 shows the sea surface temperature and the corresponding phytopigments distributions off the Algarve coast. In front of Olhos de Água, with a NW/SE orientation, there is a narrow yellow tongue with temperatures near 19ºC (duly identified on Fig. 5.3a) with the corresponding lower chlorophyll content (greenish tones also identified on Fig. 5.3b) that could correspond to a surface signature of a SGD.

It is interesting to note that the values of the water temperature measured in the submarine springs at the beach were approximately constant and around 19ºC along the whole hydrological year. However the temperature in the water column measured during the CTD campaigns did not show such constancy and the values were in the range 17.5º-18.5ºC during the 11/2012 survey and in the range 14.5º-16.0ºC in the 04/2013 survey (see Task 3 for details).

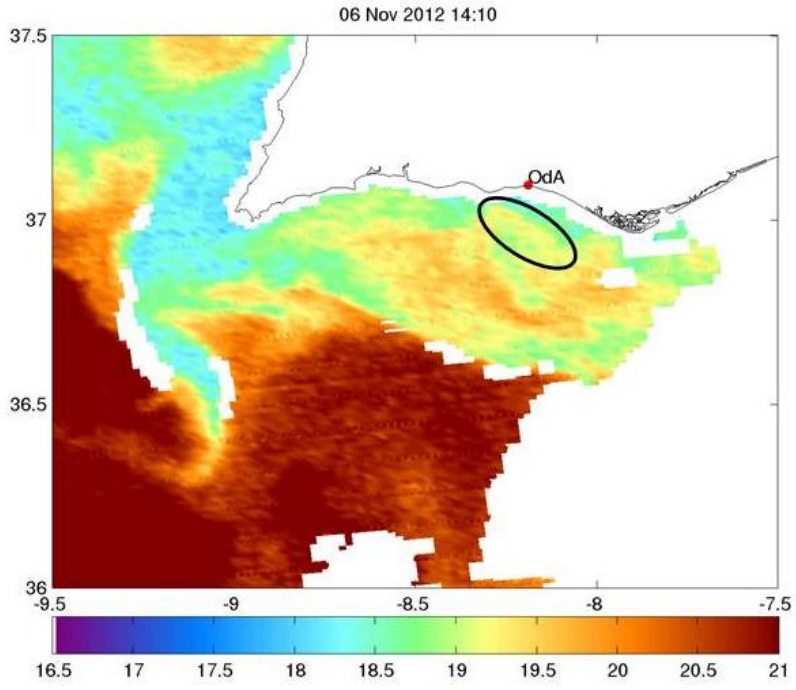

a)

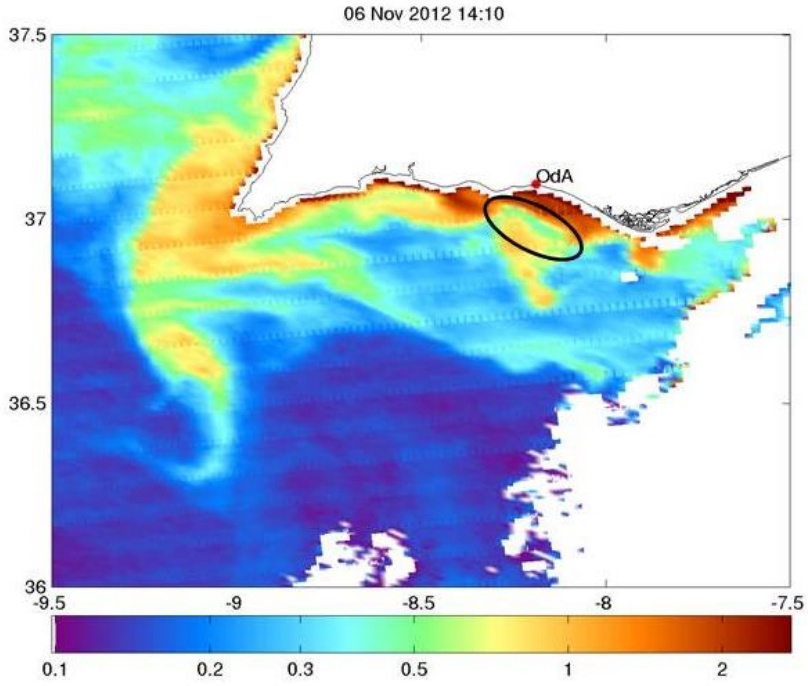

b)

Fig. 5.3 – (a) Sea surface temperature and (b) phytopigments distributions off the Algarve coast obtained with the MODIS-AQUA satellite on 6 November 2012, at 14:10 UT.

It was observed that the temperatures at the depths where the salinity minima were identified (the potential location of the SGDs) presented a decrease of its value (see Figs. 4.5, 4.7 and 4.12, in Task 3, for example). As these waters have an underground origin, their phytoplankton content is very low, which is in agreement with the surface pattern revealed by the satellite image presented in Fig. 5.3b).

If the patterns identified in Fig. 5.2 do correspond, in fact, to the surface signatures of the SGDs, these could be the result of less dense water vertically upwelled or water coming from submarine springs horizontally advected by a plume carrying the groundwater discharges over the continental shelf.

The surface patterns identified on both images obtained on 6 November 2012 (see Fig. 5.3) have relatively big dimensions (several km). To detect surface patterns on satellite imagery seems to be possible only in the case of strong submarine discharges (strong enough to upwell in the vertical) or the result of exceptionally meteorological and oceanic conditions which occurred on that particularly day or even both together.

For the second campaign which took place on 9 April 2013 (04/2013 survey), 4 SST and 1 chlorophyll distributions obtained with the MODIS-TERRA satellite, and another SST image obtained with the MODIS-AQUA satellite were available at http://oceancolor.gsfc.nasa.gov/ (level 2 data). The analysis of all these imagery obtained in the period 7-13 April did not reveal any particular pattern that could be associated with the surface signature of any potential submarine groundwater discharge.

During the last campaign, conducted on 12-13 November 2013 (11/2013 survey), 3 SST and 2 chlorophyll distributions obtained with the MODIS-TERRA satellite, and another 4 SST and 2 more chlorophyll distributions obtained with the MODIS-AQUA satellite were available at http://oceancolor.gsfc.nasa.gov/ (level 2 data). The analysis of all these distributions obtained in both days did not reveal any particular surface signatures. There is a circular pattern, located in front of Olhos de Água, only visible on the SST image obtained on 12 November 2013, at 14:00 UT, but this hypothetical pattern should also be confirmed with the CTD data, which is currently been processed.

5.3.3 LANDSAT 7 and 8 – Thermal band imagery

In the scope of using all the free information available to the scientific community, thermal bands of LANDSAT 7 and 8 satellites (resolution of 60 and 100 m respectively) were processed to detect surface patterns with small dimensions, which is more suitable for such coastal studies. LANDSAT 7 and 8 archive images are free of charge and were downloaded from the USGS application EarthExplorer (earthexplorer.usgs.gov).

The differences between Landsat-7 ETM+ Bands (µm) and Landsat-8 OLI and TIRS Bands (µm) are shown on table 5.1.Landsat 8 Operational Land Imager (OLI) and Thermal Infrared Sensor (TIRS) images consist of nine spectral bands with a spatial resolution of 30 meters for Bands 1 to 7 and 9. New band 1 (ultra-blue) is useful for coastal and aerosol studies. New band 9 is useful for cirrus cloud detection. The resolution for Band 8 (panchromatic) is 15 meters. Thermal bands 10 and 11 are useful in providing more accurate surface temperatures and are collected at 100 meters.

Landsat-7 ETM+ Bands (μm)			Landsat-8 OLI and *TIRS* Bands (μm)		
			30 m Coastal/Aerosol	0.435 - 0.451	Band 1
Band 1	30 m Blue	0.441 - 0.514	30 m Blue	0.452 - 0.512	Band 2
Band 2	30 m Green	0.519 - 0.601	30 m Green	0.533 - 0.590	Band 3
Band 3	30 m Red	0.631 - 0.692	30 m Red	0.636 - 0.673	Band 4
Band 4	30 m NIR	0.772 - 0.898	30 m NIR	0.851 - 0.879	Band 5
Band 5	30 m SWIR-1	1.547 - 1.749	30 m SWIR-1	1.566 - 1.651	Band 6
Band 6	60 m TIR	10.31 - 12.36	*100 m TIR-1*	*10.60 – 11.19*	Band 10
			100 m TIR-2	*11.50 – 12.51*	Band 11
Band 7	30 m SWIR-2	2.064 - 2.345	30 m SWIR-2	2.107 - 2.294	Band 7
Band 8	15 m Pan	0.515 - 0.896	15 m Pan	0.503 - 0.676	Band 8
			30 m Cirrus	1.363 - 1.384	Band 9

Table 5.1 - Differences between Landsat-7 ETM+ Bands (μm) and Landsat-8 OLI and TIRS Bands (μm).

For the present study, 10 LANDSAT-7 images obtained in the period 1999-2003 and 1 in 2010 were selected. The dates are listed on

Table 5.2. Note that after 2003 a defect in the ETM+ sensor of LANDSAT-7 resulted in no data stripes in the images, masking part of the scene.

1999-11-22
2000-03-29
2001-02-12
2001-04-01
2002-01-14
2002-04-20
2003-02-02
2003-03-06
2003-05-09
2003-05-25
2010-03-09

Table 5.2: Study area LANDSAT 7 selected images.

5 LANDSAT 8 Images were also processed. Their date is listed in Table 5.3.

2013-04-26
2013-06-13
2013-11-20
2013-12-06
2014-01-23

Table 5.3: Study area LANDSAT 8 selected images

The conversion of the Landsat 7 and 8 thermal bands into temperature was done using the methodology explained in Chander et al. (2009). The thermal band of LANDSAT 7is divided in two bands, as explained by these authors: “The ETM+ Level 1 product has two thermal bands, one acquired using a low gain setting (often referred as Band 6 L with a useful temperature range of 130–350 K) and the other using a high gain setting (often referred as Band 6H with a useful temperature range of 240–320 K). So, the difference is in range and thus in precision. Note that the temperature conversion was done on images without atmospheric correction incorporating an error of ~+/-1.5ºC. Thus the retrieved temperature is approximate. As we are interested in this study in temperature contrast and not on the true value, the error is not relevant.

2 images from Landsat 8 and 1 image from Landsat 7 were selected to show the performed imagery processing, see Figs. 5.4, 5.5 and 5.6.

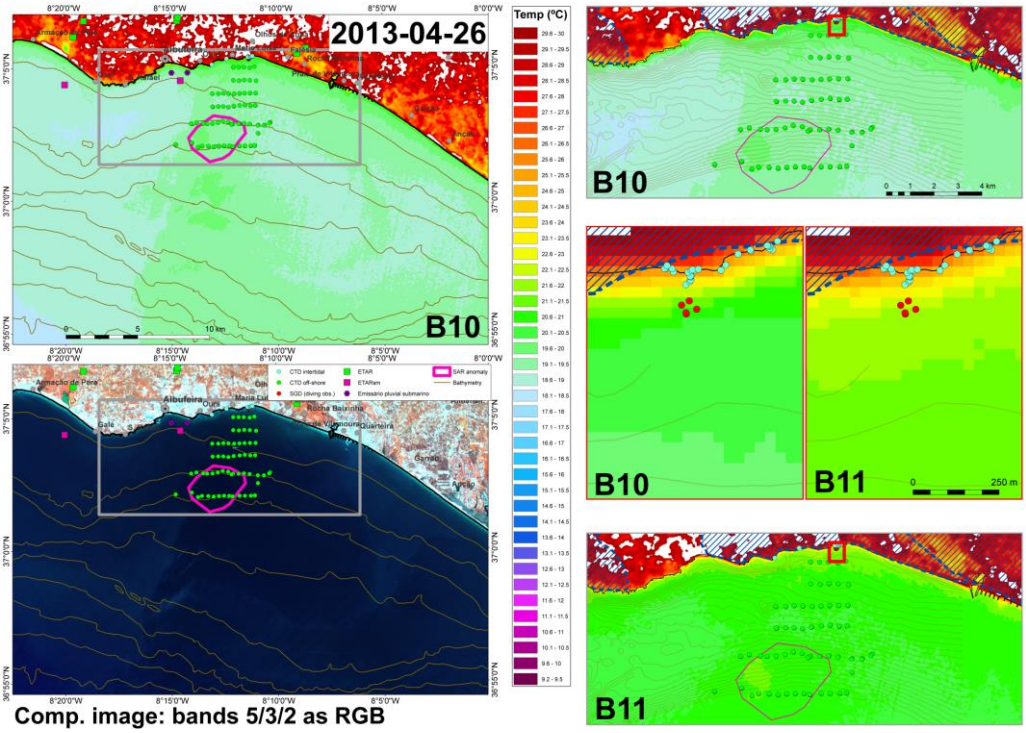

Fig. 5.4 - Landsat-8 OLI and TIRS Bands, acquisition on 26/4/2013.

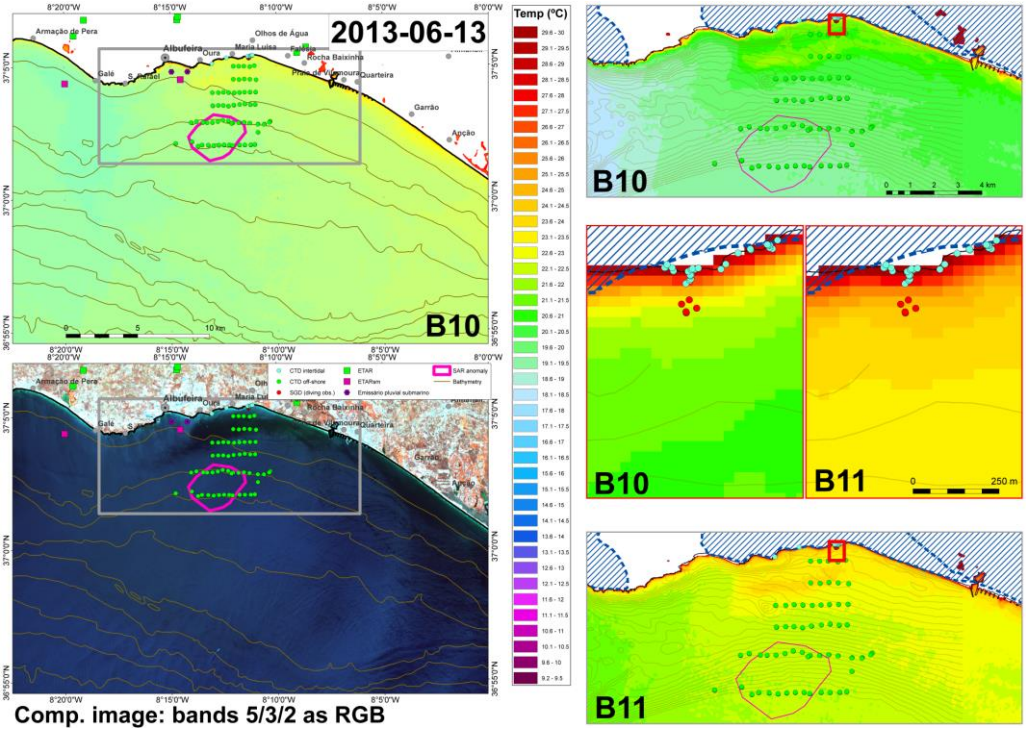

Fig. 5.5 - Landsat-8 OLI and TIRS Bands, acquisition on 13/6/2013.

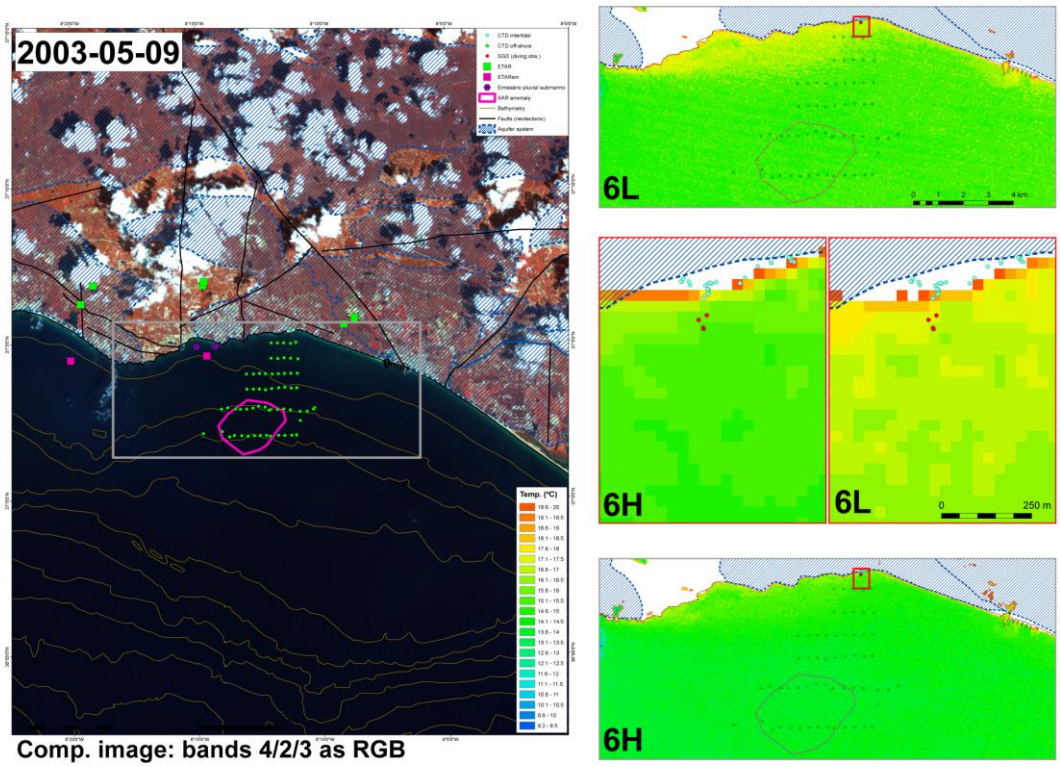

Fig. 5.6 - Landsat-7 ETM+ Bands, acquisition on 9/5/2003.

The existence of thermal anomalies that unequivocally relate tothe SGD is not clear. In first instance the analysis of most of processed images does not seem to indicate patterns that are repeating throughout the different images. This also relates to the acquisition of images whose quality often suffers interference due to atmospheric factors.

However we would like to emphasize that the LSAT8 (Fig.5.4), acquired on April 26, 2013, shows 3 slightly warmer spots (19,6to 20ºC) located above 20-30mt, 30-40mt and 40-50mt depth, which coincide with some of SGD identified in seismic profiles. The depths below spots are similar to the paleocoast lines ones and in particular the 20-30mt spot is included in the SAR image slick (Fig. 5.2).

Image LSAT8 (Fig.5.5), acquired on June 13, 2013, shows the mixture of cooler and very hot water. Located in the SAR slick place, a rectangular pattern of cooler water (19-20ºC) that interferes with this mixture and keeps cooler water in this zone of influence seems to be present.

Image of the LSAT7 (Fig.5.6), acquired on May 9, 2003, doesn't show any pattern in the SAR area but considering the temperature of the surrounding sea a patch of warmer water (17-18 °C) along the coast is present.

Taking in account the complex water dynamics off Olhos de Água and the lack of current meter temporal series we could not obviously quantify the real contribution of the SGDs to the coastal temperature distribution.

CTD profiles besides showing seafloor SGDs indicate low salinity values in the shallowest part of water column. These values are not directly correlated with seafloor SGDs. These lows could represent the intersections between water plumes (formed by low salted and less dense waters) and seawater surface. Low depths and strong flows let SGDs reach seawater surface without water mixture. Due to high water dynamics existing in the area we are not able to establish a direct relationship with the CTD salinity lows and satellites images thermal anomalies.

6. TASK 5 - Hydro – Ecological characterization and ecological impacts evaluation in the area

6.1 Objectives

The objectives of this task were i) to assess the effect of submarine groundwater discharge (SGD) over meiofauna and macrofauna in sandy and rocky areas; ii) evaluate the effect of SGD in individual physiologic conditions and found SGD indicators.

6.2 Biological marine surveys

Sampling took place according to a Control–Impact design, with seasonal replication. In order to account for the natural changes in the hydrological regime of these coastal aquifers, sampling was done in spring and summer and to have replication within seasons there were two sampling periods per season. Spring was considered since it is when the aquifers have been recharged by winter precipitation, as is characteristic of the Mediterranean climate and so it is expected that a higher volume of water is discharged. On the other hand, summer is the season of the year when the volume of discharged water is expected to reach its minimum due to a lack of refilling of the aquifers and a higher human demand for water. The Control area was specifically chosen, as it is the only area in Algarve that belongs to the same water mass as the Impact area but has no influence of any coastal aquifer system (Located in front of Arrifes beach, Albufeira). The Impact area of Olhos de Água is also a unique area within the south coast of Portugal, as to our knowledge, no other SGD occur in the coastal area of Algarve. In order to keep the design as conservative as possible, there could only be one Control area and one Impact area.

Samples were taken by SCUBA diving in subtidal soft-bottom sediments, at depths between 4 and 7 m. At each sampling period, 3 replicate meiofauna samples were randomly taken in each location (Control and Impact), each sample consisting of 2 corers with 3.5 cm of diameter and 15 cm deep, which were subsequently pooled. In the Impact location, samples were randomly collected within the area delimited by seepages, but not directly on the seepages. In parallel with each sample, two identical corers (3.5 × 15 cm) were collected: one for organic matter and one for grain size analysis. Meiofauna samples were

subsequently preserved in 4% buffered formalin and stained with Rose Bengal until further laboratory processing.

For macrofauna at each location (Control and Impact), 6 samples were randomly collected, each comprised of 3 corers with 22 cm diameter by 15 cm deep. Sediments contained in these corers were sampled with an airlift pump and all organisms were retained on a 500 µm mesh bag, which corresponded to the established minimum macrofauna size of this study. In rocky areas a percentage cover methods was used (N=6 samples of 1 m^2 each) with data being collected in situ by scuba diving team. For such propose a quadrant with 0.5 x 0.5 m^2 with 49 interception points were used (each sampled comprise 4 quadrates that were pooled or 1 m^2).

6.2.1 Meiofauna and macrofauna protocol

The technique used to separate the meiofauna from the sediment was based in the protocol by Burgess (2001), which relies on density differences. Samples were initially washed with a 500 µm sieve to remove formalin, Rose Bengal excess and macrofauna organisms, while meiofauna and sediment were retained in a 55 µm sieve. The remaining sample was placed in 500 ml PE tubes with Ludox® (DuPont) HS 40 solution in a 3:2 Ludox/sediment proportion. Samples were homogenized manually for 30 s and subsequently with an automatic vortex mixer (Cassel) for 4 min. Organisms were separated from sediment on a centrifuge (Beckman Coulter, Avanti™ J-25) at 900 × g for 5 min. The supernatant was removed from the sample by decanting and passed through a 55 µm sieve, where meiofauna was retained. Meiofauna samples were then washed with freshwater, stored in tubes and preserved in 96% ethanol. Meiofauna organisms were then identified and counted according to major taxonomic groups.

6.2.2 Sediment analysis

The method of “loss on ignition” was used for organic matter quantification. Dry weight was determined after drying the sediment samples in an oven (WTC Blinder) for 12 h at 30 °C. The samples were subsequently ached in a muffle (DINKO) at 450 °C for 4 h and the remaining sediment was weighted. The organic matter (OM) percentage was then estimated by dividing ash-free weight (the difference between ash weight and dry weight) by dry weight.

The analysis of grain fractions started by placing the sediment in hydrogen peroxide until all organic matter was oxidized and then dried at 60 °C (WTC Blinder oven). Sediment samples were then passed through a stack of sieves that comprised six fractions: silt and clay (<0.063 mm), very fine sand (0.063–0.125 mm), fine sand (0.125–0.250 mm), medium sand (0.250–0.500 mm), coarse sand (0.500–1.000 mm) and very coarse sand (>1.000 mm). The sediment retained on each fraction was then weighted and the percentage of each fraction, in relation to the total weight of each sample, calculated.

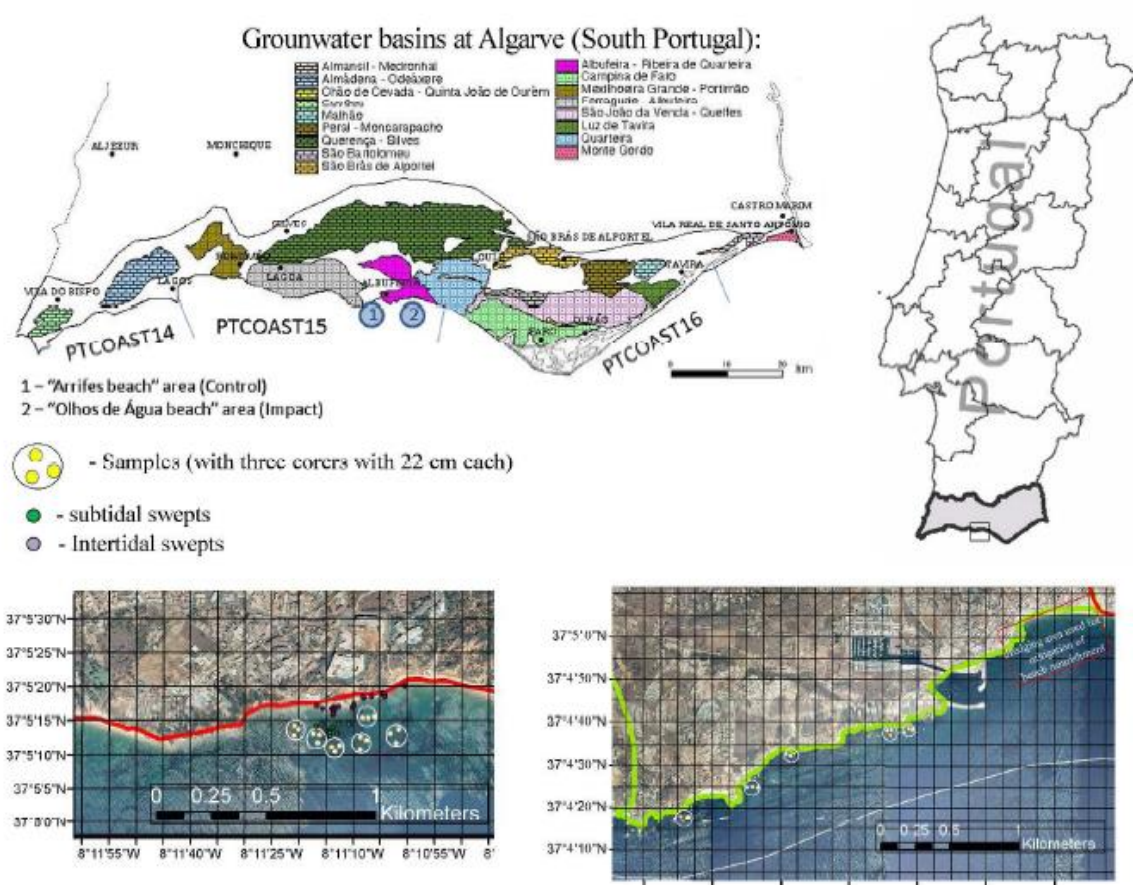

Fig. 6.1 - Location of the major aquifer systems in Algarve, the study area and respective sampling sites (Control and Impact), locations of the samples and the positions of the intertidal and subtidal seeps (upper left figure adapted from Almeida et al., 2000).

6.3 Results

Here follow the main results obtained by the biological investigations for meiofauna, macrofauna, physiological condition and benthic indicators in the study area.

6.3.1 Meiofauna

Meiofauna assemblages in the area impacted by SGD were compared with the meiofauna from a similar area, but without SGD. The major changes in the community were recorded at a seasonal level, with higher abundances and number of taxa in spring, when compared to summer (Table 6.1).

		Spring		Summer		*p* value		
		Control	Impact	Control	Impact	Season	Local	SexLo
Sediment variables	Organic matter	0.9 ± 0.1	0.8 ± 0.1	1.1 ± 0.1	1.2 ± 0.6	0.21	0.65	0.79
	Silt and clay	0.2 ± 0.0	1.4 ± 0.5	0.2 ± 0.1	0.9 ± 0.3	0.31	**	0.22
	Very fine sand	14.7 ± 0.5	39.7 ± 2.1	18.5 ± 2.6	36.4 ± 3.0	0.95	**	0.53
	Fine sand	49.3 ± 21.9	54.1 ± 2.8	57.3 ± 5.1	54.2 ± 4.0	0.80	0.42	0.86
	Medium sand	10.7 ± 0.2	2.4 ± 0.2	17.1 ± 5.5	4.5 ± 0.9	0.05	**	0.31
	Coarse sand	23.5 ± 20.7	1.6 ± 0.5	6.3 ± 1.8	2.8 ± 0.8	0.42	0.06	0.28
	Very coarse sand	1.6 ± 1.4	0.7 ± 0.1	0.6 ± 0.3	1.3 ± 0.5	0.83	0.66	0.46
Meiofauna taxa	Copepoda + nauplii	1846.2 ± 1909.9	153.3 ± 115.4	831.8 ± 752.9	1061.0 ± 1208.2	0.94	0.05	0.07
	Egg	971.4 ± 475.4	721.5 ± 1238.5	360.8 ± 195.2	523.4 ± 841.4	0.19	0.81	0.69
	Foraminifera	462.1 ± 727.1	377.3 ± 603.6	35.4 ± 14.1	268.8 ± 340.1	0.10	0.96	0.73
	Gastropoda	0	905.4 ± 40.0	0	438.6 ± 580.2	0.61	0.16	0.61
	Nematoda	15722.2 ± 11751.7	15189.3 ± 15142.2	3367.0 ± 1104.4	2405.0 ± 4369.6	*	0.87	0.96
	Nemertea	70.7 ± 20.0	938.4 ± 888.2	773.4 ± 962.6	325.4 ± 214.9	0.63	0.30	0.08
	Ostracoda	1471.3 ± 0	492.3 ± 431.7	0	396.1 ± 520.2	0.07	0.90	0.60
	Others	160.3 ± 58.9	82.3 ± 63.8	84.9 ± 80.0	207.5 ± 278.8	0.77	0.81	0.22
	Polychaeta + larvae	914.8 ± 722.7	999.7 ± 1366.7	90.5 ± 46.5	277.3 ± 224.9	*	0.51	0.95
	Turbellaria	7413.1 ± 9803.4	4682.7 ± 6269.7	871.5 ± 539.6	466.9 ± 352.8	0.07	0.88	0.97
Ecological indices	S	7.67 ± 1.15	11.50 ± 1.38	7.60 ± 1.14	7.33 ± 2.80	*	0.06	*
	N	26134.4 ± 24225.6	24578.2 ± 17952.8	6807.6 ± 1626.4	5654.1 ± 7970.7	*	0.82	0.98
	d	0.68 ± 0.07	1.10 ± 0.12	0.75 ± 0.12	0.76 ± 0.25	0.11	*	*
	H'	1.05 ± 0.33	1.19 ± 0.38	1.34 ± 0.11	1.38 ± 0.35	0.12	0.55	0.74

Table 6.1. Average and standard deviation of sediment variables, meiofauna taxa abundances and ecological indices (S – number of taxa; N – abundance; d – species richness; H′ – Shannon's diversity) in Control and Impact of Spring and Summer 2011. Two-way ANOVA (d.f.Season = 1; d.f.Local = 1; d.f.SexLo = 1; d.f.Residual = 16; d.f.Total = 19) results of variables between seasons, locations and interactions between the two factors. *p < 0.05; **p < 0.001

This may be explained by better sediment aeration during spring along with higher food availability from the sedimentation of spring phytoplankton blooms. Although no significant differences were detected by multivariate analysis on the meiofauna abundances between Control and Impact areas, pair-wise tests on the interactions between factors in number of taxa (S) and species richness (Margalef's d) suggested that the discharge of groundwater stimulated an increase in meiofauna diversity. Such effect can be observed between the meiofauna assemblages from impacted and control areas and also between periods with different discharge regimes (spring and summer) in the impacted area. These findings highlight the role that freshwater discharges from coastal aquifers have on meiofauna assemblages and suggest that SGD contribute to enhance the transfer of energy from the lower levels of the trophic web to upper levels.

6.3.2 Macrofauna

The results for macrofauna showed a significant increase in the abundance, number of species, species richness (Margalef' d) and Shannon's diversity in the area under effect of SGD (Table 6.2), when compared to the Control area.

Subtidal rocky habitats were dominated by red algae (mainly *Sphaerococcus coronopifolius* and *Asparagopsis armata*), independently of site and time of sampling. Overall, preliminary results showed that the effect of this SGD on rocky benthic communities was not clearly evident. Statistical results show that seasonal patterns may superimpose on the impact of freshwater discharges.

		Spring		Summer		*p* value		
		Control	Impact	Control	Impact	Season	Local	Se x Lo
Taxonomic groups (ind m^{-2})	Bivalvia	37 ± 30	240 ± 336	94 ± 72	131 ± 73	0.62	*	0.07
	Crustacea	179 ± 151	251 ± 136	313 ± 284	250 ± 199	0.26	0.94	0.25
	Echinodermata	22 ± 15	48 ± 63	97 ± 148	66 ± 49	0.07	0.86	0.19
	Gastropoda	42 ± 50	61 ± 0	21 ± 13	31 ± 26	0.69	0.28	0.28
	Nematoda	105 ± 35	18 ± 0	18 ± 9	18 ± 0	0.15	0.07	0.15
	Nemertea	58 ± 48	65 ± 57	18 ± 15	70 ± 38	0.81	*	0.06
	Platyhelminthes	0	26 ± 0	0	15 ± 8	0.39	*	0.39
	Polychaeta	431 ± 487	806 ± 595	236 ± 124	526 ± 367	0.05	*	0.54
	Sipunculida	53 ± 0	18 ± 12	13 ± 6	18 ± 10	0.90	0.71	0.39
Ecological indices	S	15.42 ± 8.44	27.75 ± 7.52	21.00 ± 7.78	22.67 ± 6.17	0.91	*	*
	N	694.9 ± 614.7	2189.8 ± 1234.2	733.8 ± 374.6	994.5 ± 502.0	*	**	*
	d	2.26 ± 1.10	3.52 ± 0.80	3.06 ± 1.10	3.16 ± 0.75	0.42	*	*
	H'	0.80 ± 0.10	0.75 ± 0.09	0.78 ± 0.14	0.78 ± 0.15	0.25	0.09	0.20
	J'	2.07 ± 0.51	2.47 ± 0.30	2.32 ± 0.49	2.38 ± 0.48	1.00	0.48	0.52
	1-Λ'	0.81 ± 0.08	0.86 ± 0.05	0.83 ± 0.11	0.82 ± 0.13	0.80	0.43	0.27
Feeding guilds (%)	SF	13.9 ± 8.2	22.9 ± 5.8	17.7 ± 9.7	22.0 ± 8.4	0.44	*	0.19
	H	4.1 ± 5.6	0.6 ± 0.7	4.0 ± 5.0	0.8 ± 1.0	0.78	*	0.93
	C	20.2 ± 13.0	22.0 ± 8.7	24.0 ± 16.6	23.1 ± 7.7	0.38	0.54	0.75
	DF	61.8 ± 12.9	54.5 ± 8.3	54.3 ± 18.8	54.1 ± 12.2	0.13	0.72	0.36

Table 6.2 – Average and standard deviation of environmental parameters, major macrofauna taxonomic groups, ecological indices and feeding guilds in both Control and Impact and spring and summer 2011. Results of two-way ANOVA (d.f. Season = 1; d.f. Local = 1; d.f. SexLo = 1; d.f. Residual = 44; d.f. Total = 47) for the two factors (season and location) and its interactions are presented. * p< 0.05; ** p < 0.001A higher abundance of suspension feeders was also observed at the area under influence of the SGD. The preliminary multivariate analysis confirmed that macrofauna assemblages slightly differed between the SGD impacted area and the Control, given specially attention to the variability within season when compared to variability among locals. Thus at higher trophic groups, such as macrofauna, the influence of SGD on the structure of the benthic community, as differences were few consistent in time. Nevertheless, several taxa were associated with the SGD area, namely the polychaetes Spionidae, Capitellidae, Magelonidae and Polynoidae, some already considered in others studies as indicators of SGD. The isopod Cyathura carinata, the bivalves Tellimya ferruginosa and Tellina fabula were also more abundant at the SGD area and played a role as bioindicators of freshwater discharges.

6.3.3 Physiological condition

The determination of the *in situ* physiological state of marine organisms (indicators at species level) is among the main challenges marine ecology research. Molecular methods, based on indices of nucleic acid, such as RNA/DNA ratio, have been used to test models of nutrient productivity, by demonstrating tight linkages between nearshore hydrologic processes and benthic rocky intertidal ecosystems. Near shore primary productivity and RNA/DNA of muscle tissues from key gastropod grazers (*Mytilus galloprovincialis, Patella depressa* and *Gibbula umbilicalis)* at 2 rocky intertidal sites, C-I, in Algarve coast were also compared. The results seem to be driven by differences in seasonal nearshore primary productivity and by the delivery of high-quality phytoplankton, related to the freshwater discharges. This might affect ecophysiological condition, and, indirectly, growth and reproduction of benthic species.

6.3.4 Benthic indicators

Sampling was also conducted for locate seeps (underwater springs that discharge water in subtidal zones). In this seeps samples were taken in three distinct areas: in the seepage itself; in the periphery of the seepage where no bubbling of water was observed; and the surrounding area of the seepage (Figure 6.1). Both sampling sites were located near the shore, at maximum depths of 12 meters. Significant advances were achieved at biological (indicators at species level) and ecological level (indicators at community level) with the processing of the samples in laboratory, aiming measure the impact of submarine groundwater discharges (SGD) over benthic communities. A total of 60 taxa, belonging to 10 major taxonomic groups (Bivalvia, Crustacea, Echinodermata, Gastropoda, Nematoda, Nemertea, Oligochaeta, Platyhelminthes, Polychaeta, Sipunculida), were identified during this study. Spionidae Polychaetes were the dominant taxon in the surrounding area. *Bathyporeia sp*. (Amphipoda) was the dominant taxon in the periphery of the seep, followed by Oligochaeta. The oligochaete *Lumbricillus lineatus* (identif. Müller, 1774) dominated the seepage area, accounting for more than 95% of the benthic fauna in that area. These enchytraeid oligochaetes are commonly associated with brackish water and they were strongly associated with the seepage area. Accordingly, they can be considered as indicators of submarine groundwater discharges in shallow sandy coastal areas. The effect of the discharge is felt in the trophic structure of communities under SGD as it favors the "filter-feeders" (with increased abundances and sizes) compared to grazers.

7. TASK 6 - Development of a towed fish for a CTD probe

Task 6 was an independent technological task that aimed to develop experimental towed platform, able to produce 2D profilesof the water column main parameters (for example temperature, conductivityand pH) in coastal areas, lakes, rivers and estuaries.

7.1 Objectives

This task was devoted to the development of a towed system able to use a CTD probe for acquiring data in a continuous profile at a desired water depth. This system would allow the acquisition of 2D sections of the water column main parameters (temperature, conductivity, pH etc.) in coastal areas, lakes, rivers and estuaries. This task had a theoretical component concerning the development of a towfish dynamic model and the remaining work was mostly experimental. The developments of this task wouldbe applicable in the future for different payload sensors and different scenarios.

In order to perform this work the project made use of a private company skilled in this field. The Blue Edge is a technology based company born within the innovative ambience of the Dynamical Systems and Ocean Robotics Lab, a part of the Institute for Systems and Robotics (ISR) in Lisbon, with the need to give answers to the constant demands for applying the know-how acquired.

7.2 Experimental work

The envisioned study concerned three different fields: hydrodynamics, telemetry and control.The hydrodynamic performance of the towfishwouldhave a major impact in the system overall performance. The dynamic behaviour of the towfish should be fine-tuned in order to make it naturally stable, and offer a good rejection of the disturbances imposed from surface waves which act in the towing vessel.

The telemetry link from the CTD probe to the acquisition system on board the survey vessel is the key point which will allow to accurately georeference the data acquired by the CTD probe. The vessel position must be known at exactly the same time that the CTD collects data from its sensors therefore all data must be logged with proper time tags created from a

common real-time clock. A Differential GPS system would be installed onboard the survey vessel to provide accurate position and time.

Accurate positioning of the towfish is far from trivial. Although the required depths for the present project are relatively low, considerable errors can be introduced when computing the towfish position with respect to the survey vessel. For the present project the goal was to avoid expensive systems (i.e. Acoustic USBL systems) and explore the available sensor information to achieve the best possible estimates.

The towfish should be made of light corrosion resistant aluminium alloy in order to facilitate the deployment by hand from a small survey vessel.

The results expected from this task were two fold: i) the operational towfish system for the CTD probe with telemetry and ii) an increased knowledge and experience of design and operation of towfish systems.

This task was considered an independent section of the project even if is strictly related to the main oceanographic goals.

7.3 Results

While the budget envisioned for the execution of this task was adequate, the actual duration of the work to be conducted including repeated sea trials was underestimated. Normally Blue Edge should be able to cope with the additional effort to lead to a successful execution, however the timing was not good since other projects had been recently approved and being a small company it would be extremely difficult and risky to embark in the execution of the complete work plan for the FREEZE project under the conditions described above. Doing so would originate delays that could endanger the execution of other important parts of the project.

Other alternatives were looked for, including the usage of multiple Autonomous Surface Vehicles (ASVs) equipped with conductivity sensors developed by Instituto Superior Técnico. The feedback received was extremely positive however the team was also very committed to other ongoing projects and consequently could not commit to the desired deadlines.

Under these circumstances and given that the other methods planned in the project had given interesting results it was decided to postpone this task to a next opportunity after the FREEZE project is concluded.

The idea of conducting a survey with the small MEDUSA class ASVs developed by IST is well seen by all key scientists and there is a personal commitment to look for an opportunity to make it reality either in the scope of a new or an existing project.

8. TASK 7- Dissemination

This task involved all the partners and devoted to the dissemination toward the scientific and non-scientific community. A great attention and effort was dedicated to the public outreach with the contruction of a web based platform that can be easily surfed and consulted by specialistic and non-specialistic people.

8.1 Objectives

Task 7 included the participation to national and international meetings and conferences with posters or oral presentations and scientific papers production. Also the educational aspects have been faced with the opening, inside the project, of 6 fellowships positions and 2 Master thesis have been concluded, 1 Master and a PhD are ongoing.

All the scientific and technical products are available on the public geoportal hosted by LNEG institution and dedicated to the FREEZE project at following address http://geoportal.lneg.pt/Freeze/ and subdirectories therein. All the documents could be consulted and/or downloaded by public community.

8.2 Results

8.2.1 Public Outreach

Project web site (http://www.lneg.pt/iedt/projectos/371/) was available just after the first six month of the project and a common web platform hosted by LNEG facilities at the following address: geoportal.lneg.pt/geoportal/mapas/?servico=freeze has been produced to reach a greater audience of specialist and non-specialist end-users. The public *geoportal* represents the natural evolution of a FREEZE scientific community internal GIS project, created to homogenize the different geographical datasets.

In 2011 an Interview to the Algarve Journal (15/09/2011) have been done describing the main project goals to reach non specialist people.

In June and in September of 2014 two public seminars on the FREEZE project are planned at Carlos Ribeiro Auditorium (LNEG, Lisbon) and UALG auditorium (Faro) respectively. The two institutions will economically support the seminars that will be dedicated to the disseminations of the main results achieved by the project in the scope to reach a specialistic and non-specialistic audience. National and international experts will be invited to participate and the proceedings of both conferences will be collected in an electronic book that will be published on the project portal.

8.2.1.1 FREEZE Geodatabase: A GIS Tool to Manage, Analyze, Distribute and Archive cross discipline data from the FREEZE Project in Olhos de Água – Albufeira, Algarve south of Portugal.

The FREEZE geodatabase is the result of combined efforts of all project partners to manage the geological, geophysical and oceanographic data gathered from the several surveys carried out in the Olhos de Água onshore and offshore coastal zone. The database incorporates a wide range of data types: logbooks from land surveys data, Conductivity-Temperature-Depth (CTD) sample analyses, scan-sonar data, bathymetric data, geophysical profiles, raster-image basemaps, etc.

The data have been integrated with spatial and attribute information to provide search and discovery tools combined with visualization capabilities using Geographic Information System (GIS) tools (in this case ArcGIS software) from the project collaborator's side and simple discovery services by using internet browsing tools (in this case ArcIMS Server software) from the general public side.

The background integrated FREEZE geodatabase was designed in a simple way to allow the project collaborator's a quick and easy tool to query and analyze data and also to update it when new data was collected or new analysis are achieved. The FREEZE geodatabase serves as a digital archive tool of any type of data need for the scientific purposes of the project (Fig.8.1 and Fig.8.2).

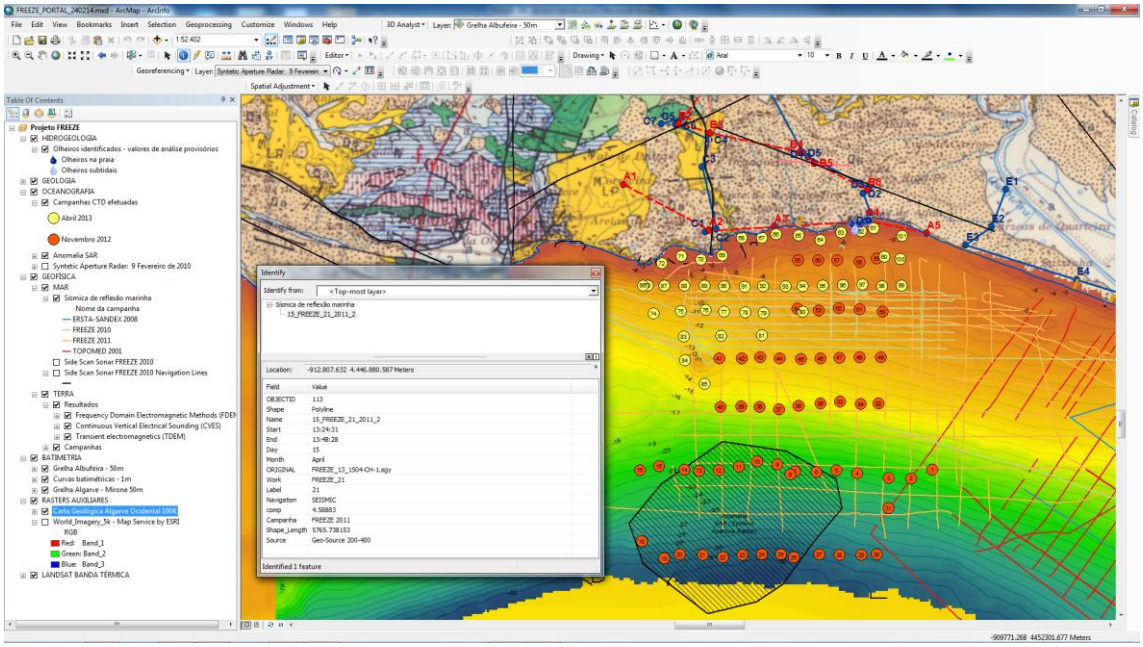

Fig.8.1 - Display of FREEZE geodatabase using ArcMap software. Data layers includes, for instance, seismic reflection profiles locations onshore and offshore (colored lines), CTD sampling sites (dots), fresh waters springs (drops), mains faults (black lines) along the Olhos de Água coastal zone. The onshore raster base map is a 100k geological map produced by national geological survey service (LNEG) and the offshore base map is a 50 m bathymetric data grid form MIRONE. The inset shows an example of the linked attribute table information from offshore seismic data.

Virtually, all the data currently collected by FREEZE project scientists are in digital format, but in several cases the data is provided in different formats, coordinate systems and without normalization. Because of that sometimes the discovery and the analysis of data is a very time consuming task.

The conversion of the information into standard digital formats accessible to all partners in the same formats, materialized by the building of the standardize FREEZE geodatabase was the response to that issue.

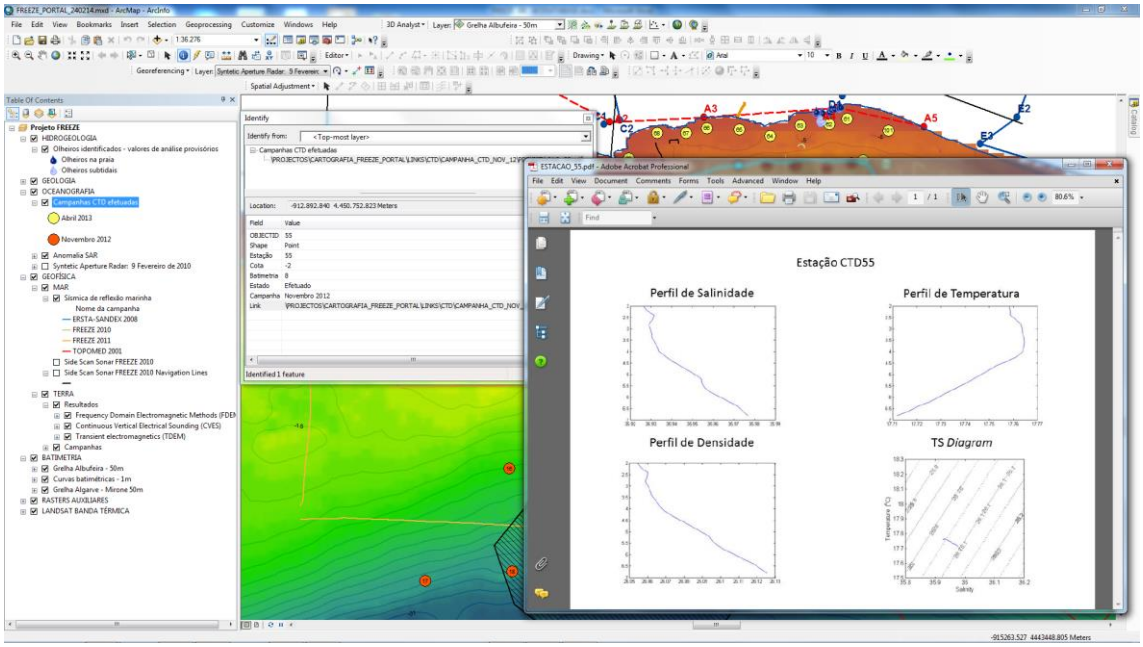

Fig.8.2 - Example of CTD analysis data stored in the FREEZE geodatabase and the hot link to the website locations (overlaid boxes) for associated sample data. Together, this information forms a permanent online digital archive of these data.

In the public geoportal (http://geoportal.lneg.pt/geoportal/mapas/?servico=freeze) the data types are organized by themes in a way to allow simple queries, analyses and cross data results can be performed across datasets (Fig. 8.3).

FREEZE geodatabase forms the backbone of a permanent online digital data-archive system. Seamless interaction between published data archives and the geodatabase allows for rapid dispersion of data to collaborators.

The system takes full advantage of ArcGIS information tools and a web server. The data files are linked either spatially or by attribute and provide to the remote user digital representations of almost any combination of data.

Data types, such CTD analyses, descriptions, seismic transects and photographs, are dynamically linked to cruise information, equipment information, scanned field logbooks, seismic-reflection profiles, etc. As an example, the linked tables allow any user with standard ArcGIS tools and a web browser to identify on a map where a CTD was taken, see a digital image analysis or view a fresh water spring photograph (Fig. 8.4).

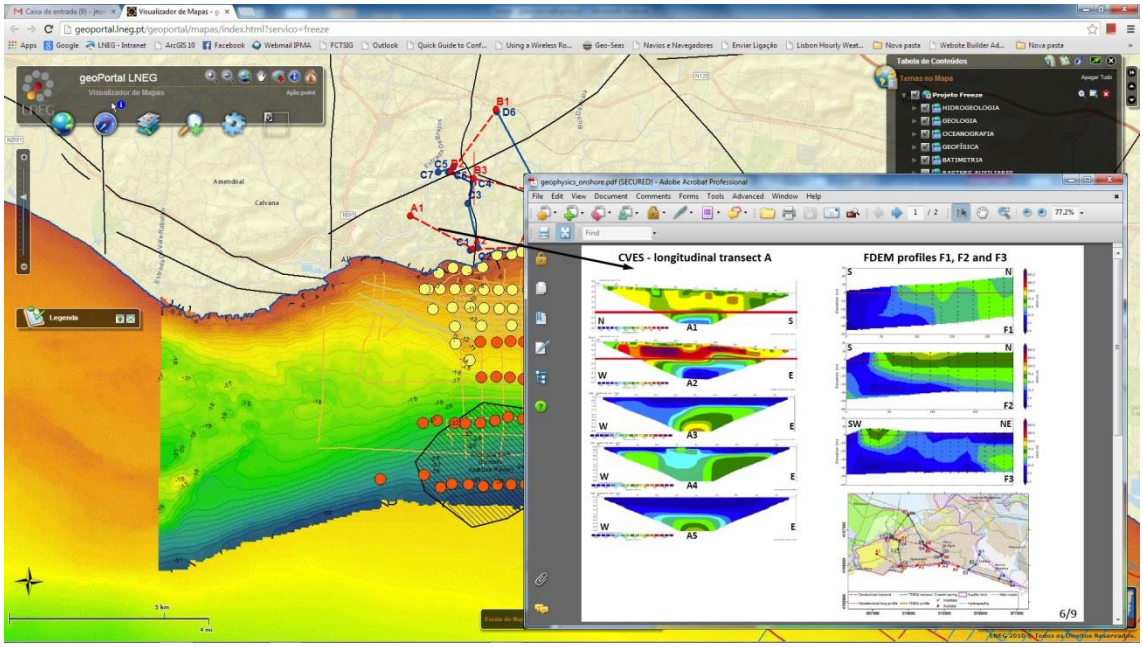

Fig.8.3 - Display of an interactive seismic transect webpage. In the example onshore seismic lines are displayed over the land cover base map. Selected seismic profile line attributes are displayed in a web browser inset window (right).

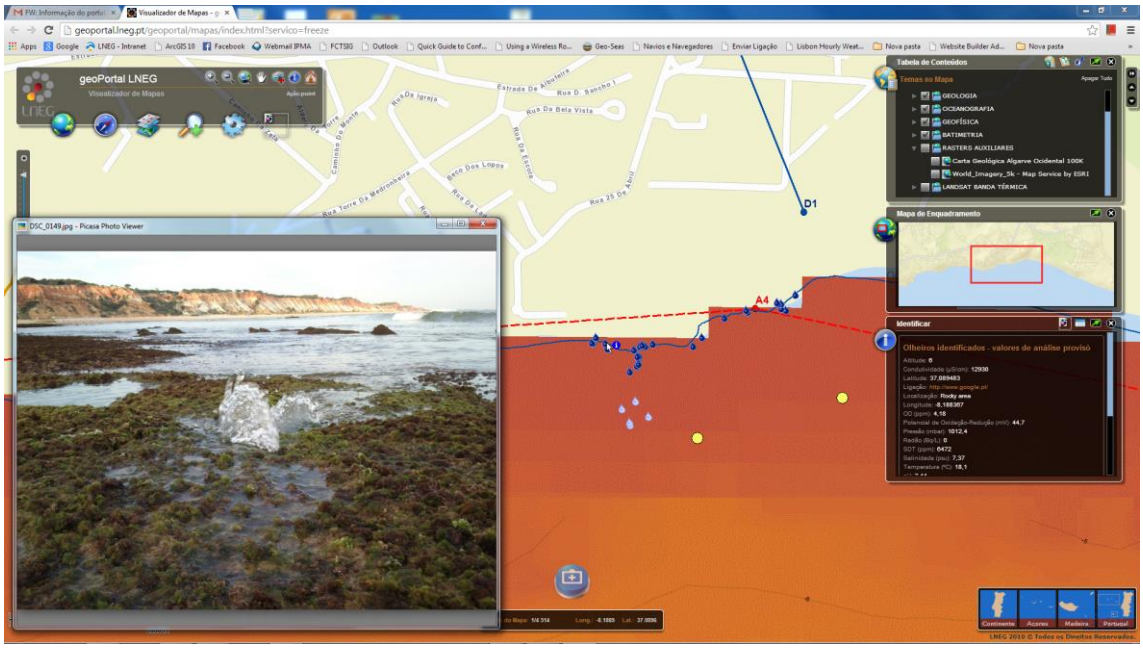

Fig.8.4 - Display of fresh water spring photograph in the webpage portal. In the example are displayed over the land cover base map. Parameters field measures attributes are displayed in a web browser inset window (right).

8.2.2 Scientific Dissemination

Posters and oral communications were submitted to numerous national and international congresses such as:

- 11º Congresso da Água (Portugal), (2012).
- ECSA 50. Estuarine Coastal and Shelf Association", Venice, Italy, 2012
- Encontro de Oceanografia Física, Quiaios, Portugal, 15-16 de Junho 2012.
- International "VII Simpósio sobre a Margem Ibérica Atlântica" (MIA 2012), Lisbon (Portugal).
- 8ºALEGG - 8ª Assembleia Luso Espanhola de Geodesia e Geofísica (Évora, Portugal, 29-31 de Janeiro, 2014).
- 1º Encontro de Oceanografia/APOCEAN, Nazaré, Portugal, 21-22 de Março 2014.
- IX Congresso Nacional de Geologia (IX CNG) e 2º Congresso de Geologia dos Países de Língua Portuguesa (2º CoGePLiP), Porto, Portugal, (2014).

8.2.2.1 References

National congresses

1. Gabriela Carrara, Judite Fernandes, Pedro Terrinha, Helena Amaral, João Noiva, Cristina Roque, Henrique Duarte, Augusto Costa, Teresa Condesso De Melo, Tibor Stigter, Simona Bronzini; Francisco Leitão, Pedro Range, David Piló, João Encarnação, Alexandra Chicharo, Luis Chicharo, Fátima Sousa, José Teixeira da Silva, Ângela Nascimento, Luís Sebastião, Luís Pinheiro, Daniela Gonçalves, Vitor Magalhães, Leonardo Azevedo; Amélia Dill, José Paulo Monteiro 2012. INVESTIGAÇÃO DAS DESCARGAS DE ÁGUAS SUBTERRÂNEAS EM MEIO MARINHO: UMA ABORDAGEM MULTIDISCIPLINAR (PROJECTO FREEZE). 11.º Congresso da Água. Associação Portuguesa dos Recursos Hídricos. Porto, 5 a 10 Fevereiro.(Oral Communication and Poster). Proceedings do 11º Congresso da Água: valorizar a água num contexto de incerteza. APRH, Porto, 6 a 8 de Fevereiro de 2012, 366-368p.

2. Costa L, Hugman R., Monteiro J.P. (2013). Modelação da Descarga de àguas Subterráneas dos Aquíferos de Abufeira-Ribeira De Quarteira e de Quarteira (Algarve,Portugal). 9º Semin. sobre Àguas Subterraneas da APRH. Lisbon, pp 82-85. https://docs.google.com/viewer?a=v&pid=sites&srcid=ZGVmYXVsdGRvbWFpbnxqcHBtb250ZWlyb3xneDoxZGQwOWVhMjdkZWQ1YjYy. Presentation available on: http://www.aprh.pt/9sas/pdf/costa.pdf.

3. Nascimento A., F. Sousa, G. Carrara, J. Fernandes & J. da Silva, (2012) "Utilização de imagens de satélite na localização das descargas de águas subterrâneas - Projecto FREEZE", "Encontro de Oceanografia Física", Praia de Quiaios, Portugal. (Poster)

4. P. Terrinha, J. Noiva, G. Carrara, J. Fernandes , C. Roque, L. Pinheiro, 2014. Neogene and Quaternary seismostratigraphy and tectonics offshore Albufeira and Quarteira: implications on the paleogeography and submarine freshwater discharges. Proceedings dos IX Congresso Nacional de Geologia (IX CNG) e 2º Congresso de Geologia dos Países de Língua Portuguesa (2º CoGePLiP), Porto, (Portugal).

5. Fátima M. Sousa, Gabriela Carrara, Judite Fernandes, Dmitri Boutov, Marisa Loureiro, Francisco Leitão, Pedro Range e Ana Machado, 2014: Descargas de Águas Subterrâneas na Plataforma Continental do Algarve. 1º Encontro de Oceanografia/APOCEAN, Nazaré – 21/22 Março 2014. (Oral Presentation)

6. R. Hugman, L.Costa, J.P. Monteiro, T.Stigter - Estimating submarine groundwater discharge from the Albufeira–Ribeira de Quarteira and Quarteira aquifer systems (Algarve, Portugal). Proceedings of III CJIG, LEG 2013 & 6th PGUE, Pólo de Estremoz da UÉvora, 04-08 outubro 2013.

International congresses

1. Gabriela Carrara, Judite Fernandes, Pedro Terrinha, Helena Amaral, João Noiva, Cristina Roque, Henrique Duarte, Augusto Costa, Teresa Condesso De Melo, Tibor Stigter, Simona Bronzini; Francisco Leitão, Pedro Range, David Piló, João Encarnação, Alexandra Chicharo, Luis Chicharo, Fátima Sousa, José Teixeira da Silva, Ângela Nascimento, Luís Sebastião,Luís Pinheiro, Daniela Gonçalves, Vitor Magalhães, Leonardo Azevedo; Amélia Dill, José Paulo Monteiro (2012). Submarine fresh groundwater discharge investigation: a multidisciplinary approach. Livro de Actas do 7º Simpósio sobre a Margem Ibérica Atlântica - MIA12., 16-20 December 2012, Lisbon.D. (Oral Presentation)

2. F. Leitão, J. Encarnação, D. Piló, P. Range, A. Chicharo, L. Chicharo (2012). Effect of groundwater discharges on subtidal benthic communities. ECSA 50. Estuarine Coastal and Shelf Association,Venice, Italy.(Oral Presentation)

3. Piló, A. Chicharo, J. Encarnação, F. Leitão, P. Range, L. Chicharo (2012). In situ physiological state of intertidal benthic macroinvertebrates under the effect of groundwater discharges. ECSA 50. Estuarine Coastal and Shelf Association, Venice, Italy (Poster) http://w5w.estuarinecoastalconference.com/index.html.

4. Alain P. Francés, Elsa C. Ramalho, Judite Fernandes, Michel Groen, Joel de Plaen, Rui Hugman, Mohamed A. Khalil, Fernando A. Monteiro Santos 2014. Hydrogeophysics contribution to the development of hydrogeological conceptual model of coastal aquifers – Albufeira-Ribeira de Quarteira aquifer case study. Proceedings da 8ª Assembleia Luso Espanhola de Geodesia e Geofísica", (eds. B. Caldeira, J. Barrenho, J.F. Borges, J. Pombinho, M.J. Costa, M.R. Duque, M. Bezzeghoud e R. Salgado), ISBN: 978-989-98836-0-4, 593 pp.

5. Sousa F.M., G. Carrara, J. Fernandes, D. Boutov, M. Loureiro, F. Leitão, P. Range e A. Machado, 2014: "Descargas de Águas Subterrâneas na região dos Olhos de Água – alguns resultados das campanhas CTD", p. 503-507 de Proceedings da 8ª Assembleia Luso Espanhola de Geodesia e Geofísica, (eds. B. Caldeira, J. Barrenho, J.F. Borges, J. Pombinho, M.J. Costa, M.R. Duque, M. Bezzeghoud e R. Salgado), ISBN: 978-989-98836-0-4, 593 pp.

6. Monteiro, J. P.; Costa; L.; Hugman, R. Stigter, T.; Nunes, L. (2013). Modelação de àguas Subterráneas do Algarve Central Aplicada a Simulação de Descarga Submarina para o Oceano Atlántico e do Caudal de Base da Ribeira de Quarteira (Portugal). Actas do 11º Simpósio de Hidráulica e Recursos Hídricos dos Países de Língua Portuguesa (SILUSBA). Maputo, Moçambique. Org. APRH, ABRH, AMCT, INGRH. Doc. elect. CD-ROM 11pp. https://docs.google.com/viewer?a=v&pid=sites&srcid=ZGVmYXVsdGRvbWFpbnxqcHBtb250ZWlyb3xneDoxNjE5NmM0ZDUwNTNiMGEw

7. R. Hugman, T. Stigter, J.P. Monteiro (accepted) Integrating improved conceptual knowledge into a 3-D variable density numerical model for a heavily exploited coastal aquifer with submarine spring discharge in South Portugal. in Proceedings of 23rd Saltwater Intrusion Meeting, Husum, Germany, 16 - 20 June 2014.

Some papers have been also published and/or submitted on/to national and international journal since 2012:

- Encarnação J, Leitão F., Piló D., Range P., Chicharo A., Chicharo L.(2013). Effect of submarine groundwater discharge on coastal meiofauna assemblages in south Portugal (Algarve). Estuar Coast Shelf Sci 130:202–208. DOI:10.1016/j.ecss.2013.04.013 (IF: 2.32)
- Encarnação J, Leitão F*., Piló D., Range P., Chicharo A., Chicharo L. (2012). Local and temporal variations in near-shore macrobenthic communities associated with submarine groundwater discharges. Marine Ecology (accepted).
- R. Hugman, T. Stigter, J.P. Monteiro, L. Costa and L. Nunes. Modelling the spatial and seasonal distribution of groundwater discharge for different water use scenarios under epistemic uncertainty - Case study in South Portugal. Environmental Earth Sciences, http://link.springer.com/journal/12665, (2013, submitted, final revision).
- Leitão F, Encarnação J, Range P, Schmelz, R.M., Chicharo A, Chicharo L.. Submarine groundwater discharges create unique benthic communities in coastal marine environment. (2013 submitted, Ecological Indicators).

Scientific work is still in progress due to the intriguing results obtained until now and some papers in the topics of oceanography, hydrogeology and tectonics are in preparation to be submitted on ISI journals in the next future.

8.2.3 Education

Great attention was dedicated in education inside project; as a result two master thesis have been produced inside the project and a total of seven fellowship positions have been opened to permit the project development in the field of remote sensing, hydrogeology, geophysics and data management.

The first master thesis, as a result of an international collaboration between Portugal and Swiss in the field of hydrogeology, was concluded and presented at the end of 2011 at Neuchatel University.

- Simona Bronzini, (2011). ETUDE HYDROGÉOLOGIQUE DE LA ZONE D'ALBUFEIRA(ALGARVE, PORTUGAL) ET ANALYSE DES MÉCANISMES DE SALINISATION DES EAUX SOUTERRAINES. Master en hydrogéologie et géothermie, Spécialisation en hydrogéologie, Centre d'hydrogéologie, Université de Neuchâtel, Swiss. 93 pp.

The second one was in the field of marine ecology and has been concluded and presented in December 2012 at Lisbon University.

- João Encarnação. (2012). Avaliação do impacto das descargas submarinas de água subterrânea nas comunidades de meiofauna e macrofauna bentónicas, Olhos de Água (Algarve). 2012. Dissertação Para Obtenção Do Grau De Mestre Em Ecologia Marinha. Faculdade de Ciências da universidade de Lisboa. Universidade De Lisboa Departamento De Biologia Animal. 65p.

http://repositorio.ul.pt/bitstream/10451/7829/1/ulfc_tm_joao_encarnacao.pdf

In addition to their original depository these thesis are also available on the following link:

http://geoportal.lneg.pt/Freeze/thesis

8.2.4 Ongoing researches

Nevertheless the large amount of work done during the last four years, a lot of questions still remain unsolved and constitute the base for further investigations and modelling. As a matter of fact, a Master and a PhD are still ongoing:

- Rui Hugman, PhD (SFRH/BD/80149/2011): "Applicability of Different Numerical Approaches to Defining Boundary Conditions and Density-Driven Flow in Groundwater Flow and Transport Models – From Regional Scale Management to Submarine Groundwater Discharge". Algarve University. Supervisors: Jose Paulo Monteiro e Tibor Stigter.

- Joel De Plaen, MSc Thesis (see MSc Thesis Proposal on the link http://geoportal.lneg.pt/Freeze/thesis/proposal_joel_12-03.pdf): Submarine Fresh Groundwater Discharge Study, Algarve, Portugal: How the groundwater flow in carbonated rocks affect the spatial extent, the hydrochemical pattern and the isotopic signature of submarine groundwater discharge?. VU University, Faculty of Earth and Life Sciences, Amsterdam.Supervisor: Koos Groen and Co-supervisor: Michel M. A. Groen, from VU University. On-site supervisor: Tibor Y. Stigter from Algarve University.

9. TASK 8 – Project Managing

The FREEZE project was a multidisciplinary project with five scientific units and more than 30 scientists to coordinate.

9.1 Objectives

The main goal of this task was the coordination of the activities and over all the integration of the different partners inside the same task. One of the main characteristic of this project was the capability to join different scientific visions and approaches on the same topic. This goal has been accomplished by a great number of restricted working group meetings focused on those common activities such as onshore or offshore campaigns, data analyses and dissemination products.

At the same time, due to the adverse economic condition, coordination was extremely important in order to carefully analyze the best economic solutions finalized to the accomplishment of the main project goals.

Additional activities such as the financial management of the project, signature of the institutional protocols and terms of acceptance, were carried out by the project leader during the whole project.

Another time consuming task was the preparation of the numerous surveys performed at sea. This activity, carried out by the PI and Dr. J. Fernandes, included all the procedures to obtain licenses and authorizations from the marine authorities (Capitania of Albufeira), the prospecting of available vessels and equipment, the evaluation of the most adequate case by case, equipment hiring and activation procedures of insurance.

9.1.1 Deviation and justification

In the first plenary meeting (8th of February 2010) a workflow was established for each task and their mutual interactions in the project. Partners decided to start Task 2 and 4 in 2010 and postpone TASK 3 in 2011 when the results deriving from the previous tasks would have been available.

Task 5 was anticipated respect the submitted project proposal and started in 2010 to allow the study of the microfauna distribution (plantos and bentos) in the area from the coast towards open sea and permitting the preliminary environmental characterization. Thus, it allowed a better and faster analyse of the interactions between SGDs and biological communities.

The project team, with a great effort, accomplished the aim to save money in the geophysical campaign organization (as suggested by the project evaluators). In fact the real costs were about 31411,56 euros instead of planned 71000 euros. In addition, it was verified that the field work had to be reinforced as well as the human resources and equipment due to the high volume of data to manage. For these reasons a variation of the money distribution was requested and accepted by FCT on 13th of December 2010.

In 2011 the methodology used in satellite images mapping (task 4) revealed excellent results that, combined with the structural and geomorphological results coming from the marine geophysical data, permitted the oceanographic cruise planning. The area was better confined permitting a detailed acquisition, uncertainties and costs reductions. Profiting of the TOPOMED-FREEZE campaign boat facilities, the oceanographic cruise was planned just after the end of the geophysical survey (April 2011). Unfortunately due to adverse weather conditions the oceanographical survey was aborted. After April 2011, in order to perform the oceanographic campaign, a smaller and cheaper boat (XegueDive) was found. New equipment was bought and prepared to permit the CTD deployment on this mean. As this boat also allows to work nearer the coast 9 CTD stations were added to the initial plan. Having in mind that the survey was inside the area reserved for beach summer activities (Olhos de Água beach) from June to late September, the CTD campaign was postponed for the beginning of October but was never executed. During 2011, due to the incoming economic crisis, Financial Ministry imposed to public administration to drastically reduce the expenses, as a result since the beginning of October 2011 till the end of the year, it was impossible to conciliate good weather conditions to work at sea with the availability of financial support from involved Institutions to pay the boat expenses. The cruise was postponed for 2012and LNEG requested a change of the initially planned budget distribution in order to: a) open a fellowship, dedicated to the processing of seismic and bathymetric data acquired in Task 2and b) reinforce the field work missions of Task 1.

In April 2012 the first oceanographic cruise has been carried out successfully and the first Portuguese shallow CTD dataset have been acquired. Immediately CTD data processing phase started. In the meanwhile the hydrological field work onshore was very intense with a

great amount of data collection. A consistent portion of the budget initially planned for data acquisition was devoted to fellowships in order to accomplish all the planned objectives so three (3) fellowships have been opened at LNEG in November 2012 for hydrogeology and data management. This last topic was necessary due to the freeze geoportal infrastructure building and to the inclusion of Freeze metadata inside oceanographical and geophysical European databases (EMODNET and GEOSEAS) in which the PI was already actively involved.

In 2012, Portugal experienced the restructuration of State Laboratories with the creation of the new Institute of Sea and Atmosphere (IPMA, D.L n.68/2012 on 20th March, 2012). LNEG-UGM unit, to which the PI belonged, moved and was included into IPMA. This transition of human, financial and material resources ended in March 2013, determining an important slowing down of the normal project administration with forced inactivity for some project actions. In fact, as a consequence of a governmental order published on 12 September 2012, it was almost impossible execute the Freeze budget in general and the budget amount transferred to IPMA was literally frozen.

This critical situation, joined with the imposition of austerity regime since 2011 by Portuguese Government, demanded a financial reorganization of the project itself.Most of the budget dedicated to Services and acquisition have been transferred to human resources to assure the data analyses and elaboration of the acquired data .

Thus considering that 1) execute the CTD campaigns was fundamental to fulfill the project goals, 2) the adverse contingent metereological condition didn't permit the survey acquisition before April 2013, 3) the new international cooperation arosen in the meanwhile with the Amsterdam University interested in the project results and 4) the very promising resuts obtained from the first CTD analyses after an initial 6 month extension further 6 months extension have been asked and obtained (up to the end of 2013) in order to fullfil the initial proposed tasks.

Resuming the project had the following main deviations respect the initial plan:

1) delay to 2011 of TASK 3. The task was completely executed and the main goals accomplished.
2) advancing of TASK 5 in 2010. The task successful accomplished its goals.
3) Task 6 has been postponed to a next opportunity after the FREEZE project is concluded. As before mentioned the budget envisioned for the execution of this task was adequate, the actual duration of the work to be conducted including repeated sea trials was underestimated. Normally Blue Edge should be able to cope with the

additional effort to lead to a successful execution, however the timing was not good since other projects had been recently approved and being a small company it would be extremely difficult and risky to embark in the execution of the complete work plan for the FREEZE project under the conditions described above. Doing so would originate delays that could endanger the execution of other important parts of the project. The non-completion of task 6 didn't affect the FREEZE financial administration, no expenses have been addressed to the project and the budget allocated by IPMA for this task will be returned to FCT.

4) One year of extension up to the end of 2013 due to economic crisis started in 2011.

The financial execution was the following:

In 2010 the reduced costs for the first geophysical campaign offshore allowed to save 39588,44 euros. Considering that the field work, the human resources and equipment had to be reinforced due to the high volume of data to manage a variation of the LNEG budget distribution was requested to and accepted by FCT on 13th of December 2010.

In 2011 LNEG requested a change of the initially planned budget distribution in order to: a) open a fellowship, dedicated to the seismic and bathymetric processing and b) reinforce the field work missions.

In 2012 a consistent part of the LNEG budget (19500 eur) initially planned for data acquisition was devoted to fellowships in order to accomplish all the planned objectives so 3 fellowships have been opened at LNEG in November 2012 for hydrogeology and data management.

Following the last request of project extension some variation in the budget distribution have been operated inside the participant Institutions and between them:

UALG transferred 2645, 68 euros from its human resources budget to equipment budget in order to conclude the ongoing working action at field.

LNEG transferred 1500 euros from its acquisition budget to equipment budget in order to conclude the ongoing working action at field.

IPMA transferred 1800 euros from its mission budget to LNEG missions budget in order to conclude the ongoing working action at field.

IPMA transferred 1000,00 euros from its mission budget to reinforce FFCUL mission budget (833,33 euros) and FFCUL gastos gerais (166,67 euros) in order to conclude the ongoing working action at field.

9.2 Results

Many project actions required specific contribution from experts that weren't initially involved into the proposal.

9.2.1 People added

- Cristina Roque was included into the team in the scope to reinforce the geological seismic stratigraphic interpretation since September 2012.
- José Dias Alexandre was included into the team in the scope to reinforce the on shore geophysical data acquisition since March 2012.
- Mohamed Khalil was included into the team in the scope to reinforce the on shore geophysical data acquisition and processing since April 2013.
- João Nuno da Palma Nascimento into the team in the scope to reinforce the interpretation of hydrogeological and hydrogeochemical data using geostatistic methods since April 2013.
- Luis Filipe Tavares Ribeiro into the team in the scope to reinforce the interpretation of hydrogeological and hydrogeochemical data using geostatistic methods since April 2013.
- Rui Twohig Hugman into the team in the scope to reinforce the development of 3D hydrogeological model since January 2013
- Elsa Cristina Lopes Rodrigues Ramalho has been added to the team in the scope to reinforce the on shore geophysical data acquisition since April 2013.

Some national and international scientific collaboration have been also established with Aveiro University, Estrutura de Missão para a Extenção da Plataforma Continental (EMEPC, Portugal) and Vrije Universiteit (Amsterdam University) .

Blueedge Company was contracted to perform some technical services.

9.2.2 Fellowship positions opened

- 1 fellowship position has been opened at IO in 2010 for remote sensing data analyses.
- 1 fellowship position has been opened at UGM-LNEG in 2011 for geophysical (seismic and bathymetric) data processing
- 1 fellowship position has been opened at UALG in 2011 for bio-ecological analysis.
- 3 fellowship positionshave been opened at UAS-LNEG in November 2012 for hydrogeology and data management.
- 1 fellowship position has been opened at IPMA for project data management.

9.2.3 Plenary Meetings

During the first year of the project two plenary meetings in Lisbon (8/2/2010) and Faro (5/5/2010) have been organized to permit the partner knowledge and better tuning task organization.

At the beginning of the second year (25th March 2011), a plenary meeting was organized in Lisbo,n where the partners presented their main results and planned the actions for the second year.

On 6th March 2012, the partners attended the plenary meeting in Lisbon and the state of the art of the second year and planned the actions for the next year.

On 15th February 2013, a plenary meeting was held in Lisbon. Partners communicated the actions performed during 2012 and the main obtained results.

On 24th October 2013, the last plenary meeting was organized in Faro at Algarve University. Partners decided the final actions needed to conclude the various tasks.

9.2. Working group Meetings

Due to the multidisciplinary character of the project and the numerous activity to coordinate many restricted meetings between the PI and the single units were organized.

2010

- UGM and UAS internal meeting for task work organization (9/03/2010);
- UGM and UAS field work planning and FREEZE 2010 geophysical survey planning (23/04/2010);
- UAS and IST-Algarve on-shore work planning (05/05/2010);
- IST, IO, LNEG-UAS, LNEG-UGM and Blueedge meeting dedicated to the bathymetric processing strategy (28/05/2010);
- LNEG-UAS, FCUL (Prof. Susana Barbosa) da FCUL on Radon acquisition and analysis(26/10/2010).
- IO, LNEG-UAS, LNEG-UGM on remote sensing data at Oceanographic Institute (28/10/2010);
- UAS and IST-Algarve on-shore work planning at Olhos de Água (08/11/2010);
- IO, LNEG-UAS, LNEG-UGM on remote sensing data at Oceanographic Institute (03/12/2010).

2011

- IO, LNEG-UGM, LNEG-UAS dedicated to SAR images analysis at Institute of Oceanography (18/01/2011);
- IO, LNEG-UGM, LNEG-UAS and do Prof. José Carlos of Porto University dedicated to SAR images analysis at Institute of Oceanography (09/02/2011);
- LNEG-UGM, LNEG-UAS and Blueedge on bathymetric modelling (25/02/2011);
- Internal LNEG meeting dedicated to data preparation for the FREEZE 2011 geophysical survey (14/04/2011);
- IO and LNEG-UAS, LNEG-UGM at Institute of Oceanography for the state of the art of remote sensing data (21/07/2011);
- IO and LNEG-UAS, LNEG-UGM at Institute of Oceanography (27/09/2011);LNEG-UGM, LNEG-UAS and Blueedge for task 6 actions (15/11/2011);

2012

- IO Team Periodic meeting (19/03/2012 and 06/07/2012;
- UALG Team Periodic meeting (01/08/2012 and 19/10/2012);,
- IST Team operative meeting on 15/10/2012;,
- LNEG-UAS Team and IPMA operative meetings on 04/12/2012 and 13/12/2012;.

2013:

- IO team Periodic meeting (28/01/2013);
- LNEG-UAS, Blueedge, IST-team and IPMA (14/02/2013);

- IO, LNEG-UAS and IPMA teams for April oceanographic survey planning and discussion on first results of previous one (13/03/2013);
- LNEG-UAS, IPMA teams and Prof. Costa Almeida on Albufeira-Ribeira de Quarteira aquifer system boundaries (20/03/2013);
- LNEG-UAS, IST-UALG and IPMA teams at Algarve University for hydrological data discussion and new activity planning (21/03/2013);
- LNEG-UAS, IPMA teams and Prof. Mário Cachão on Albufeira Miocene sequences (26/03/2013);
- LNEG-UAS, IPMA teams and Dr. Paulo Oliveira on Algarve coastal oceanography (04/06/2013);
- LNEG-UAS, IPMA, IST teams and Prof. Michel Groen and Joel de Plaen of VU university for onshore geophysical survey and spring monitoring (06 and07/06/2013;
- LNEG-UAS, IO and IPMA teams to discuss and compare oceanographic survey results of November 2012 and April 2013 campagns 811/07/2013);
- LNEG-UAS, LNEG-UIG and IPMA teams for final details of Freeze gis platform developing on LNEG geoportal (19/07/2013);
- LNEG-UAS, IO and IPMA teams for discussing new outputs of CTD data (11/09/2013);LNEG-UAS, IO and IPMA teams for planning the new CTD campaign foreseen in November 2013;
- LNEG-UAS,IO and IPMA-teams on analyses and processing strategy of new November CTD dataset;;

9.3 Ongoing research

The new hydrological model is a clear improvement on our knowledge on the aquifer system of Albufeira-Quarteira.

Many questions still remain open for example which is the real aquifer circulation, which is the sedimentary distribution and the real stratigraphy of Olhos de Água offshore area.

An accurate calibration deriving by direct sampling (i.e. coring) is fundamental for seismic profile interpretation as well as the acquisition of new profiles oriented perpendicularly respect the new tectonic features identified by the geological work.

In addition currentometer datasets, even already collected, will allow a better understanding and constrain of the shallow water oceanographic settings.

10. REFERENCES

- Almeida, C. (1985) - Hidrogeologia do Algarve Central. Dissertação para a Obtenção do Grau de Doutor em Geologia. Departamento de Geologia da FCUL, 333 pág.
- Almeida, C. e J. A. Crispim (1987) - Traçagens com uranina no Algar do Escarpão (Albufeira, Algarve). ALGAR, Bol. da Soc. Portuguesa de Espeleologia, nº 1, pp. 9-16.
- Almeida, C. and Silva, M. L. 1990. Hidrogeologia do miocénico entre Albufeira e Ribeira de Quarteira. Geolis IV (1 and 2), 199-216.
- Almeida, C.A.C., Lourenço da Silva, M., 1992. Hidrogeologia do sistema aquífero de Quarteira (Algarve). Geolis, VI(1 e 2): 18.
- Almeida, C., Mendonça, J. J. L., Jesus, M. R. and Gomes, A. J. 2000. Sistemas Aquíferos de Portugal Continental - Sistema Aquífero: Albufeira-Ribeira de Quarteira (M6). Instituto da Água.
- Ambar I., M.R. Howe, 1979: “Observations of the Mediterranean outflow II: the deep circulation in the vicinity of the Gulf of Cádiz”, Deep-Sea Research 26A, 555-568.
- Ambar I., N. Serra, M.J. Brogueira, G. Cabeçadas, F. Abrantes, P. Freitas, C. Gonçalves, N. Gonzalez, 2002: “Physical, chemical and sedimentological aspects of the Mediterranean outflow off Iberia”, Deep-Sea Research II 49, 4163-4177.
- Ascough, P., Cook, G. and Dugmore, A., 2005. Methodological approaches to determining the marine radiocarbon reservoir effect. Progress in Physical Geography 29, 4 (2005) pp. 532–547
- Aunay, B. et al., 2007. A multidisciplinary approach for assessing the risk of seawater intrusion in coastal aquifers: The case of the Roussillon Basin (France). Aquifer Systems Management: Darcy’s Legacy in a World of Impending Water Shortage: Selected Papers on Hydrogeology 10: 459.
- Auken, E. et al., 2010. The use of airborne electromagnetic for efficient mapping of salt water intrusion and outflow to the sea. The use of airborne electromagnetic for efficient mapping of salt water intrusion and outflow to the sea.

- Azerêdo, A.C., Duarte, L.V., Henriques, M.H. & Manuppella, G. (2003) – Da dinâmica continental no Triásico aos mares do Jurássico Inferior e Médio. Cadernos de Geologia de Portugal, Instituto Geológico e Mineiro, 43 p.
- Bakker, M., Schaars, F., 2005. TheSea Water Intrusion (SWI) package manual Part I: Theory user manual and example, version 1.2, www.modflowswi.googlecode.com.
- Barazzuoli, P., Nocchi, M., Rigati, R., Salleolini, M., 2008. A conceptual and numerical model for groundwater management: a case study on a coastal aquifer in southern Tuscany, Italy. Hydrogeology Journal, 16(8): 1557-1576.
- Baringer M.O., J.F. Price, 1997: "Mixing and Spreading of the Mediterranean Outflow", Journal of Physical Oceanography 27(8), 1654-1677.
- Bratton, J. F., Böhlke, J. K., Manheim, F. T. and Krantz, D. E., 2004. Ground water beneath coastal bays of the Delaware Peninsula: Ages and nutrients. Ground Water, 42, 1021-1034.
- Bronzini, S., 2011. Etude hydrogéologique de la zone d'Albufeira (Algarve, Portugal) et analyse des mécanismes de salinisation des eaux souterraines. Master en hydrogéologie et géothermie, spécialisation en hydrogéologie Thesis, Université de Neuchâtel, Switzerland, 83 pp.
- Burgmann, R., Rosen, P. A., & Fielding, E. J., 2000. Synthetic aperture radar interferometry to measure Earth's surface topography and its deformation. Annual Review of Earth and Planetary Sciences, 28, 169–209.
- Burnett, W.C., Bokuniewicz, H., Huettel, M., Moore, W. S. and Taniguchi, M., 2003. Groundwater and pore water inputs to the coastal zone. Biogeochemistry 66: 3–33.
- Cachão, M., Marques da Silva, C., Santos, A., Domènech, R., Martinell, J., Mayoral, E. (2009) - The bioeroded megasurface of Oura (Algarve, south Portugal): implications for the Neogene stratigraphy and tectonic evolution of southwest Iberia. Facies (2009) 55:213–225. DOI 10.1007/s10347-008-0172-2
- Carrara G., Matias L., W. Geissler et al. NEAREST 2008 Cruise Preliminary Report r/v Urania,1st Aug 2008 - 4th Sept 2008. 2008 CNR- reports.
- Carrara, G., et. al. 2012. Submarine fresh groundwater discharge investigation: a multidisciplinary approach, VII Simpósio sobre a Margem Ibérica Atlântica, Lisbon.

- Carvalho Dill A, Stigter, T (2008). Near shore Radio Frequency-Electromagnetics in hydrogeological studies. In: Proc. International Geological Congress (CD-ROM), HYH-01 General contributions to hydrogeology, Oslo, 6-14 August 2008.

- Carvalho Dill A, Turberg P, Müller I, Parriaux A, 2009. The combined use of Radio-Frequency Electromagnetics (RF-EM) and Radiomagnetotellurics (RMT) methods in non-ideal field conditions for delineating hydrogeological boundaries and for environmental problems.Environmental Geology 56(6): 1071-1091 DOI: 101007/s00254-008-1208-1.

- Carvalho Dill A, Stigter T. Y., Brito R., Chícharo M. A. and Chícharo L. 2014. The combined use of radio frequency-electromagnetic surveys and chemical and biological analyses to study the role of groundwater discharge into the Guadiana estuary. Ecohydrology. 7(2), 291–300. Published online in Wiley Online Library(wileyonlinelibrary.com).DOI: 10.1002/eco.1345

- Carvalho, J., Torres, L., Rocha, R., Dias, R., Mendes-Victor, L., 2006. A geophysical study of the S. Marcos–Quarteira fault, Portugal. Journal of Applied Geophysics, 60(2): 153-164.

- Carvalho, J., et al. (2012). "Connecting onshore structures in the Algarve with the southern Portuguese continental margin: The Carcavai fault zone." Tectonophysics 570–571(0): 151-162.

- Carvalho, J., Ramalho, E., Dias, R., Pinto, C., Ressurreição, R., 2012. A Geophysical Study of the Carcavai Fault Zone, Portugal. Pure and Applied Geophysics, 169(1-2): 183-200.

- Chander, G., Markham, B.L., Helder, D.L., 2009. Summary of current radiometric calibration coefficients for Landsat MSS, TM, ETM+, and EO-1 ALI sensors. Remote Sens. Environ., 113(5): 893-903.

- Church T.M., 1996 – An underground route for the water cycle, Nature 380: 579-580.

- Costa, A. M. 2013. Dos ensaios de aquífero aos modelos de simulação de fluxo. Algumas considerações e exemplos. 9º Seminário sobre Águas Subterrâneas. Universidade Nova.

- Costa, F. E., Brites, J. A., Pedrosa, M. Y., Silva, A. V. (1985) - Carta Hidrogeológica da Orla Algarvia, esc. 1:100 000. Notícia Explicativa. Serviços Geológicos de Portugal, Lisboa.

- Creel, L., 2003. Ripple effects: population and coastal regions, Making the link. Population Reference Bureau.

- Crusius, J., Koopmans, D., Bratton J. F., Charette, M. A., Kroeger, K. D., Henderson, P., Ryckman, L., Halloran, K. and Colman, J. A., 2005. Submarine groundwater discharge to a small estuary estimated from radon and salinity measurements and a box model. Biogeosciences, 2, 141-157.

- Crusius, J., Trescott, A., Bratton, J., Koopmans, D. and Giblin, A., 2006. Strengths and limitations of groundwater discharge estimates based on radon and radium isotopes: An example from a small Massachusetts estuary. Eos Trans. AGU, 87, Ocean Sci. Meet. Suppl., Abstract OS15B-04.

- Custodio, E., 2010. Coastal aquifers of Europe: an overview. Hydrogeology Journal, 18(1): 269-280.

- Danielsen, J.E., Auken, E., Jørgensen, F., Søndergaard, V., Sørensen, K.I., 2003. The application of the transient electromagnetic method in hydrogeophysical surveys. Journal of Applied Geophysics, 53(4): 181-198.

- Dale R.K., Miller D.C. 2008. Hydrologic interactions of infaunal polychaetes and intertidal groundwater discharge. Marine Ecology Progress Series, 363, 205-215.

- Day-Lewis, F.D., White, E.A., Johnson, C. D., Lane Jr., J.W. 2006. Continuous resistivity profiling to delineate submarine groundwater discharge—examples and limitations. The Leading Edge 25, 724 (2006); DOI:10.1190/1.221005.

- De Montety, V. et al., 2008. Origin of groundwater salinity and hydrogeochemical processes in a confined coastal aquifer: Case of the Rhône delta (Southern France). Applied Geochemistry, 23(8): 2337-2349.

- Dias, J.M.A., Boski, T., Rodrigues, A., Magalhães, F., 2000. Coast line evolution in Portugal since the Last Glacial Maximum until present - a synthesis. Marine Geology 170 (2000) 177±186.

- Dias, R.P. (2001) – Neotectónica da Região do Algarve. Dissertação de doutoramento, Fac. Ciências, Univ. Lisboa, 369 p.
- Dias, R.P. & Cabral, J. (2002) – Neotectonic activity of the Algarve region (S of Portugal). Comunicações do Instituto Geológico e Mineiro, Tomo 89, pp. 193-208.
- DiGiacomo P.M., L. Washburn, B. Holt and B.H. Jones, 2004: "Coastal pollution hazards in southern California observed by SAR imagery: stormwater plumes, wastewater plumes, and natural hydrocarbon seeps". Marine Pollution Bulletin, 49: 1013-1024.
- Dingman, S.L., 2002. Physical hydrology. Prentice Hall, Upper Saddle River, 646 pp.
- Doherty J (2002) Model-Independent Parameter Estimation, 4th ed. Watermark Numer Comput 279.
- Domenico PA, Schwartz FW (1997) Physical and Chemical Hydrogeology, 2nd ed. 528.
- Dörfliger, N., 2013. Entre terre et mer, les eaux souterraines du littoral. Géosciences (BRGM), 17: 74-81.
- Duk-jin Kim, Wooil M. Moon, Guebuem Kim, Sang-Eun Park, Hyoseong Lee. Submarine groundwater discharge in tidal flats revealed by space-borne synthetic aperture radar. Remote Sensing of Environment 115 (2011) 793–800.
- Elsendoorn, B., Hoogeveen, H., Vuyck, P., 1982. Geo-electrisch onderzoek van de Miocene aquifer tussen Olhos de Agua en Quarteira, Algarve (Portugal). VU University, Faculty of Earth and Life Sciences, Amsterdam.
- Encarnação J, Leitão F, Range P, et al. (2013). The influence of submarine groundwater discharges on subtidal meiofauna assemblages in south Portugal (Algarve). Estuar Coast Shelf Sci 130:202–208.doi: 10.1016/j.ecss.2013.04.013
- Ferretti, A.; Prati, C.; Rocca, F., 2000. Nonlinear Subsidence Rate Estimation Using Permanent Scatterers in Differential SAR Interferometry. IEEE Trans. Geosci. Remote Sens. , 38, 2202-2212.
- Ferretti, A; Prati, C.; Rocca, F., 2001. Permanent Scatterers InSAR Interferometry. IEEE Trans. Geosci. Remote Sens. 39, 8-20.

- Fetter, C.W., 2001. Applied Hydrogeology. Prentice Hall PTR, 598 pp.
- Fiúza A.F.G., M.E. de Macedo, M.R. Guerreiro, 1982: “Climatological space and time variations of the Portuguese coastal upwelling”, OceanologicalActa5, 31-40.
- Fiúza A.F.G., 1983: “Upwelling Patterns off Portugal”, in: Suess E., Thiede J. (Eds.), Coastal Upwelling Plenum, New York, pp. 85-98.
- Fleury, P., Bakalowicz, M., de Marsily, G., 2007. Submarine springs and coastal karst aquifers: A review. Journal of Hydrology, 339(1–2): 79-92.
- Folkard A.W., P.A. Davies, A.F.G. Fiúza, I. Ambar, 1997: “Remotely sensed sea surface thermal patterns in the Gulf of Cádiz and the Strait of Gibraltar: variability, correlations and relationships with the surface wind field”, Journal of Geophysical Research 102(C3), 5669-5683.
- Francés, A.P., Reyes-Acosta, J.L., Balugani, E., van der Tol, C., Lubczynski, M.W., 2011. Towards an improved assessment of the water balance at the catchment scale : a coupled model approach. In: J.M. Fernández, N.S. Martin (Ed.), Estudios en la zona no saturada del suelo: volumen X: ZNS11 proceedings, 19-21 October, Salamanca, Spain, pp. 321-326.
- Gabriel, A. K., Goldstein, R. M., & Zebker, H. A., 1989. Mapping small elevation changes over large areas: Differential radar interferometry. Journal of Geophysical Research, 94, 9183–9191.
- Garcia-Lafuente J., J. Delgado, F. Criado-Aldeanueva, M. Bruno, J. Del Rio, J.M. Vargas, 2006: “Water mass circulation on the continental shelf of the Gulf of Cádiz”, Deep-Sea Research II 53, 1182-1197.
- Garcia-Solsona, E., Garcia-Orellana, J., Masqué, P., Rodellas, V., Mejías, M., Ballesteros, B., and Domínguez, J. A., 2010. Groundwater and nutrient discharge through karstic coastal springs (Castelló, Spain). Biogeosciences, 7, 2625–2638. doi:10.5194/bg-7-2625-2010.
- Geirnaert, W., van Beeres, P.H., de Vries, J.J., Hoogeveen, H., 1982. Hidrogeologic studies in the East Algarve, Portugal. Part I: Geo-electric survey of the Miocene aquifer between Quarteira and Olhão, Algarve, Portugal, III Semana de Hidrogeologia, 10 - 14 May, Lisbon, Portugal, pp. 2-22.

- Groves CG, Howard AD (1994) Early development of karst systems: 1. Preferential flow path enlargement under laminar flow. Water Resour Res 30:2837–2846. doi: 10.1029/94WR01303

- Henderson, R. et al., 2010. Marine electrical resistivity imaging of submarine groundwater discharge: sensitivity analysis and application in Waquoit Bay, Massachusetts, USA. Hydrogeology Journal, 18(1): 173-185.

- Hinsby, K., Condesso de Melo, M.T., Dahl, M. 2008. European case studies supporting the derivation of natural background levels and groundwater threshold values for the protection of dependent ecosystems and human health. Science of the total environment, 401 (1), p.1-20.

- Hugman R, Stigter TY, Monteiro JP, Nunes L (2012) Influence of aquifer properties and the spatial and temporal distribution of recharge and abstraction on sustainable yields in semi-arid regions. Hydrol Process 26:2791–2801.doi: 10.1002/hyp.8353.

- Hugman, R., Costa, L., Monteiro, J.P., Stigter, T., Nunes, L., 2013. Modelling the spatial and seasonal distribution of submarine groundwater discharge for different water use scenarios under epistemic uncertainty. Environmental Earth Sciences, Submitted (Special Issue: Sustainability & Water Resources).

- Jackson, L.E., Kurtz, J.C., Fisher, W.S., 2000. Evaluation Guidelines for Ecological Indicators.Environmental Protection Agency, Washington, DC. Report No. EPA/620/ R-99/005, 110 pp.

- Johannes, R. E. 1980. The ecological significance of the submarine discharge of groundwater. Marine Ecology Progress Series 3, 365-373.

- Kennedy A.D., Jacoby C.A. 1999. Biological indicators of marine environmental health: meiofauna – a neglected benthic component? Environmental Monitoring and Assessment, 54, 47-68.

- Kok, A. et al., 2010. Using Ground based Geophysics and Airborne Transient Electromagnetic Measurements (SkyTEM) to map Salinity Distribution and Calibrate a Groundwater Model for the Island of Terschelling - The Netherlands.

- Langevin, C.D., Thorne, D.T., Jr., Dausman, A.M., Sukop, M.C., Guo, W., 2007. SEAWAT Version 4: A Computer Program for Simulation of Multi-Species Solute and

Heat Transport, U.S. Geological Survey Techniques and Methods Book 6, Chapter A22.

- Legchenko, A., Ezersky, M., Camerlynck, C., Al-Zoubi, A., Chalikakis, K., 2009. Joint use of TEM and MRS methods in a complex geological setting. Comptes Rendus Geosciences, 341(10-11): 908-917.

- Leote, C., Severino Ibánhez, J., Rocha, C. 2008. Submarine Groundwater Discharge as a nitrogensource to the Ria Formosa studied with seepage meters. Biogeochemistry 88:185–194. DOI 10.1007/s10533-008-9204-9.

- Li, L., Barry, D., Stagnitti, F. and Parlange, J., 1999. Submarine groundwater discharge and associated chemical input to a coastal sea. Water Resources Research, 35, 3253-3259.

- Lofi J, Pezard P, Bouchette F, Raynal O, Sabatier P, Denchik N, Levannier A, Dezileau L, Certain R (2012) Integrated Onshore-Offshore Investigation of a Mediterranean Layered Coastal Aquifer. Ground Water:no-no. doi:10.1111/j.1745-6584.2012.01011.x

- Lopes, J. B. S. L. 1841. Corografia ou Memoria Economica, Estadistica, e Topografica do Reino do Algarve. Academia Real das Sciencias de Lisboa, Lisboa.

- Lopes FC, Cunha PP, Le Gall B (2006) Cenozoic seismic stratigraphy and tectonic evolution of the Algarve margin (offshore Portugal, southwestern Iberian Peninsula). Marine Geology 231:1-36. doi:http://dx.doi.org/10.1016/j.margeo.2006.05.007

- Manuppella, G., Marques, B. & Rocha, R.B. (1988) – Évolution tectono-sédimentaire du bassin de l'Algarve pendant le Jurassique. 2nd Int. Symposium on Jurassic Stratigraphy, Lisboa, pp. 1031-1046.

- Manuppella, G. (coord.) (1992) – Carta Geológica da Região do Algarve, escala 1/100 000, Notícia Explicativa. Serv. Geol. Port., Lisboa, 15 p.

- Manuppella, G., Ramalho, M., Telles Antunes, M., Pais, J., 2007. Sheet 53-A (Faro), Carta Geológica de Portugal (1:50 000). Laboratório Nacional Energia e Geologia, Lisbon.

- Martínez-Loriente S., Gráçia E., Bartolomé R.,Sallares V., Connors C., Perea H., Lo Iacono C., Klaeschen D., Terrinha P., Dañobeitia J.J. and Zitellini N. (2013) - Active

deformation in old oceanic lithosphere and significance for earthquake hazard: Seismic imaging of the Coral Patch Ridge area and neighboring abyssal plains (SW Iberian Margin). Geochemistry, Geophysics, Geosystems Volume 14, Issue 7, pp. 2206-2231.

- Massonnet, D., & Feigl, K. (1998). Radar interferometry and its application to changes in the Earth's surface. Reviews of Geophysics, 36, 441–500.

- Matias, H., et al. (2011). "Salt tectonics in the western Gulf of Cadiz, southwest Iberia." AAPG Bulletin 95(10): 1667-1698.

- Mauritzen C., Y. Morel, J. Paillet, 2001: “On the influence of Mediterranean water on the central waters of the North Atlantic Ocean”, Deep-Sea Research I 48, 347-381.

- McNeill, J.D., 1980. Electromagnetic terrain conductivity measurement at low induction numbers. TN-6, Geonics, Ontario - Canada.

- Mejías M, Ballesteros BJ, Antón-Pacheco C, Domínguez JA, Garcia-Orellana J, Garcia-Solsona E, Masqué P (2012) Methodological study of submarine groundwater discharge from a karstic aquifer in the Western Mediterranean Sea. Journal of Hydrology 464–465:27-40. doi:http://dx.doi.org/10.1016/j.jhydrol.2012.06.020

- Michael, H. A., Mulligan, A. E., & Harvey, C. F. Seasonal Water Exchange between Aquifers and the Coastal Ocean. Seasonal_SGD_26_Supplement.

- Miller, D. C. andUllman, W. J. 2004. Ecological consequences of ground water discharge to Delaware Bay, United States. Ground Water - Oceans Issue 42 (7), 959–970.

- Montagna P.A., Kalke R.D. 1992. The effect of freshwater inflow on meiofaunal and macrofaunal populations in the Guadalupe and Nueces estuaries, Texas. Estuaries, 15(3), 307-326.

- Mongelli, G., Monni, S., Oggiano, G., Paternoster, M., Sinisi, R., 2013. Tracing groundwater salinization processes in coastal aquifers: a hydrogeochemical and isotopic approach in the Na-Cl brackish waters of northwestern Sardinia, Italy. Hydrol. Earth Syst. Sci., 17(7): 2917-2928.

- Monteiro, J.P.; Santos, J.; Martins, R.R. (2002) - Avaliação dos Impactes Associados a Alterações no Regime de Exploração de Sistemas Aquíferos do Algarve Central

Usando Modelos Numéricos. Univ. Sevilha. In actas do III Congresso Ibérico sobre Gestão e Planificação da Água [Evaluation of the Impacts Associated to Changes in Exploration Regime of Aquifers in the Central Algarve Using Numerical Models]. Resumo pp717-724 e documento electrónico em CD-Rom 10pp.

- Monteiro, J.P.; Martins, R.R.; Nunes, P.; Diogo, A. (2003) - Evolução do Uso de Águas Subterrâneas nas Redes Urbanas de Abastecimento Público Entre Albufeira e Quarteira (Algarve Central). in Ribeiro L. & Peixinho de Cristo F. (eds.) As Águas Subterrâneas no Sul da Península Ibérica. Assoc. Intern. Hidrog. APRH publ., pp83-93.

- Monteiro, J.P., Oliveira, M.M., Costa, J.P., 2007. Impact of the Replacement of Groundwater by Dam Waters in the Albufeira-Ribeira de Quarteira and Quarteira Coastal Aquifers, XXXV AIH Congress. Groundwater and Ecosystems, Lisbon, Portugal, pp. 489-490.

- Moore, W. S. 1999. The subterranean estuary: a reaction zone of ground water and sea water. Marine Chemistry 65, 111-125.

- Moore, W. S., Sarmiento, J. L. and Key, R. M. 2008. Submarine groundwater discharge revealed by 228Ra distribution in the upper Atlantic Ocean. Nature Geoscience 1, 309-311.

- Morais, P., Borges, T. C., Carnall, V., Terrinha, P., Cooper C. & Cooper, R., 2007. Trawl-induced bottom disturbances off the south coast of Portugal: direct observations by the 'Delta' manned submersible on the Submarine Canyon of Portimão. Marine Ecology 2007, 28 (Suppl. 1), 112–122 a 2007 The Authors. Journal compilation a 2007 Blackwell Publishing Ltd.

- Morais, P., Chícharo, M.A., Chícharo, L. 2009. Changes in a temperate estuary during the filling of the biggest European dam. Science of The Total Environment, In Press.

- Moura, D. & Boski, T. (1999) – Unidades litostratigráficas do Pliocénico e Plistocénico no Algarve. Comunicações do Instituto Geológico e Mineiro, t. 86, pp. 85-106.

- Nicolau R (2002) Modelação e mapeamento da distribuição espacial da precipitação – Uma aplicação a Portugal Continental (Modeling and mapping of the spatial distribution of rainfall). Universidade Nova de Lisboa.

- Noiva, J., 2009. Caracterização de estruturas tectónicas activas da região sul de Portugal com recurso a ferramentas SIG: O caso da falha de São Marcos-Quarteira de Lisboa., Tese de Mestrado da Universidade Nova.

- Noiva, J., et al. (2010). Holocene morphologic changes offshore the Quarteira region, Algarve, south Portugal. EGU Meeting, Vienna, Austria, EGU.

- Oliveira MM (2006) Recarga de Águas Subterraneas - Metodos de Avaliaçao, 1st ed. 474.

- Oude Essink, G.H.P., 2001. Density Dependent Groundwater Flow - Salt water Intrusion and Heat Transport, Utrecht University.

- Palain, C. (1976) – Une série détritique terrigéne, les “Grés de Silves”: Trias et Lias inférieur du Portugal. Mem. Serv. Geol. Portugal, N. S., Lisboa, 25, 377 p.

- Palain, C. (1979) – Connaissances stratigraphiques sur la base du Mésozoique portugais. Ciências da Terra, Univ. Nova Lisboa, 5, pp. 11-28.

- Pais J, Legoinha P, ElderWeld H, Sousa L, Estevens M (2000) The Neogene of Algarve (Portugal). Cienc Terra 14:277–288

- Pais, J., et al. (2012). The Paleogene and Neogene of Western Iberia (Portugal): A Cenozoic Record in the European Atlantic Domain. The Paleogene and Neogene of Western Iberia (Portugal), Springer Berlin Heidelberg: 1-138.

- Porcelli, D. and Swarzenski, P.W., 2003. The behaviour of U- and Th-series nuclides in groundwater and the tracing of groundwater. Reviews in Mineralogy and Geochemistry, 52, 317-361.DOI: 10.2113/0520317

- Post, V., Abarca, E., 2010. Preface: Saltwater and freshwater interactions in coastal aquifers. Hydrogeology Journal, 18(1): 1-4.

- Post, V.E.A., 2005. Fresh and saline groundwater interaction in coastal aquifers: Is our technology ready for the problems ahead? Hydrogeology Journal, 13(1): 120-123.

- Post, V.E.A., Groen, M., Groen J., Kooi, H., 2007. Using seaborne TDEM measurements to detect the offshore extension of fresh groundwater systems. Abstract Offshore Geophysics IAH 2007.

- Post, V.E.A. et al., 2013. Offshore fresh groundwater reserves as a global phenomenon. Nature, 504(7478): 71-78.
- Potter R.A., M.S. Lozier, 2004: “On the warming and salinification of the Mediterranean outfow waters in the North Atlantic, Geophysical Research Letters 31, L01202.
- Poulsen, S.E., Rasmussen, K.R., Christensen, N.B., Christensen, S., 2010. Evaluating the salinity distribution of a shallow coastal aquifer by vertical multielectrode profiling (Denmark). Hydrogeology Journal, 18(1): 161-171.
- Povinec P.P., P.K. Aggarwal, A. Aureli, W.C. Burnett, E.A. Kontar, K.M. Kulkarni, W.S. Moore, R. Rajar, M. Taniguchi, J.-F. Comanducci, G. Cusimano, H. Dulaiova, L. Gatto, M. Groening, S. Hauser, I. Levy-Palomo, B. Oregioni, Y.R. Ozorovich, A.M.G. Privitera e M.A. Schiavo, 2006: “Characterization of Submarine Groundwater Discharge Offshore South-Eastern Sicily”, Journal of Environmental Radioactivity, 89, 81-101 (doi: 10.1016/j.jenvrad.2006.03.008).
- Presidência do Conselho de Ministros, 2009. Resolução do Conselho de Ministros n.º 82/2009 de 8 de Setembro de 2009, Diário da República, 1.ª série — N.º 174, pp. 6056-6088.
- Ramalho, M.M. (1988) – 400 milhões de anos de história do Algarve. Anais do Município de Faro, Faro, XVII, 45 p.
- Razack, M., Drogue, C., Romariz, C. et Almeida, C., 1980. Étude de l’effet de marée océanique sur un aquifére carbonate cotier (MIOCÈNE DE L’ALGARVE − PORTUGAL). Journal of Hydrology, 45 (1980) 57-69.
- Reis, E., Gago, C., Borges, G., Matos, M., Cláudio, A., Mendes, E., Silva, A., Serafim, J., Rodrigues,A., Correia, S., 2007. Contribuição para o Cálculo do Balanço Hídrico dos Principais Sistemas Aquíferos do Algarve. Ministério do Ambiente, do Ordenamento do Território e do Desenvolvimento Regional, Comissão de Coordenação e Desenvolvimento Regional do Algarve.
- Rey, J., 1983. Le Crétacé de l’Algarve: éssai de synthèse. Comum. Serv. Geol. Portugal, Lisboa, 69 (1), pp. 87-101.
- Rey, J., 2006. Les Formations Crétacées de l'Algarve Occidental et Central. Comunicações Geológicas, 93: 41.

- Rocha, R., Marques, B., Antunes, M. T. (1989) – Carta Geológica de Portugal na escala 1:50 000 e Notícia Explicativa da Folha 52-B ALBUFEIRA. Serviços Geológicos de Portugal. Lisboa. 36 pág.

- Roque, C., et al. (2012). "Pliocene and Quaternary depositional model of the Algarve margin contourite drifts (Gulf of Cadiz, SW Iberia): Seismic architecture, tectonic control and paleoceanographic insights." Marine Geology 303–306(0): 42-62.

- Roque, C. (2007). Tectonoestratigrafia do Cenozóico das Margens Continentais Sul e Sudoeste Portuguesas: Um modelo de correlação sismostratigráfica. Deparatamento de Geologia. Lisboa, Universidade de Lisboa. PhD: 316.

- Sallarès, V., et al. (2013). "Seismic evidence of exhumed mantle rock basement at the Gorringe Bank and the adjacent Horseshoe and Tagus abyssal plains (SW Iberia)." Earth and Planetary Science Letters 365(0): 120-131.

- Sánchez R., P. Relvas, 2003: “Spring-summer climatological circulation in the upper layer in the region of Cape St. Vincent, Southwest Portugal”, ICES Journal of Marine Science 60, 1232-1250.

- Santos, F.A.M., 2004. 1-D laterally constrained inversion of EM34 profiling data. Journal of Applied Geophysics, 56: 123-134.

- Schiavob, M.A., Hauserb, S., Cusimanoa, G., Gattoa, L., 2006. Geochemical characterization of groundwater and submarine discharge in the south-eastern Sicily. Continental Shelf Research 26, pp.826–834.

- Silva, M. L (1988) - Hidrogeologia do Miocénico do Algarve. Dissertação para a Obtençãodo Grau de Doutor em Geologia. Departamento de Geologia da FCUL, 377 pág.

- Silva, A.C.F., Tavares P., Shapouri M., Stigter T.Y., Monteiro J.P., Machado M., Cancela da Fonseca L., Ribeiro L. (2102) – Estuarine biodiversity as an indicator of groundwater discharge. Estuarine, Coastal and Shelf Science 97, pp. 38-43.

- Sousa F.M., G. Carrara, J. Fernandes, D. Boutov, M. Loureiro, F. Leitão, P. Range e A. Machado, 2014: “Descargas de Águas Subterrâneas na região dos Olhos de Água – alguns resultados das campanhas CTD”, p. 503-507 de “Proceedings da 8ª Assembleia Luso Espanhola de Geodesia e Geofísica”, (eds. B. Caldeira, J.

Barrenho, J.F. Borges, J. Pombinho, M.J. Costa, M.R. Duque, M. Bezzeghoud e R. Salgado), ISBN: 978-989-98836-0-4, 593 pp.

- Stigter, T.Y., Carvalho Dill, A., Malta, E.-j., Santos, R., in press. Nutrient sources for green macroalgae in the Ria Formosa lagoon – assessing the role of groundwater. Chapter in: Ribeiro, L., Stigter, T.Y., Chambel, A., Condesso de Melo, M.T., Monteiro, J. P., Medeiros, A. (Eds) Selected papers on Hydrogeology - Groundwater and Ecosystems, Chapter 13. Taylor & Francis.

- Street, J.H., Grossman, E.E. and Paytan, A., 2006. Submarine groundwater discharge and nutrient subsidies to the leeward shores of Maui, Moloka'i and Hawai'i estimated using radium isotopes. Eos Trans. AGU, 87, Ocean Sci. Meet. Suppl., Abstr. OS15B-03.

- Swarzenski P. W., Bratton, J. and Crusius, J., 2004. Submarine groundwater discharge and its role in coastal processes and ecosystems. USGS OFR 2204-1226.

- Taniguchi M., Burnett W.C., Cable J.E. and Turner J.V. (2002) – Investigation of submarine groundwater discharge. Hydrological Processes, 16, 2115-2129. DOI:10.1002/hyp.1145

- Teixeira, S.B., 1998. Identificação e caracterização de arribas Holocénicas submersas ao largo do Algarve (Portugal). Com. In. Geol. Min. 84 (1), 35±38.

- Teixeira, S.B., 2000. Litologia dos balastros das praias do Algarve Central (Portugal). Com. 3º Simpósio sobre a Margem Continental Ibérica Atlântica, Faro, pp. 139-140.

- Teixeira, S.B. & Macedo, F. (2001). “Prospecção de manchas de empréstimo ao largo de Albufeira. DRAOT Internal Report, 59 p.

- Teixeira, S. B., 2005. Evolução Holocénica do Litoral em Regime Trangressivo: o caso da costa de Quarteira (Algarve, Portugal). Iberian Coastal Holocene Paleoenvironmental Evolution, COASTAL HOPE 2005 – Proceedings, 121-124.

- Terrinha, P.A.G. (1998) – Structural Geology and Tectonic Evolution of the Algarve Basin, South Portugal. PhD Thesis, Imperial College, London, 430 p.

- Terrinha, P., et al. (2003). "Tsunamigenic-seismogenic structures, neotectonics, sedimentary processes and slope instability on the southwest Portuguese Margin." Marine Geology 195 (1-4): 55-73.

- Terrinha, P., et al. (2013). A Bacia do Algarve: Estratigrafia, Paleogeografia e Tectónica. Geologia de Portugal no contexto da Ibéria. Geologia de Portugal, Volume II, Geologia Meso-cenozóica de Portugal. R. Dias, A. A. Araújo, P. Terrinha and J. C. R. Kullberg, Escolar Editora. II: 29-166.

- Terrinha, P., Noiva, J., Carrara, G., Fernandes, J., Roque, C., Pinheiro, L.,2014. Neogene and Quaternary seismostratigraphy and tectonics offshore Albufeira and Quarteira: implications on the paleogeography and submarine freshwater discharges. Proceedings dos IX Congresso Nacional de Geologia (IX CNG) e 2º Congresso de Geologia dos Países de Lí-ngua Portuguesa (2º CoGePLiP), Porto, (Portugal).

- Trabelsi, R., Abid, K., Zouari, K., Yahyaoui, H., 2012. Groundwater salinization processes in shallow coastal aquifer of Djeffara plain of Medenine, Southeastern Tunisia. Environmental Earth Sciences, 66(2): 641-653.

- UNESCO, 2004. Submarine groundwater discharge. Management implication, measurements and effects. International hydrological Program (IHP), IHP-Vi, Series on Groundwater, 5. ISBN 92-9220-006-2.

- USGS, 2006. Submarine groundwater discharge science plan. A report to USGS-Coastal and Marine Geology Program Managers prepared by the USGS Submarine Groundwater Discharge Team.

- Vargas J.M., J. Garcia-Lafuente, J. Delgado, F. Criado, 2003: “Seasonal and wind-induced variability of sea surface temperature patterns in the Gulf of Cádiz, Journal of Marine Systems 38, 205-219.

- Vouillamoz, J.M. et al., 2012. Quantifying aquifer properties and freshwater resource in coastal barriers: A hydrogeophysical approach applied at Sasihithlu (Karnataka state, India). Hydrology and Earth System Sciences, 16(11): 4387-4400.

- Waltham, A C, Bell, F G and Culshaw, M G. 2005. Sinkholes and Subsidence: Karst and Cavernous Rocks in Engineering and Construction. Springer. ISBN 3-540-20725-2.

- Waska, H. and Kim, G. 2011. Submarine groundwater discharge (SGD) as a main nutrient source for benthic and water-column primary production in a large intertidal environment of the Yellow Sea. Journal of Sea Research 65, 103-113.

- Webera, N., Chaumillonb, E., Tessonc, M., Garlana, T., 2004. Architecture and morphology of the outer segment of a mixed tide and wave-dominated-incised valley, revealed by HR seismicreflection profiling: the paleo-Charente River, France. Marine Geology 207,17–38.

- Weinberger, R., V. Lyakhovsky, G. Baer, and Z. B. Begin (2006), Mechanical modeling and InSAR measurements of Mount Sedom uplift, Dead Sea basin: Implications for effective viscosity of rock salt, Geochem. Geophys. Geosyst., 7, Q05014, doi:10.1029/2005GC001185.

- Werner, A.D. et al., 2013. Seawater intrusion processes, investigation and management: Recent advances and future challenges. Advances in Water Resources, 51(0): 3-26.

- Wessel, P. and W. H. F. Smith, Free software helps map and display data, EOS Trans. AGU, 72, 441, 1991.

- Wessel, P., W. H. F. Smith, R. Scharroo, J. F. Luis, and F. Wobbe, Generic Mapping Tools: Improved version released, EOS Trans. AGU, 94, 409-410, 2013.

11. AKNOWLEDGMENTS

We are gratefully to the University of Algarve for boat supply and all the people that in various ways have permitted the successfully realization of the campaign.

We thank Engº Rui Santos (Câmara Municipal de Albufeira) for the access to the municipality boreholes, Edite Reis (ARHA) to provide the borehole data and the digital terrain model, Teresa Cunha (LNEG) to provide the digital geological cartography and PANGEO processed data and Manuel Silva (LNEG) for the geoelectrical field work.

Authors are gratefully to all people that in various ways gave them the possibility to access fundamental datasets. In particular we thank José da Silva (Porto University) and Prof. Joaquim Luis (Algarve University) for allowing the using of SAR images and the Algarve bathymetric grid, respectively.

Special thanks are addressed to António Massapina and Isolete Correia, directors of Marinas de Albufeira e de Vilamoura, respectively, that ever placed a berth to our disposal during the various offshore surveys.

We also thank Algarve Seafaris Lda., that placed its offices at Marina de Vilamoura to our disposal allowing us to perform the initial and final checks of our CTD probe at the beginning and the end of each CTD survey.

We personally thank the great disponibility and collaboration of Francisco Leitão (SFRH/BPD/63935/2009), Pedro Range (SFRH/BPD/69959/2010) and Rui Hugman (SFRH/BD/80149/2011), FCT Post-Doc and PhD fellows respectively, in the project acquisition phases.

Special thanks to FCT for funding the Project Freeze.